

# PREDICTION OF REMAINING USEFUL LIFE OF AN END MILL CUTTER

SEOW XIANG YUAN

Report submitted in partial fulfillment of the requirements  
for the award of the degree of  
Bachelor of Engineering (Hons.) in Manufacturing Engineering

Faculty of Manufacturing Engineering

UNIVERSITI MALAYSIA PAHANG

JUNE 2016

### **SUPERVISOR'S DECLARATION**

I hereby declare that I have checked this thesis and in my opinion, this thesis is adequate in terms of scope and quality for the award of the degree of Bachelor of Engineering in Manufacturing

Signature :

Name of supervisor : DR. MEBRAHITOM ASMELASH GEBREMARIAM

Position : SENIOR LECTURER

Date : 10/6/2016

**STUDENT'S DECLARATION**

I hereby declare that the work in this thesis is my own except for quotation and summaries which have been duly acknowledged. The thesis has not been accepted for any degree and is not concurrently submitted for award of other degree.

Signature :

Name : SEOW XIANG YUAN

ID Number : FA12046

Date : 10/6/2016

## ACKNOWLEDGEMENTS

A final year project is a golden opportunity for learning and self-development. I consider myself very lucky and honoured to have a wonderful and respectful supervisor to lead us through in the completion of this project.

My most grateful thanks to Dr. Mebrahitom Asmelash Gebremariam who in spite of extraordinary busy with his own duties, took out time to listen, guide and keep me on the correct path. I do not know where we would have been without him. Very humble thanks to my supervisor, Dr. Mebrahitom.

I would like to thank the person in charge of the lab FKM, Mr Asmizam for being highly helpful and fully supportive in this project although he is busy with his own stuffs in the duration of the project. This has enabled me to finish this project in the time given.

Last but not least, there were so many people who shared valuable information in the successful completion of this project.

## **ABSTRACT**

This thesis presents a comparison between methods for tool life prediction. The main objective of the thesis is to have an accurate prediction of the RUL and select the best method for prediction. An experiment has been conducted using Kistler dynamometer and Olympus metallurgical microscope on a HASS VF-6 milling machine to acquire the sensor force signals and actual tool wear respectively. The force signal gives the significant statistical features of the data. The features are extracted using statistical measure and reduced using a stepwise regression model. The prediction methods are Support Vector Regression and Neural Network. Both the models are trained using the MATLAB software. The results of the models are compared against each other to select the best method. Moreover, the methods are also applied on data taken from PHM Society. This data serves as a preliminary result and fundamental knowledge for my own experiment. The models trained in this project are compared with the existing models. These results show that the proposed methods are suitable for predicting the remaining useful life.

## ABSTRAK

Tesis ini membentangkan perbandingan antara kaedah untuk ramalan hayat alat. Objektif utama tesis ini adalah untuk mempunyai ramalan yang tepat daripada RUL dan memilih kaedah yang terbaik untuk ramalan. Satu eksperimen telah dilakukan dengan menggunakan Kistler dinamometer dan Olympus mikroskop logam pada HASS VF-6 pengilangan mesin untuk memperoleh isyarat kuasa sensor dan penggunaan alat sebenar masing-masing. Isyarat kuasa memberikan ciri-ciri statistik besar daripada data. Ciri-ciri yang diekstrak menggunakan kaedah statistik dan dikurangkan dengan menggunakan model regresi langkah demi langkah. Kaedah ramalan adalah Support Vector Regresi dan Neural Network. Kedua-dua model dilatih menggunakan perisian MATLAB. Keputusan model dibandingkan antara satu sama lain untuk memilih kaedah yang terbaik. Selain itu, kaedah ini juga digunakan pada data yang diambil daripada PHM Society. Data ini berfungsi sebagai hasil awal dan pengetahuan asas untuk percubaan saya sendiri. Model-model dilatih dalam projek ini dibandingkan dengan model yang sedia ada. Keputusan ini menunjukkan bahawa kaedah yang dicadangkan adalah sesuai untuk meramalkan baki hayat berguna.

**TABLE OF CONTENTS**

	<b>Page</b>
<b>SUPERVISOR'S DECLARATION</b>	iii
<b>STUDENT'S DECLARATION</b>	iv
<b>ACKNOWLEDGEMENTS</b>	v
<b>ABSTRACT</b>	vi
<b>ABSTRAK</b>	vii
<b>TABLE OF CONTENTS</b>	viii
<b>LIST OF TABLES</b>	xii
<b>LIST OF FIGURES</b>	xiv
<b>LIST OF SYMBOLS</b>	xx
<b>LIST OF ABBREVIATIONS</b>	xxii
<b>CHAPTER 1 INTRODUCTION</b>	
1.1 Introduction	1
1.2 Problem Statement	2
1.3 Objectives	3
1.4 Project Scope	3
<b>CHAPTER 2 LITERATURE REVIEW</b>	
2.1 Introduction	5
2.2 Factors Affecting Tool Life	5

2.3	Climb Milling and Conventional Milling	6
2.4	Cutting Force in End Milling	8
	2.4.1 Calculations of $F_F$	10
	2.4.2 Calculations of $F_b$	11
2.5	Cutting Parameters in Milling Process	12
2.6	Wear Mechanism of End Mill	16
2.7	Remaining Useful Life (RUL)	20
2.8	Tool Cutter Condition Monitoring	22
2.9	Prediction Method	23
	2.9.1 Artificial Neural Network (ANN)	24
	2.9.2 Support Vector Regression (SVR)	27
2.10	Summary	29

### **CHAPTER 3 DURABILITY ASSESSMENT METHODS**

3.1	Introduction	31
3.2	Flow Chart	32
3.3	Project Descriptions	33
	3.3.1 Design of Experiment	34
	3.3.2 CAD Program	39
	3.3.3 Tool Wear Measurement	43
	3.3.4 Signal Acquisition and Processing	49
	3.3.5 Features Extraction and Reduction	53
	3.3.6 Support Vector Machine Regression Model Training	54
	3.3.7 Artificial Neural Network Model Training	57
	3.3.8 Predict for Remaining Useful Life	63
3.4	Hardware and Software Application	64
	3.4.1 MAKINO Milling Machine	64
	3.4.2 HAAS Milling Machine	66
	3.4.3 Wire Cut Machine	67



3.4.4	Metallurgical Microscope	68
3.4.5	End Mill Insert	69
3.4.6	Workpiece Material	70
3.4.7	Dynamometer	71
3.4.8	Amplifier	73
3.4.9	Mastercam	75
3.4.10	MATLAB	76

## **CHAPTER 4 RESULTS AND DISCUSSIONS**

4.1	Introduction	78
4.2	PHM Society Data Analysis	79
4.2.1	Raw Data Features Extraction	81
4.2.2	Features Reduction and Selection	82
4.2.3	Support Vector Regression (SVR) Model	83
4.2.4	Artificial Neural Network Model	85
4.2.5	Remaining Useful Life (RUL) Prediction	89
4.2.6	Performance Assessment	90
4.3	Actual Tool Wear Measurement	93
4.4	Raw Data Features Extraction	95
4.5	Features Reduction and Selection	95
4.6	Support Vector Regression (SVR) Model	97
4.7	Artificial Neural Network Model	100
4.8	Remaining Useful Life (RUL) Prediction	106
4.9	Performance Assessment	108

## **CHAPTER 5 CONCLUSION AND RECOMMENDATIONS**

5.1	Introduction	112
5.2	Conclusion	112

5.3	Recommendations	113
	<b>REFERENCES</b>	114
	<b>APPENDICES</b>	119
A	Budget Plan	119
B	Gantt Chart	120
C	CAD Program	122

**LIST OF TABLES**

<b>Table No.</b>	<b>Title</b>	<b>Page</b>
2.1	ANOVA for surface roughness	15
2.2	ANOVA for surface roughness	15
2.3	Important statistical features	25
3.1	Experiment setting	39
3.2	Wire cut machine specification	68
4.1	Cutting Condition	79
4.2	Significant statistical features	81
4.3	Stepwise regression parameters	82
4.4	Features selection result from stepwise regression	82
4.5	Support vector machine regression model	83
4.6	Artificial Neural network setting	85
4.7	Mean Square Error and regression of the model	86
4.8	Performance assessment for SVM Regression model	91
4.9	Performance assessment for neural network model	92
4.10	Important statistical features	95
4.11	Stepwise regression setting	96
4.12	Features selection result from stepwise regression	97

4.13	Support vector machine regression model	98
4.14	Neural network setting	102
4.15	Mean Square Error and regression of the model	103
4.16	Performance assessment for models trained	110

**LIST OF FIGURES**

<b>Figure No.</b>	<b>Title</b>	<b>Page</b>
2.1	Conventional Milling and Climb milling	8
2.2	Milling process	9
2.3	Graph for cutting force	14
2.4	Graph for surface roughness	14
2.5	Central wear and flank wear	16
2.6	Schematic illustration of tool wear	17
2.7	Chipping and catastrophic fracture on end mill	19
2.8	Concept illustration of remaining life of an asset	20
2.9	Remaining useful life (RUL)	21
2.10	Prognostics approach	24
2.11	ANN architecture	26
2.12	ANN output graph	26
2.13	Health indicator result using EM-PCA (left) and ISOMAP (right)	28
2.14	Result of SVR model	29
3.1	Flow chart	32
3.2	Raw material	34

3.3	Wire cutting of material	34
3.4	Material surface after wire cut	35
3.5	Surface finish from face milling process	35
3.6	Experiment setup	36
3.7	Edge finding process	37
3.8	Cutting process	37
3.9	Tool holder and insert	38
3.10	Mastercam Mill X5 software	40
3.11	Stock dimension setup	40
3.12	Tool parameters	41
3.13	Linking parameters	41
3.14	Tool path design	42
3.15	Tool path illustration	42
3.16	Tool wear measurement	43
3.17	Tool wear measurement process	44
3.18	Computer and microscope system	45
3.19	Light level on microscope	46
3.20	Specimen preparation	46
3.21	Microscope software	47

3.22	Table height adjustment	47
3.23	Image capture	48
3.24	Wear measurement	48
3.25	Data acquisition and export process	49
3.26	Dynoware	50
3.27	Amplifier Connection	51
3.28	Measuring time and sampling rate	51
3.29	Sensor data measurement	52
3.30	Data exportation	52
3.31	Exported data	53
3.32	Features extraction	53
3.33	Features reduction	54
3.34	Support Vector Machine regression model training	55
3.35	Predictors and respond	56
3.36	<i>fitrsvm</i> function code	57
3.37	<i>predict</i> function code	57
3.38	Artificial Neural Network model training	58
3.39	Neural fitting app	59
3.40	Data loading	59

3.41	Validation and test data	60
3.42	Neurons selection and network architecture	60
3.43	Training of network	61
3.44	Retraining interface	62
3.45	Network result saving	62
3.46	Predicting remaining useful life	63
3.47	Makino KE55 CNC milling machine	64
3.48	Specifications for Makino KE55	65
3.49	HAAS milling machine VF-6	66
3.50	Control unit	66
3.51	Sodick VZ 300L wire cut machine	67
3.52	Olympus BX51M metallurgical microscope	68
3.53	End mill insert	69
3.54	Insert specification	70
3.55	Workpiece physical data	71
3.56	Dynamometer 9257B	72
3.57	Dynamometer technical data	73
3.58	Amplifier type 5070A	74
3.59	Amplifier specifications	75



3.60	Mastercam logo	76
3.61	MATLAB Logo	77
4.1	Raw data from force sensor during first cutting process (left) and final cutting process (right)	80
4.2	Raw data from vibration sensor during first cutting process (left) and final cutting process (right)	80
4.3	Raw data from acoustic sensor during first cutting process (left) and final cutting process (right)	81
4.4	Comparison between actual wear and predicted wear of SVR	84
4.5	Neural network architecture	85
4.6	Mean Square Error	87
4.7	Regression plot	87
4.8	Comparison between actual wear and predicted wear of neural network	88
4.9	Comparison between actual RUL and neural network RUL	89
4.10	Comparison between actual RUL and Support Vector Regression RUL	90
4.11	Actual tool wear of end mill	93
4.12	Tool wear after first cutting process	94
4.13	Tool wear after last cutting process	94
4.14	Comparison between actual wear and predicted wear of SVR	100
4.15	Neural network architecture	101
4.16	Mean Square Error	104

4.17	Regression plot	104
4.18	Comparison between actual wear and predicted wear of neural network	105
4.19	Illustration for remaining useful life calculation	107
4.20	Comparison between actual RUL and Support Vector Regression RUL	107
4.21	Comparison between actual RUL and Artificial Neural Network RUL	108

**LIST OF SYMBOLS**

$C$	Force Coefficient
$C$	Penalty function
$\epsilon$	Epsilon
$\mathcal{E}(t)$	Difference between predicted and actual RUL
$\epsilon$	Mean of total difference between predicted and actual RUL
$e$	Exponent
$F$	Total cutting force
$F_B$	Bottom force
$F_F$	Flank force
$h$	Instantaneous uncut chip thickness
$N$	Number of cuts
$R^2$	R squared
$RUL_{\text{actual}}$	Actual remaining useful life
$RUL_{\text{predicted}}$	Predicted remaining useful life
$t$	Current time
$t_f$	Final time
$V$	Voltage
$W$	Axial length

$\Sigma$  Summation

$\omega$  Angle

**LIST OF ABBREVIATIONS**

AE	Acoustic emission
AISI	American Iron & Steel Institute
ANN	Artificial Neural Network
ANOVA	Analysis of Variance
CART	Classification and Regression Tree
CNC	Computer Numerical Control
CMS	Condition Monitoring System
DAQ	Data Acquisition
EM-PCA	Expected Maximization Principal Component Analysis
ESR	Electro-Slag-Refining
GUI	Graphical User Interface
HP	Horse Power
HSS	High Speed Steel
MAPE	Mean Absolute Percentage Error
MSE	Mean Square Error
PHM	Prognostics and Health Management
PVD	Physical Vapor Deposition
QP	Quadratic Programming

RMS	Root Mean Square
RUL	Remaining Useful Life
SMO	Sequential Minimal Optimization
SVR	Support Vector Regression
TCM	Tool Condition Monitoring
WPD	Wavelet Packet Decomposition

## **CHAPTER 1**

### **INTRODUCTION**

#### **1.1 INTRODUCTION**

Machining process is a widely used method of production method to remove excess material to get the desired dimension. Machining processes can be classified into traditional machining process or nontraditional machining process. Traditional machining processes are milling, turning, and etc. while the nontraditional machining processes are electrical discharge cutting, chemical milling, and etc.

Milling process is one of the most adaptable traditional machining process where a rotating cutter removes the material while traveling along different axes with respect of the workpiece. Milling is able to produce a part with very compact shape but still very close to the tolerance and with a very fine finishing surface.

Due to the ability of milling process to produce workpiece with intricate profiles or complicated shape, it has been classified as commonly used machining process. An end mill is used in the machining process to remove the material on the workpiece. This cutter can be either having a straight shank for a small size cutter or a tapered shank for an end mill with bigger diameter. The cutter has different kinds of geometry such as cylindrical end mill, ball end mill, bull nose end mill, and other geometries [1]. The end

mill is installed on a tool holder and mounted on the spindle of the milling machine. Generally, the cutter is made from high speed steel (HSS) but it may be made from carbide or cobalt and come with a protective coating to increase its surface hardness [2].

The quality of the end milling is related to the milling parameters such as cutting speed, feed, cutting time, material removal rate, and etc. Other than these parameters, the quality of the surface is also depending on the condition of the cutting tools. The quality and wear of the end mill will affect directly the result of the end milling process. Normally the wear pattern found in the ends mill are flank wear on the cutting edge and center wear on the tool tip [2]. A worn end mill will give a damaged surface to the workpiece, thus it is very important for us to understand the wear mechanism of the end mill and remaining useful life of it.

This research paper is focus on estimating the amount of wear and predicting the remaining useful life of an end mill. A few different prediction methods have been established to know the remaining tool life of the cutter. The approaches available are Artificial Neural Network [3], Fuzzy Neural Network [4], Support Vector Regression [5], and etc. Different prediction methods were investigated in this research paper to determine the best approach for remaining useful life prediction. The data driven approach is selected to be investigated in this research paper.

## **1.2 PROBLEM STATEMENT**

In the manufacturing sectors nowadays, end milling process is a machining process that is widely adopted. The condition of the tool cutter is very important as it represents the remaining useful tool life of the cutter. The failure of a cutting tool occurs when it has come to the end of its service life. A worn tool will cause the workpiece to



have inferior quality and increased surface roughness. In some cases, if the wear of the tool was not detected, it may cause damage to the milling machine or may even cause accidents. This has negatively impact the usefulness of milling process [5].

Therefore, it is important to conduct this research to determine the best approach to estimate the wear of an end mill and predict its remaining useful life. The main focus of this research will be on the data driven type of prediction method with the help of MATLAB software in the analysis of data. This research will investigate different prediction methods using MATLAB to increase the reliability of the tool life prediction model. This allows us to reduce the manufacturing costs by reducing the scrap produced due to the broken tools and the service life of the end mill cutter can be fully utilized before it is disposed away.

### **1.3 OBJECTIVES**

The objectives of this project are:

1. To predict the remaining useful life of an end mill cutter.
2. To investigate and compare different prediction methods available using MATLAB software.
3. To propose the best approach to predict the remaining tool life end mill cutter.

### **1.4 PROJECT SCOPE**

The scope of this project is to investigate the methods available to estimate the wear of the end mill and predict its remaining useful life. The prognostics prediction approaches for remaining tool life can be classified into three types which are model based

approach, data driven approach, and hybrid approach [5]. In this paper we will focus on investigate and compare the different data driven approaches for useful tool life estimation.

In the model based approach, a mathematical model is used to illustrate the performance for the physical parts. The model is used to predict the future degradation, thus predict the remaining useful life. In data driven method, the data acquired from the sensors will be monitored and implemented into the suitable models. Later these models will be used to predict the remaining useful life of the cutter by evaluate the health indicator of the system. The hybrid approach is the combination of the two approaches [5].

The software that will be used for analysis in this paper is MATLAB. It provides the user an environment to carry out different kinds of calculations [6]. The limitation of the MATLAB is it is not a general programming language such as C++ or FORTRAN. It is also not suitable for other applications other than scientific calculations. MATLAB is an interpreted language, thus slower than the compiled language such as C++ [7].

## **CHAPTER 2**

### **LITERATURE REVIEW**

#### **2.1 INTRODUCTION**

The main purpose of this chapter is to provide the knowledge relevant to this project by reviewing several literatures. The different researches done by the researchers were reviewed. The literatures are in the form of journal, articles, publications, website, and other reliable sources. This is to establish a connection between the available researches to this project. This chapter also helps in the selection of most appropriate method for this project. The cutting force, cutting parameters, wear mechanism of end mill, remaining useful life, and prediction methods available were discussed and reviewed in this chapter.

#### **2.2 FACTORS AFFECTING TOOL LIFE**

The tool life of an end mill can be affected by many different variables, such as the type of milling method, cutting forces, machining parameters and other uncertainty in the machining environment.

The cutting speed is the most influencing factor in affecting the tool life. The temperature will increase when the cutting speed increases. The heat is mainly focus on the tool than the workpiece. The hardness of the tool will increase due to the changing in the matrix of the material and this condition will accelerate the abrasion of the tool. The flank wear will be dominant when the cutting speed is increased. Other than that, the tool life is influenced by the feed rate also. The chip will pass through the tool face at a greater surface area when using a fine feed compared to a coarse feed in swarf removal. The resultant pressure will offset the advantage as to cope with the greater chip [8].

Besides that, the tool geometry will affect the tool life. The tool will become weak when the rake angle is large because it will reduce the cross section of the tool and the heat absorption by the metal. The form stability of the tool the wear rate will be affected by both the chemical and physical properties of the workpiece material. The tool will wear more when cutting a harder material. The cutting fluid can reduce the friction coefficient at the tool chip interface thus helping in lengthen the tool life. It acts as a coolant when the tool is under high speed milling operation or it can also act as a lubricant in a normal low speed milling [8].

### **2.3 CLIMB MILLING AND CONVENTIONAL MILLING**

The climb milling and conventional milling can produce a very different result in the milling process. By understanding the main difference between these two milling methods, we will be able to extend the tool life, improve the product quality, and increase the utilization of the machine [9].

In the conventional milling, the forces needed is lower and it is more favorable for roughing process. The cutter will revolve in the direction oppose to the table feed and

the workpiece will be fed into the rotation of the tool cutter. The chip starts with a minimum width and reaches its maximum width at the end of the cut. On the other hand, the climb milling method is able to produce a very nice surface finish and is suitable for most cases. The cutter will revolve in the direction same as the table feed. The cutter will meet the workpiece at the maximum thickness, thus largest chip will be produced first. The combination of the direction of the table feed and the rotation of the tool cutter will have the tendency to bring the chips away from the workpiece [9]. Figure 2.1 shows the climb milling method and conventional milling method.

Characteristic of conventional milling:

- Suitable for rough and abrasive surface.
- Cause more rubbing between the tool and workpiece, thus cause premature failure of tool.
- The tooth of cutter makes contact with the workpiece at the bottom of cut.
- It exerts an upward force on the workpiece and causes more workpiece movement.
- It requires more torque than climb milling.
- It gives worse surface finish as the chips are brought upward and dropped at the front cutter.
- The chip starts with zero thickness until maximum at the end of cut.
- The tool deflection tends to be parallel to the cut direction.

Characteristics of climb milling:

- It is suitable for solid carbide cutter.
- It gives improved surface finish and helps to extend the tool life by up to 50%.
- The tooth of cutter makes contact with the workpiece at the top of cut.

- It exerts a downward force on the workpiece, thus able to reduce workpiece movement.
- It requires less torque compared to conventional milling.
- The initial spindle load is higher and it increases when the tool cutter gets dull.
- The chip starts with maximum thickness and decreases to zero thickness.
- The tool deflection tends to be perpendicular to the cut direction

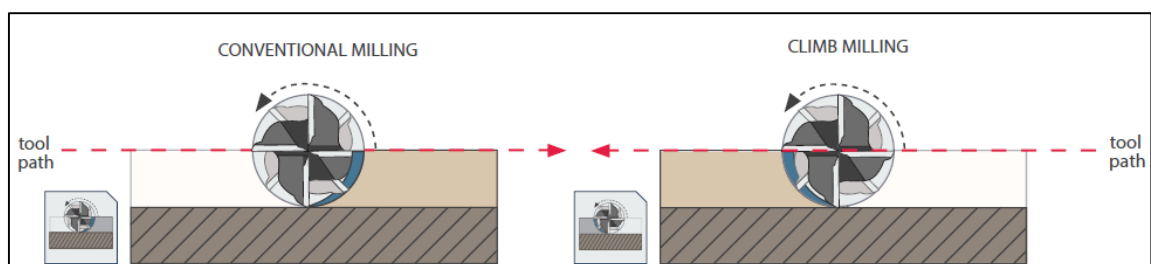


**Figure 2.1:** Conventional Milling and Climb milling [9]

Source: Climb & conventional milling enhancing tool life & machine performance. (n.d.), 48(888).

## 2.4 CUTTING FORCE IN END MILLING

Cutting force is very important in machining process and it is crucial in the choosing of optimal machining parameters. The summation of a definite number of elementary cutting forces that are due to the discrete cutting edges of the tools are determined using the numerical integration force the total cutting forces. There are two types of force model available to obtain the coefficient for cutting force which are orthogonal to oblique cutting transformation cutting method and direct calibration method [10].

The first method is established from the analysis of generic oblique cutting. It uses the shear yield, angle of shear, and angle of friction obtained from the tests. A database will be established using the experimental data and this database will be used to deduce the coefficient of cutting force and the force model. The limitation of this method is that a large number of tests are needed to have enough data in the setup of database. On the other hand, the second method uses a cutter and workpiece combination to determine the coefficient directly from the milling tests. The limitation of this method is that there is always a deviation in the predicted value for the cutting force at the maximum and minimum when compared to the measured values. The average thickness of the chip is very different from the instantaneous thickness of the chip [10].

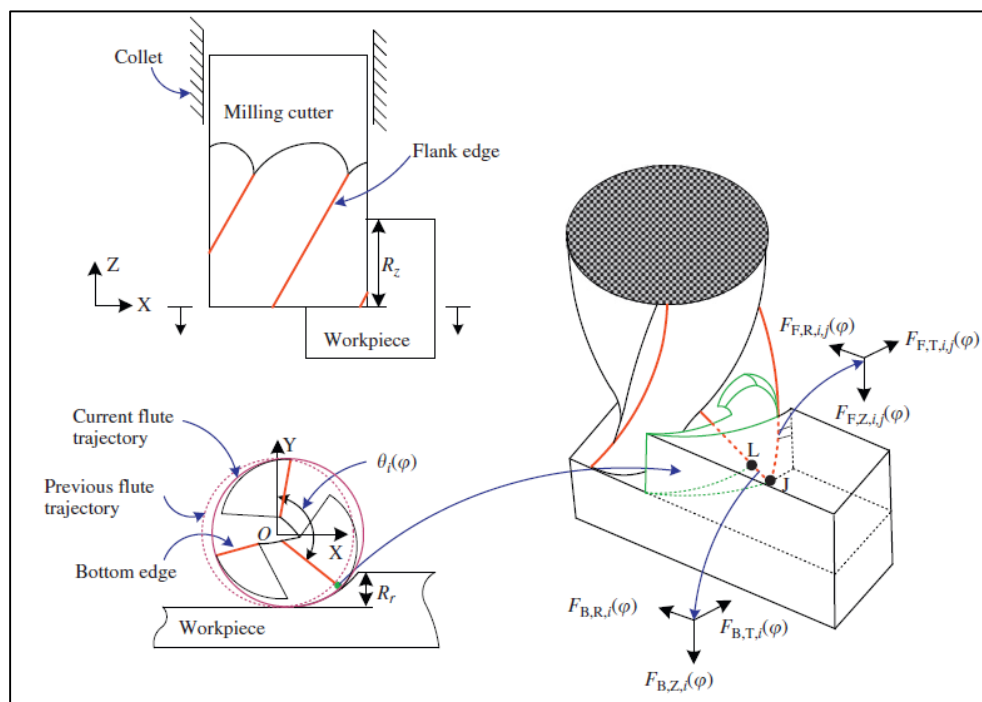


**Figure 2.2:** Milling process [10]

Source: Cutting force modeling for flat end milling including bottom edge cutting effect.

Figure 2.2 shows the end milling operation by a flat end mill. It can be seen from the figure that the flank edge and the bottom are both engage with the workpiece during the calculation. Therefore the total cutting force is calculated by the summation of force at the flank edge and the force at the bottom edge. The total applied cutting force can be considered as:

$$F = F_F + F_B \quad (2.1)$$

The force components are illustrated in the figure 2.2 above [10].

#### 2.4.1 Calculations of $F_F$

The available cutting area of the tool cutter is separated into N different element that symbolize the cutting length same as tool axis direction. As an example, we will split the cutting part into 5 discrete parts during the milling process with the cutting depth at 5mm, the length of each individual cutting element will be 1mm. Forces exerted on the jth axial cutting discrete element of the ith flute at the  $\omega$  are as following [10]:

$$\mathbf{F}_{F,i,j} = \begin{bmatrix} F_{F,T,i,j}(\omega) \\ F_{F,R,i,j}(\omega) \\ F_{F,Z,i,j}(\omega) \end{bmatrix} = \begin{bmatrix} [g_{F,i,j}(\omega)]C_{F,T,i,j} \\ [g_{F,i,j}(\omega)]C_{F,R,i,j} \\ [g_{F,i,j}(\omega)]C_{F,Z,i,j} \end{bmatrix} h_{F,i,j} W_{F,i,j}(\omega) \quad (2.2)$$

The axial length of discrete part is represents as  $W_{F,i,j}(\omega)$ .

The  $[g_{F,i,j}(\omega)]C_{F,p,i,j}$  ( $p = T,R,Z$ ) has been shorten to  $C_{F,p,i,j}$  for convenience. They are shown as an exponential functions to show the effect of size.



$$C_{F,T,i,j} = c_T [g_{F,i,j}(\omega)]^{m_T} \quad (2.3)$$

$$C_{F,R,i,j} = c_R [g(\omega)]^{m_R} \quad (2.4)$$

$$C_{F,Z,i,j} = c_Z [g_{F,i,j}(\omega)]^{m_Z} \quad (2.5)$$

The tangential, axial, and rotational forces will be able to change into x-direction, y-direction, and z-direction by

$$[F_{F,X,i,j}(\omega) \quad F_{F,Y,i,j}(\omega) \quad F_{F,Z,i,j}(\omega)]^T = \mathbf{T}_{F,i,j}(\omega) \mathbf{F}_{F,i,j} \quad (2.6)$$

Where,

$$\mathbf{T}_{F,i,j}(\omega) = \begin{bmatrix} -\cos\theta_{i,j}(\omega) & -\sin\theta_{i,j}(\omega) & 0 \\ \sin\theta_{i,j}(\omega) & -\cos\theta_{i,j}(\omega) & 0 \\ 0 & 0 & 1 \end{bmatrix} \quad (2.7)$$

The overall forces that acts on the *i*th edge during cutting can be written as:

$$[F_{F,X,i}(\omega) \quad F_{F,Y,i}(\omega) \quad F_{F,Z,i}(\omega)]^T = [\sum_j F_{F,X,i,j}(\omega) \quad \sum_j F_{F,Y,i,j}(\omega) \quad \sum_j F_{F,Z,i,j}(\omega)]^T \quad (2.8)$$

#### 2.4.2 Calculations of $\mathbf{F}_b$

This is the cutting force induced at the bottom of the end mill and it is separated into three components which are tangential component, radial component, and axial component. We can treat this force to be a function of linearity of distance of the line connecting L and J as shown in the figure 2.2 above. This  $\overline{LJ}$  line is the width of the uncut chip at the bottom. The cutting force can be obtain as [10]:

$$\mathbf{F}_{B,i} = \begin{bmatrix} F_{B,T,i}(\omega) \\ F_{B,R,i}(\omega) \\ F_{B,Z,i}(\omega) \end{bmatrix} = \begin{bmatrix} C_{B,T}(w_{B,i}(\omega)) \\ C_{B,R}(w_{B,i}(\omega)) \\ C_{B,Z}(w_{B,i}(\omega)) \end{bmatrix} w_{B,i}(\omega) \quad (2.9)$$

The  $w_{B,i}(\omega)$  is the length of  $\bar{LJ}$  and is almost same as the  $h_{F,i,1}(\omega)$ . The  $C_{B,q}(w_{B,i}(\omega))$  is shorten as  $C_{B,q}$  in the following content for the purpose of simplicity.

The forces in the x-direction, y-direction and z-direction exerted on the  $i$ th bottom edge can be acquired by

$$[F_{B,X,i}(\omega) \quad F_{B,Y,i}(\omega) \quad F_{B,Z,i}(\omega)]^T = \mathbf{T}_{B,i}(\omega) \mathbf{F}_{B,i} \quad (2.10)$$

Where

$$\mathbf{T}_{B,i}(\omega) = \begin{bmatrix} -\cos\theta_i(\omega) & -\sin\theta_i(\omega) & 0 \\ \sin\theta_i(\omega) & -\cos\theta_i(\omega) & 0 \\ 0 & 0 & 1 \end{bmatrix} \quad (2.11)$$

$\theta_i(\omega)$  is almost same as the  $\theta_{i,1}(\omega)$ .

By summing all the cutting forces caused by the cutter's flank edge and cutter's bottom edge, we will be able to get the total force component in x-direction, y-direction, and z-direction that acts on the tool cutter at any rotation angle  $\omega$ .

$$F_s(\omega) = \sum_{i=1}^{N_f} [F_{F,s,i}(\omega) + F_{B,s,i}(\omega)] \quad s = X, Y, Z \quad (2.12)$$

## 2.5 CUTTING PARAMETERS IN MILLING PROCESS

The parameters in milling process play an important role for determining the quality of milling products. The different parameters such as spindle speed, incline angle, feed rate, cutter diameter, depth of cut, feed per tooth, and other parameters will affect

the outcome of milling process. There are many researches have been done to determine the optimal parameters for milling process. A few of the researches done are being studied and reviewed in the following paragraphs to show their results and conclusions.

First of all, the milling parameters for aluminum alloy 6082 has been researched by K. Siva Kumar and Bathina Sreenivasulu. Their aim was to determine the optimal parameters for the milling operation of aluminum alloy. The Taguchi technique and ANOVA analysis using MINITAB software to understand the relationship between the parameters and the result of experiment [11].

In their study, it has been shown that the surface roughness will increase when the depth of cut is increased, but the increase in the feed will reduce the surface roughness. The depth of cut is the main influencing parameter when compared to the speed and feed. The material removal rate will increase when the feed is increased but the material removal rate will reduce when we increase the cutting depth. The depth of cut is the parameter that will influence the material removal rate more than the speed and feed [11].

Furthermore, the milling process parameters for stainless steel AISI 304 to improve its surface finish has been studied by Ahmad Hamdan, Ahmed A. D. Sarhan and Mohd Hamdi. The main objective of this research was to determine the best combination of different parameters to achieve the best appearance for the milled surface and reduced force needed during the operation. The results from the experiments are analyzed using the Taguchi technique and Pareto ANOVA.

Figure 2.3 and figure 2.4 show the signal to noise ratio for cutting force and surface roughness. The result shows that there is one parameter which is feed rate that will has a more significant effect followed by the cutting speed and depth of cut. The lubrication mode does not shows any statistically significant. These parameters were

tested with the optimal level of value and it has generated a result of 25.5% reduction in the machining force and 41.3% better surface finish [12].

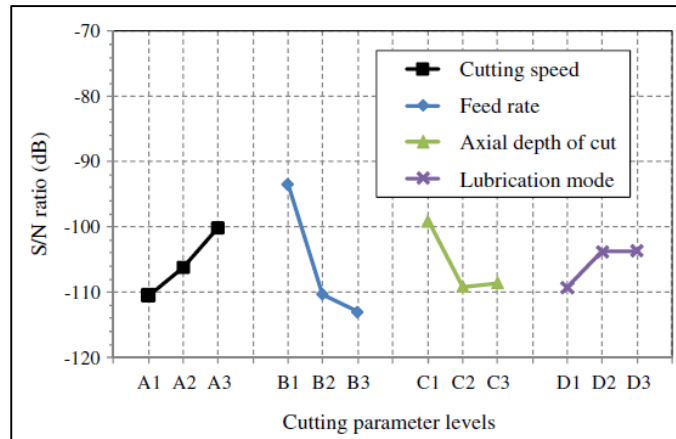


**Figure 2.3:** Graph for cutting force [12]

Source: An optimization method of the machining parameters in high-speed machining of stainless steel using coated carbide tool for best surface finish.

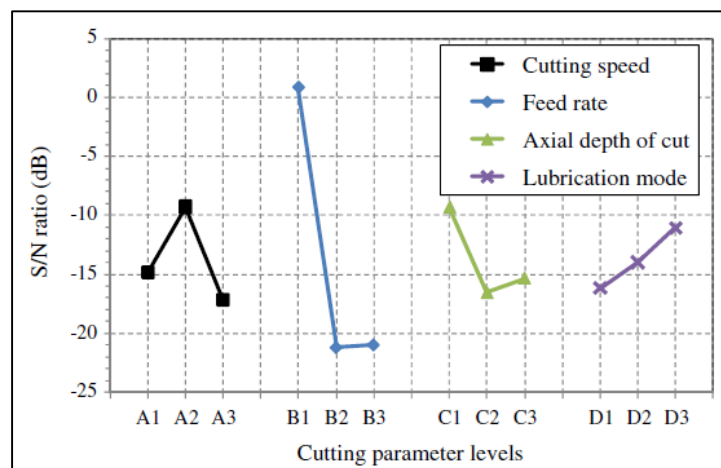


**Figure 2.4:** Graph for surface roughness [12]

Source: An optimization method of the machining parameters in high-speed machining of stainless steel using coated carbide tool for best surface finish.

Besides that, the process parameters for Ti-6Al-4V have been studied by Vijay S and Krishnaraj V to reduce the cutting force and improve the surface finish of the machined product. The parameters like depth of cut, speed and feed are being considered in this research. The Taguchi method and ANOVA are used in this research to help in find the improved parameters setting.

**Table 2.1:** ANOVA for surface roughness

Source	DOF	SS	P Value	% Contribution
F(mm)	3	108049	0.122	27.48
CS (m/min)	3	17356	0.715	4.41
DOC (mm)	3	193728	0.041	49.27
Error	6	74007	-	18.82
Total	15	393141	-	99.98

Source: Machining Parameters Optimization in End Milling of Ti-6Al-4V.

**Table 2.2:** ANOVA for surface roughness

Source	DOF	SS	P Value	% Contribution
F(mm)	3	5.7131	0.047	52.20
CS (m/min)	3	1.0243	0.504	9.35
DOC (mm)	3	1.8707	0.285	17.09
Error	6	2.3358	-	21.34
Total	15	10.9438	-	99.98

Source: Machining Parameters Optimization in End Milling of Ti-6Al-4V.

According to the ANOVA result in table 2.1, this research has concluded that the depth of cut is most influencing in the surface roughness of the product followed by the influence of feed per tooth then cutting speed. According to the ANOVA result in table 2.2, the surface roughness is influenced the most by the feed per tooth and then followed by the depth of cut then cutting speed [13].

## 2.6 WEAR MECHANISM OF END MILL

During the milling process, the temperature at the contact zone between the cutter and the workpiece will increase significantly when the cutting speed is increased. This may cause the temperature to exceed the thermal stability limit of cutter material. This can cause a drastic drop in the tool life of the cutter.

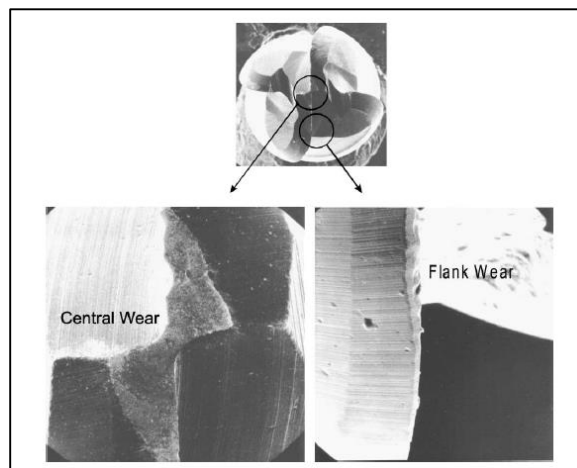


**Figure 2.5:** Central wear and flank wear [2]

Source: Wear mechanisms of cutting tools in high-speed cutting processes.

Figure 2.5 shows the most common tool wear which are central wear and flank wear. The flank wear occurs at the cutting edge of the cutter while the central wear occurs at the center of the cutter. When the feed velocity is too low, a buildup edge burr will occur and this will change the geometry of the tool tip. This can adversely affect the useful life of the cutter and the surface finish of the product. In contrast, when the feed velocity is high enough, the flank wear will be dominant. It will be significant at the beginning of the milling and stabilized after some time [2].

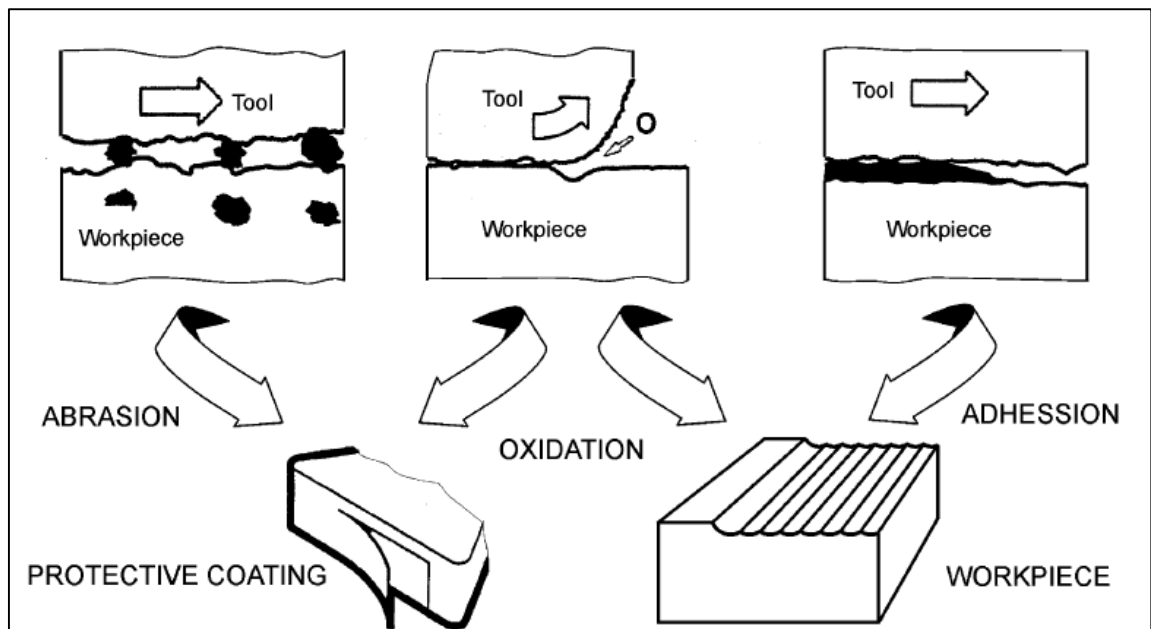


**Figure 2.6:** Schematic illustration of tool wear [2]

Source: Wear mechanisms of cutting tools in high-speed cutting processes.

Figure 2.6 shows the illustration of wear mechanism for a coated end mill. The tool wear mechanism is commonly a result of mechanical interaction and chemical interaction between the cutter and the workpiece. The thermo-dynamic wear can be

caused by thermally loaded motion such as abrasion with workpiece and adhesion of cutter coating. Besides that, the thermos-chemical wear due to the chemical processes at elevated temperature are diffusion and oxidation. The thermos-chemical becomes more evident under high speed milling operation as the cutting edge heated up to enhance the oxidation and diffusion [2].

During the cutting process, the hard oxide particles from end mill coating will rub against the hard inclusion in the workpiece and this will cause the coating of the end mill to be peeled off by abrasion. The abrasion process will become severe after the coating has been removed from the end mill. There is also a strong adhesive force existed between the flank edge of the end mill and the surface of the workpiece. This adhesion can cause a significant wear on the cutting edge of the end mill [2].

Besides that, according to the research done by W.Y.H. Liew and X. Ding in the paper “Wear progression of carbide tool in low-speed end milling of stainless steel”, the increment of cutting speed from 25 meter per minute to 50 meter per minute on modified AISI 420 stainless steel has no effect on the tool wear but the increment in the hardness of the workpiece will reduce the tool life of end mill. There is also a wear mechanism called attrition wear which will occur when the cutting speed is too slow and the buildup edge is formed. This build up edge will cause the carbon particles on the end mill to be removed and left behind empty cavities [14].

The end mill will form a crack when the protective coating on it has been removed as it is less resistant to the cracking. An impact or collision between the end mill and workpiece may also cause a crack on the tool. This crack will normally spread along the direction of cutting edge. This crack can make the edge of end mill to be weaker and more susceptible to chipping. The fracture will also occur at the location of crack and it will grow and merge with other fracture to become a large fracture surface or catastrophic



failure. The figure 2.7 shows the illustration of chipping/fracture and catastrophic fracture on an end mill [14].

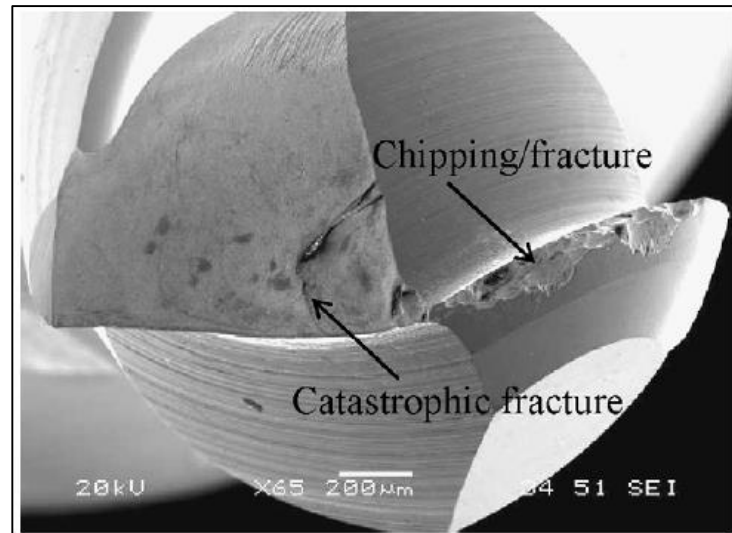


**Figure 2.7:** Chipping and catastrophic fracture on end mill [14]

Source: Wear progression of carbide tool in low-speed end milling of stainless steel.

In their research, they also found out that the use of cutting fluid is very efficient in extending the tool life when cutting the modified AISI 420 stainless steel. The coolant is able to reduce the adhesive force between the cutter and the workpiece and improves its surface finish. The cutting fluid acts as a coolant when it is under high speed cutting and it behaves as a lubricant in low speed cutting. Its effectiveness in increasing the tool life is due to the lubricating at the cutting interface [14].

## 2.7 REMAINING USEFUL LIFE (RUL)

The remaining useful life is defined as how long the asset will be in a good service condition until it becomes unusable. The useful life may be affected by many variables such as the frequency of use, the using condition, maintenance measure, and other variables. The figure 2.8 below shows a simple representation of the remaining useful life concept for an asset.

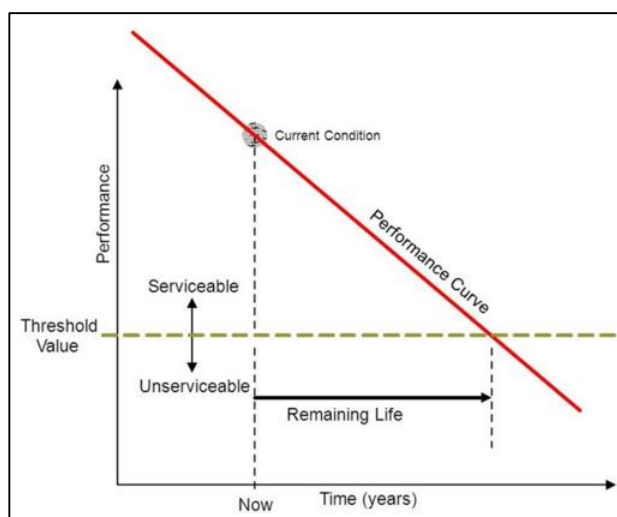


**Figure 2.8:** Concept illustration of remaining life of an asset

In the figure 2.8, it is assumed that the performance of an asset will deteriorate in a straight line, but in actual life it will follow a curved line deterioration. The asset will deteriorate faster when it is reaching the end of its physical life. The threshold value is the point for us to judge whether the asset is still serviceable or not. The time for the asset to have its performance to deteriorate from current level to the threshold value is the remaining useful life of the asset.

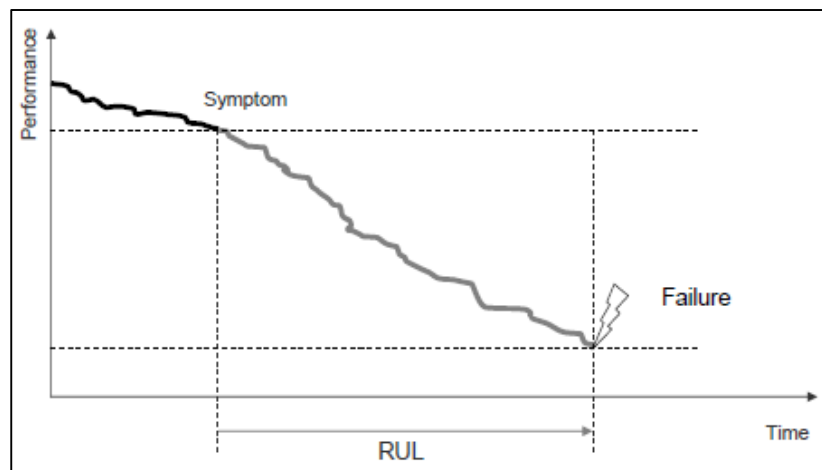


**Figure 2.9:** Remaining useful life (RUL) [5]

Source: Health assessment and life prediction of cutting tools based on support vector regression.

The figure 2.9 shows the remaining useful life (RUL) of a cutter tool. The symptom is the point where we started to monitor the wear of the cutter and predict its remaining service life. The failure point is where the cutter has reached its maximum useful life and failed catastrophically. The negative gradient of the graph shows that the performance of the cutter deteriorates follow the time. The length of time between the times we selected the symptom of tool wear until its catastrophic failure is called the remaining useful life (RUL).

The prediction of remaining useful life is very important as it can be taken as a measure to prevent wastage. The available remaining tool life of the cutter can be fully utilized before it is replaced. It also assists in the reduction of surface quality problem and dimension accuracy problem of the workpiece which can be caused by using a worn out cutter. Therefore, the RUL prediction should has the capability to estimate the best timing

for a tool change where most of the tool life has been utilized, but before it reached the failure condition. This allows us to change the cutter conveniently [3].

## **2.8 TOOL CUTTER CONDITION MONITORING**

The Condition Monitoring System (CMS) is able to monitor the real condition of the tool and the process. It may not be able to indicate the problem in early stage, but it is needed to control and carry out correction decision, such as stop the process for the moment, update the process parameters, or ask for human interception. This system has the potential to make our machining system more robust and reliable [15].

The purpose of the condition monitoring is to detect any abnormality in the machining process and the wear pattern of the machine component. The machining process interacts with the elastic structure of a cutting tool forms the machining system. The cutting tool interacts with the workpiece to create the cutting forces.

The wear pattern of a tool has been researched widely from the past with the focus on the wear detection, remaining useful life prediction, and the timing of the tool fracture or breakage. The techniques used were with the help of sensor or without the present of a sensor. The sensor based tool condition monitoring (TCM) are normally based on the cutting force measured using the rotating dynamometer or the multi-channel table type dynamometer, vibration signal using a multi-channel accelerometer, audible sound from the machining process, and the high frequency emission of sound using the acoustic emission sensor. On the other hand, the sensor free monitoring system uses the internal drive signal such as the spindle motor current, spindle motor power, and feed motor current. The measurement may combine the different kind of quantities unit [15].

However, the use of external sensor will not be always practical because it will make the system becomes more complicated. Different types of sensors will be mounted on the machines near the machining area and all these sensors will experience the heat, coolant, and chips from the machining process. This may shorten the service life of the sensors and affect the accuracy of the measurements. These sensors also need extra cost for maintenance and calibration to make sure that they are functioning properly [15].

The wiring of the sensors is another issue that must be considered especially in more advanced machining operations. External sensors also require additional maintenance and calibration in order to function properly [15].

## **2.9 PREDICTION METHOD**

The estimation for tool life commonly can be performed using a method called prognostics and health management (PHM). This PHM method is able to cut down the cost for maintenance, increase the machine availability and come up with a better maintenance plan. PHM is better than the predetermined maintenance schedule by determining the best timing for a maintenance work to be undergone. This is important as the operating costs will be raised if we perform a premature maintenance, but a late maintenance may even bring in more damage not only in term of costs but also the danger to the employees safety. The main objective of this system is to detect the upcoming failure fast enough to take preventive measures.

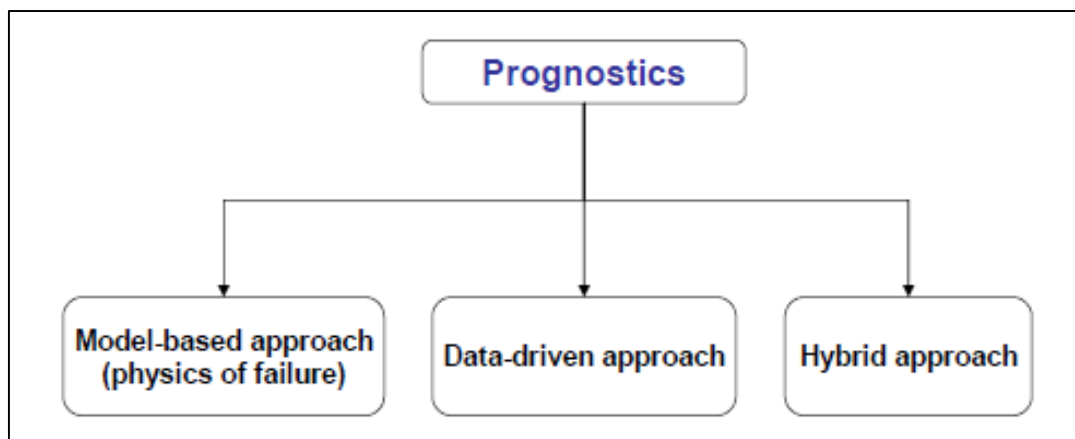


Figure 2.10: Prognostics approach [5]

Source: Health assessment and life prediction of cutting tools based on support vector regression.

The figure 2.10 shows the approaches under the prognostics method. It is classified into model based approach, data-driven approach, and hybrid approach. The focus of this project will be on the data-driven- approach.

### 2.9.1 Artificial Neural Network (ANN)

Artificial Neural Network is one of the available data-driven approach to estimate the remaining useful life. According to the research done by Amit Kumar Jain and Bhupesh Kumar Lad in “Predicting Remaining Useful Life of High Speed Milling Cutters based on Artificial Neural Network”, they have used an ANN network to estimate the remaining tool life in a high speed milling operation. The machine used was a high speed milling machine and the ball nose end mill was made with tungsten carbide to mill on a stainless steel workpiece. The data used for analysis was force signal from a dynamometer

in the feed direction. There were 315 cutting process with a distance of 27.2m before the flank wear was measured [3].

Table 2.3: Important statistical features [3]

S.No	Important Statistical Features
1	Average force
2	Standard deviation
3	Skewness
4	Kurtosis
5	Maximum force level
6	Total Amplitude of Cutting Force
7	Root mean squared

Source: Predicting remaining useful life of high speed milling cutters based on Artificial Neural Network

The table 2.3 shows the statistical features that can be collected from the cutting force signal. The stepwise regression will be used to select the most relevant features among this seven features for a best correlation. This is because the computational performance will become insufficient for us to develop the correlation model if we included too many features. The signal number 1, 2, 5 and 7 are selected to build the correlation model due to their prominent influence [3].

The figure 2.11 shows the basic architecture of ANN. This network is suitable to predict the remaining useful tool life due to its nonlinear characteristics, easy to adapt, and is capable to approximate the arbitrary function. This network consists of three layers which are the input layer, hidden layer and the output layer. The network tool box in the MATLAB is used to train the ANN model. There was two sets of data prepared for the training and validating of the model to prevent over fitting problem. The training process

will stop when there is a rising in the Mean Square Error (MSE) of the validating data set. The set up that gives us the lowest error percentage will be the best model use to predict the RUL [3].

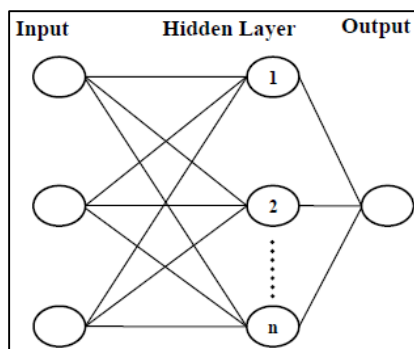


**Figure 2.11:** ANN architecture [3]

Source: Predicting remaining useful life of high speed milling cutters based on Artificial Neural Network

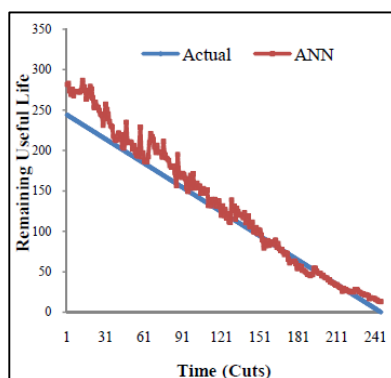


**Figure 2.12:** ANN output graph [3]

Source: Predicting remaining useful life of high speed milling cutters based on Artificial Neural Network



The output of the ANN model is shown at the figure 2.12. The ANN model gives a prediction life which is very similar to the actual remaining useful life. There is over prediction at the beginning of the early stage, but this favorable as the cutter is still new and no immediate actions need to be taken yet. When it is approaching to the end of the service life, the prediction life becomes more accurate. This is very suitable for us to predict the failure of tool cutter early enough. Therefore, it is concluded that ANN is a very suitable approach to predict the remaining useful life of a tool cutter [3].

### **2.9.2 Support Vector Regression (SVR)**

The Support Regression Vector (SVR) technique has been studied by T. Benkedjough, Kamal Medjaher, Noureddine Zerhouni and S. Rechak in the research for estimating the remaining useful tool life of an end mill on high speed milling. They have utilized three dynamometer, three accelerometer, and one acoustic emission sensor in the acquisition of signal data. Six end mills are used in the experiment where data from three cutters are used for the training process and three cutters are used for testing process [5].

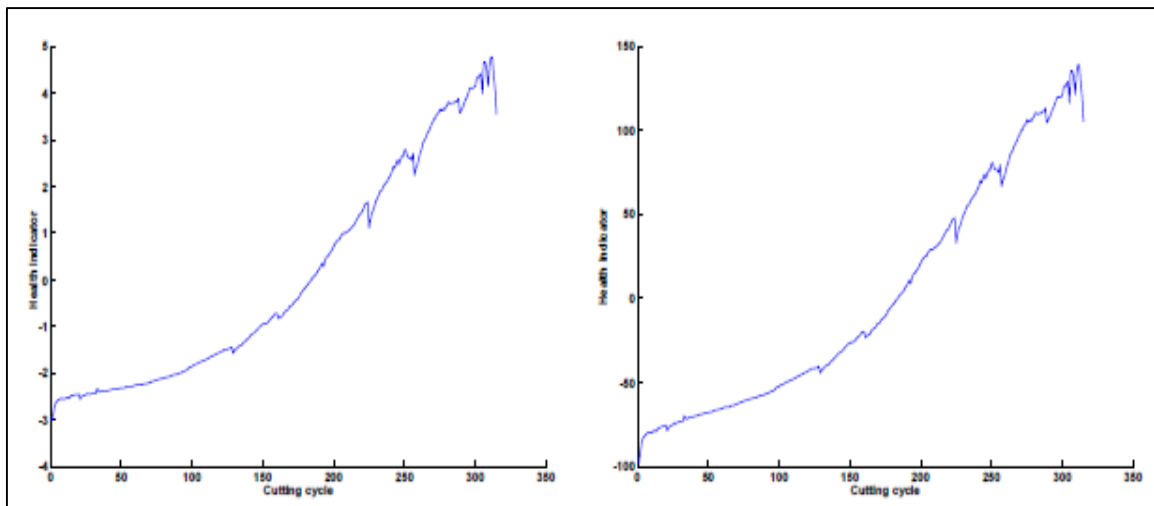


**Figure 2.13:** Health indicator result using EM-PCA (left) and ISOMAP (right) [5]

Source: Health assessment and life prediction of cutting tools based on support vector regression.

The data from the sensors will be fused to have a more suitable and accurate result from the result get from a single sensor. After the fusion, the features will be extracted using the Wavelet Packet Decomposition (WPD) method. The detailed energy coefficient for the signal in the first six level of decomposition is calculated. The higher discrimination of the signal can be retain as the WPD can analyze higher frequency domain of a signal. After this, the features extracted will be reduced. The method used here were two nonlinear reduction method which are EM-PCA and ISOMAP. A trend will be obtained from these reduction methods and the trend is also called as a health indicator. Both of the trends have the same progression but different magnitude. The figure 2.13 shows the health indicators obtained from the reduction techniques [5].

The health indicator will be mapped to the regression model using the technique of support vector regression. Different kernel can be used for the SVR, but the Gaussian kernel will give a lowest learning error. Finally, the regression model will be used in a

power model to estimate the RUL of an end mill. The figure 2.14 shows the prediction result using the SVR model. The blue color line is the real RUL while the red color line is the predicted RUL [5].

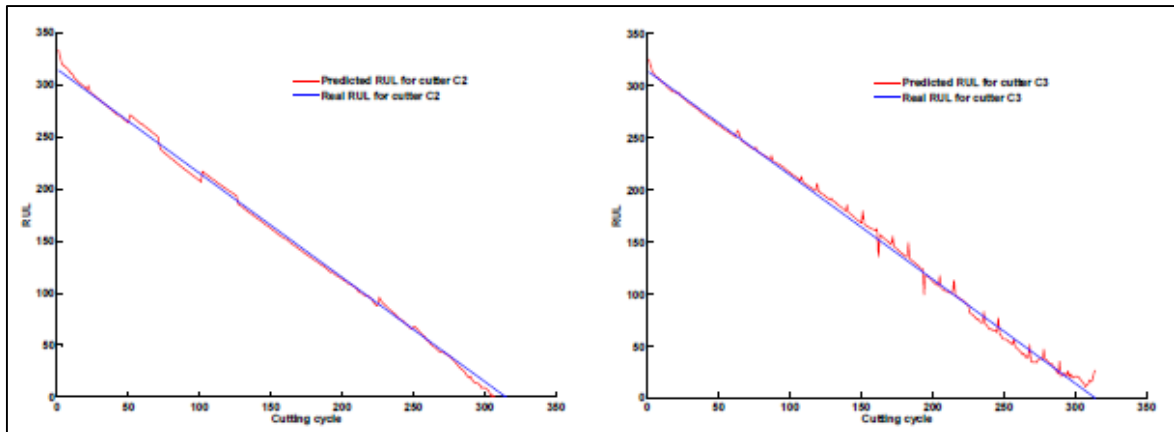


**Figure 2.14:** Result of SVR model [5]

Source: Health assessment and life prediction of cutting tools based on support vector regression.

## 2.10 SUMMARY

According to the literature review, it has shown that the climb milling method is more suitable for the project. The surface finish using this cutting method is very nice and the tool life is longer compared to the conventional milling method. The torque needed is lower so a lower force for cutting needed. The cutting force is very important in machining process and crucial in the choosing of optimal machining parameters. The summation of a definite number of elementary cutting forces that are due to the discrete cutting edges of the tools are determined using the numerical integration force the total

cutting forces. From the review of cutting force, the cutting force can be determined summing the force on the flank edge engage with the workpiece during cutting and the bottom edge force in contact with the workpiece.

Other than that, the cutting parameters have a significant effect on the life according to the studies done by researchers. The cutting force has the most significant on the tool life. Other factors such as feed, depth of cut, usage of cutting fluid, and etc. also will affect the tool life of cutter. The wear mechanism of the tool wear has been reviewed based on the research done. Normally, the wear pattern on the end mill are flank wear and central wear. The wear of the end mill will progress due to the mechanical interaction or chemical interaction between the workpiece and the tool cutter.

Besides that, the definition of remaining useful life of a tool cutter has been discussed according to the definition. The cutter is said to be at the end if its service life when the flank wear has exceeded the threshold value of wear. The tool cutter condition monitoring system is used to monitor the tool life during its service. The monitoring can be online by sensors will be used to monitor the condition of the tool continuously during the operations while the offline method will use the data from the sensors after the operations have finish to monitor the tool condition of the end mill.

Furthermore, the data driven prediction method is believed to be more appropriate for the project following the literature review. This method is easier to conduct and more cost efficient, The Artificial Neural Network (ANN) and Support Vector Machine (SVR) methods have been reviewed and they have shown that the prediction of remaining useful life is accurate using these two methods. These two methods use the data acquired from the sensors to extract the important features and use these features to train the prediction model. The train model will be able to give an accurate result on the prediction which is almost same as the actual remaining useful life.

## **CHAPTER 3**

### **METHODOLOGY**

#### **3.1 INTRODUCTION**

This chapter provides an insight of what will be done in this project and how it will be carried out. A flow chart will be used to show the process flow of the project and the Gantt chart will provide the timeline that this project will follow. The detail methods used in the research project will be explained and specific tool life prediction method to be used is as per the analysis outcome in the literature review of the previous chapter. The prediction method selected in this project was data driven method. Besides that, the equipment and software needed will be introduced and briefly explained in this chapter.

### 3.2 FLOW CHART

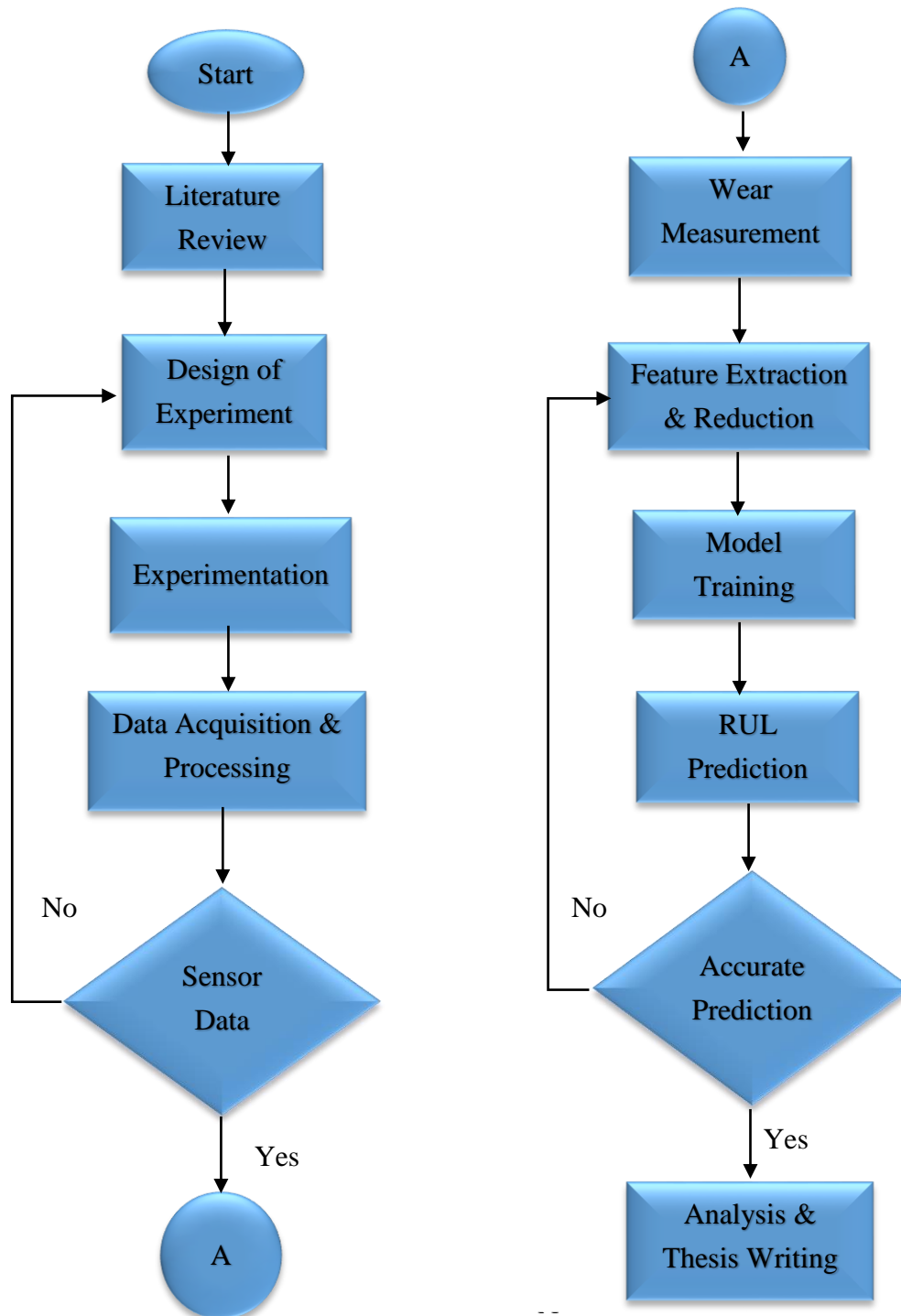


**Figure 3.1:** Flow chart

### 3.3 PROJECT DESCRIPTIONS

The equipment needed for this project was a Haas VF-6 milling machine. One CTPM240 coated carbide insert was selected to use in the experiment. The workpiece material was Uddeholm Stavax ESR stainless steel. Dynamometer was installed on the machine to collect data during the experimental cutting process to track the wear evolution of the cutter. The data from the dynamometer was amplified before fed into the DAQ system of the computer. Seven important statistical features were extracted from the dynamometer data. The features were extracted using the statistical method in MATLAB.

The features will then be reduced stepwise regression. It is a standard procedure to include or remove the elements from a multilinear model according to their importance in the regression model. The features selected through this process were used as input to train the Support Vector Regression model and Artificial Neural Network model. The generated models will predict its RUL. The predicted life was compared with the actual life to know the accuracy of this prediction model.

After the prediction has been done using the SVR model and Artificial Neural Network (ANN) model, the performance was compared against each other to get a best prediction method. Other than that, one more set of SVR model and ANN model was trained using the raw data from Prognostics and Health Management (PHM) Society to compare the performance between the trained model and the existing model.

### 3.3.1 Design of Experiment

The material used in the experiment was cut into the desired workpiece using the wire cut machine. Figure 3.2 shows the raw material before any preparation process. Figure 3.3 shows the cutting process in the wire cut machine and figure 3.4 the surface of the workpiece after the cutting process.



**Figure 3.2:** Raw material

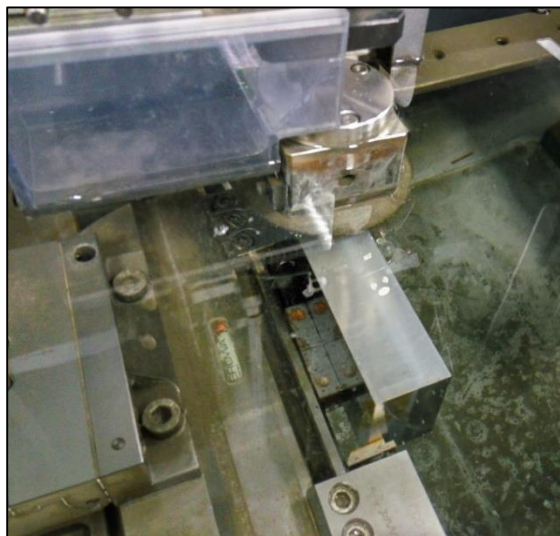


**Figure 3.3:** Wire cutting of material



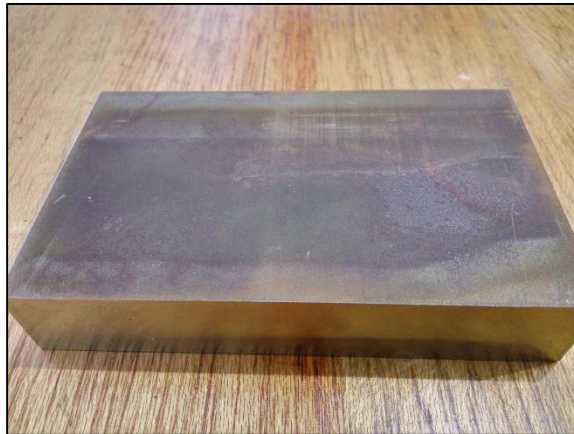


**Figure 3.4:** Material surface after wire cut

As shown in the figure 3.3, the surface finish of the wire cut was in dark color as the cutting was carried out the discharge of electricity between the copper wire and the workpiece to erode the material. The material has undergone a face milling on a Makino KE55 milling machine to remove the hard particles on the surface. Figure 3.5 shows the surface finish of the workpiece after the face milling process.



**Figure 3.5:** Surface finish from face milling process

The main equipment used in this project was the Haas VF-6 milling machine. A Kistler dynamometer was installed on the milling machine table to read the cutting force

on the material. The workpiece was clamped on top of the dynamometer. The dynamometer was connected to the amplifier to amplify its reading to a readable value before sending it to the DAQ system of the computer. Figure 3.6 shows the experiment setup. The dynamometer was mounted on the milling machine and the workpiece was clamped on top of the dynamometer. The dynamometer was connect to a Kistler amplifier before the data was fed into the DAQ system of the computer.

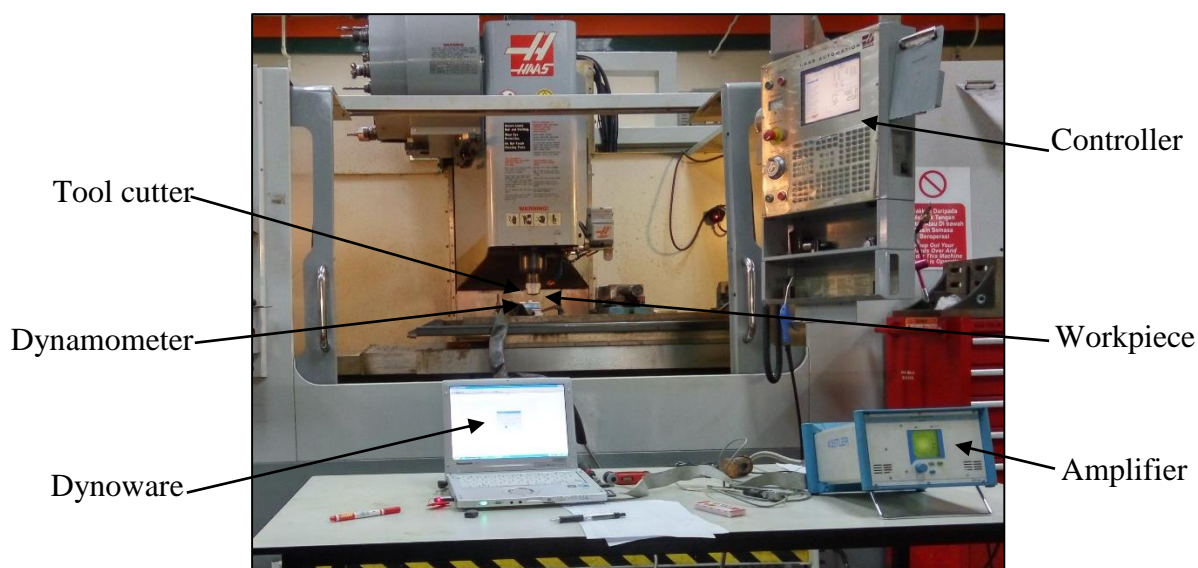


**Figure 3.6:** Experiment setup

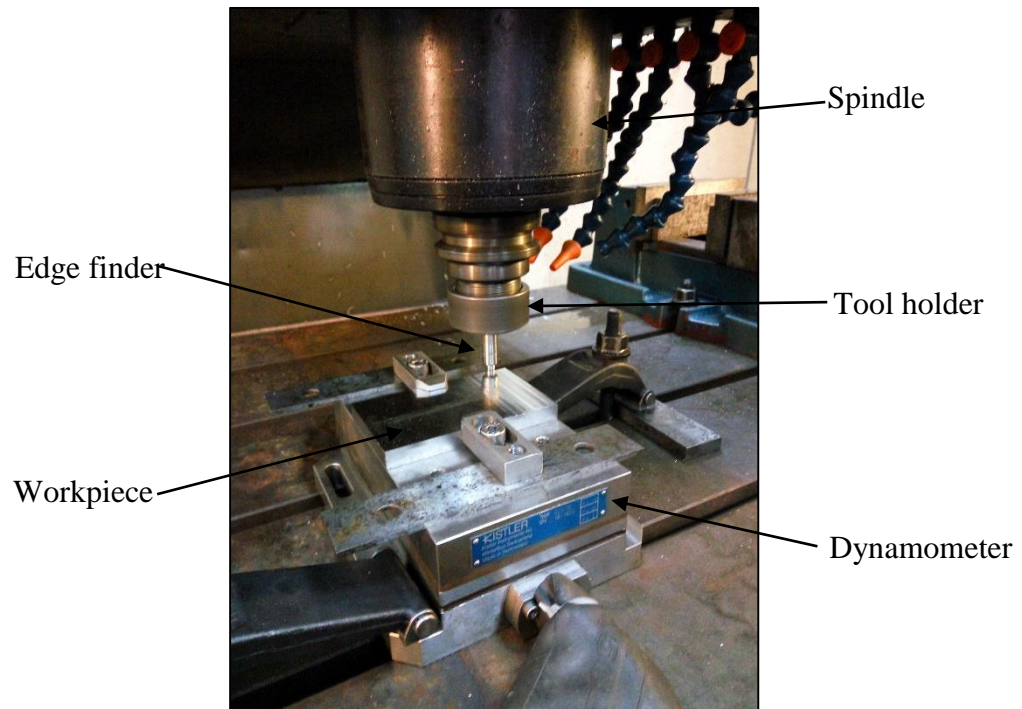


**Figure 3.7:** Edge finding process

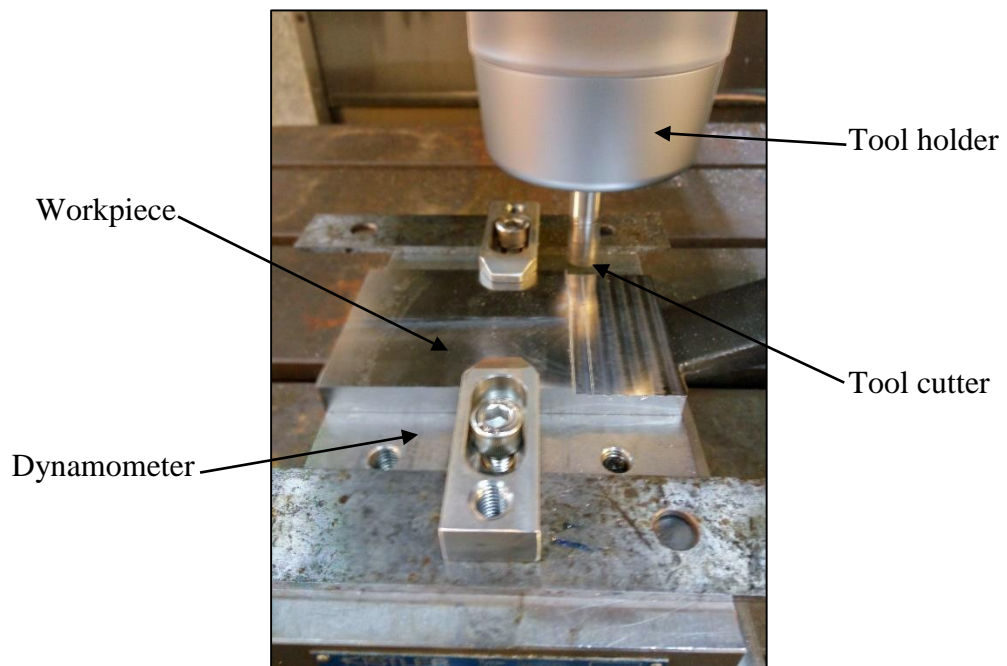


**Figure 3.8:** Cutting process

Figure 3.7 shows the edge finding process on the workpiece. The origin for the x-axis and y-axis will be found in this process and the origin was set at the center of the workpiece. Figure 3.8 shows the cutting process during the experiment. Every time the cutter cut through a distance of 60mm and then will be removed from the tool holder for wear measurement.

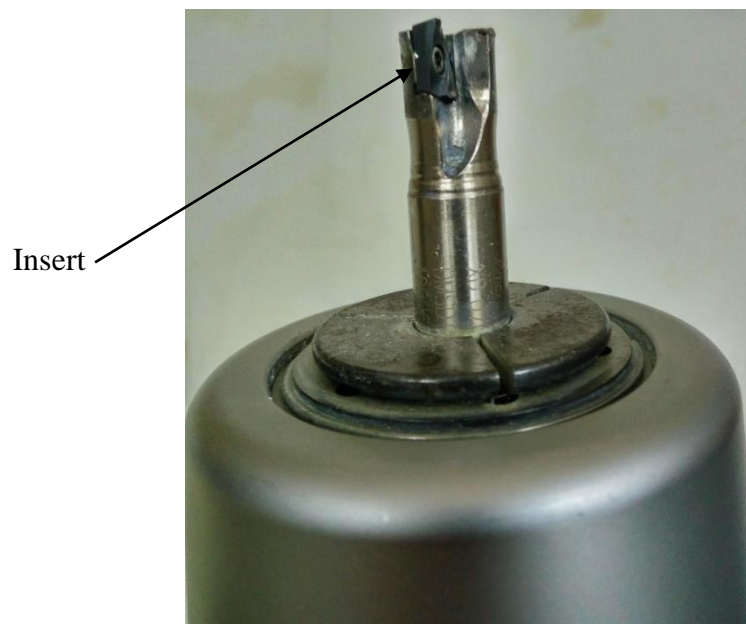


**Figure 3.9:** Tool holder and insert

Figure 3.9 shows the tool used for the experiment. A Ceratizit coated carbide insert was used for the experiment. One single insert was mounted on the tool holder for the cutting process. The cutting speed was set at 170 m/min. The axial depth of cut on the workpiece was 0.1mm and the feed was 0.06mm/tooth. The spindle speed and federate were calculated using the available information. The calculated spindle speed and feed rate were 4509 rpm and 270mm/min respectively.

The dimension of the workpiece was 100mm x 60mm x 10mm. The total cutting length in this project was 60mm x 50 = 3000mm and with a total cutting time of  $13.5s \times 50 = 675s$ . Table 3.1 shows the experiment setting and parameters for this project.

**Table 3.1:** Experiment Setting

<b>Experiment Setting</b>	<b>Value</b>
<b>Cutting speed</b>	170 m/mm
<b>Feed</b>	0.06 mm/tooth
<b>Depth of cut</b>	0.1 mm
<b>Spindle speed</b>	4509 rpm
<b>Feed rate</b>	270 mm/min
<b>Total cutting length</b>	3000 mm
<b>Total cutting time</b>	675 s

### 3.3.2 CAD Program

The G-code for the CNC machining process was created using the Mastercam software and sent to the controller of the milling machine. Figure 3.10 to 3.15 show the steps to generate the tool path program. Figure 3.10 shows the interface of Mastercam Mill X5 software while figure 3.11 shows the stock dimension setup in the software. Moreover, the setting for tool parameters are shown in the figure 3.12 and the tool linking parameters are shown in the figure 3.13.

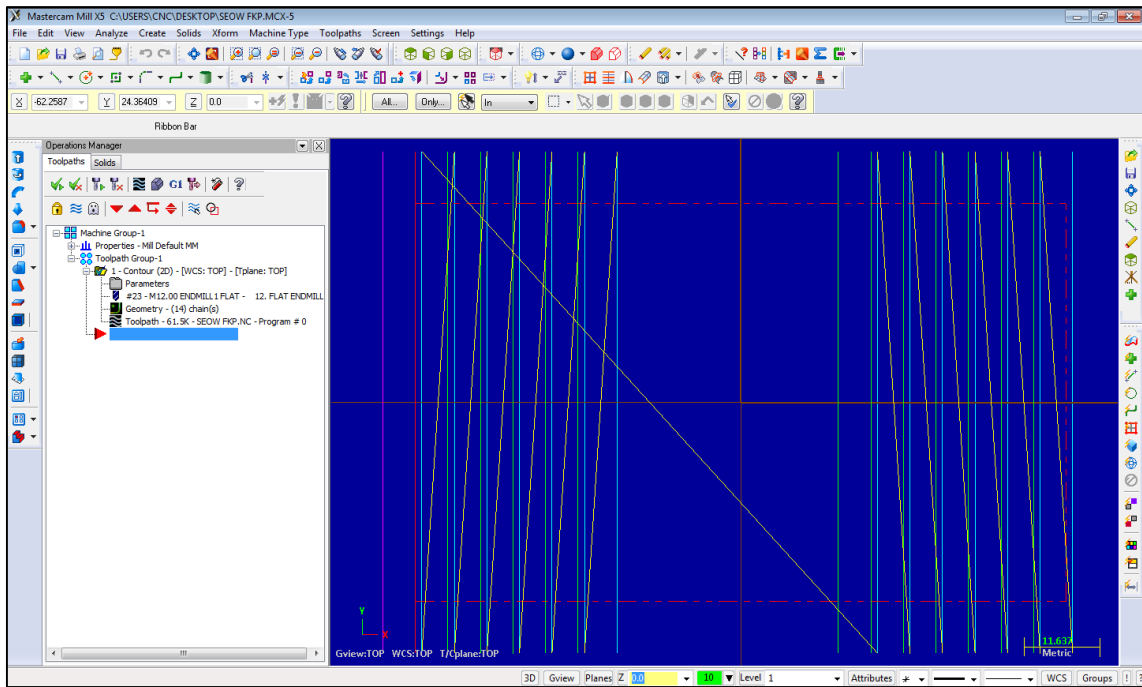


Figure 3.10: Mastercam Mill X5 software

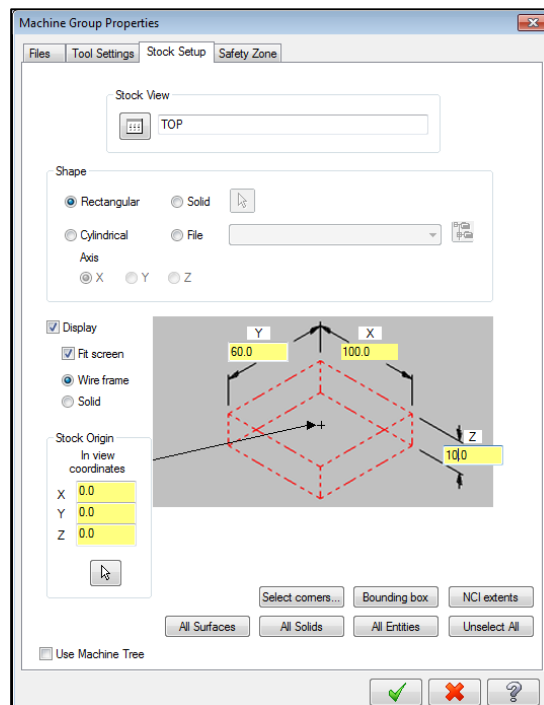


Figure 3.11: Stock dimension setup

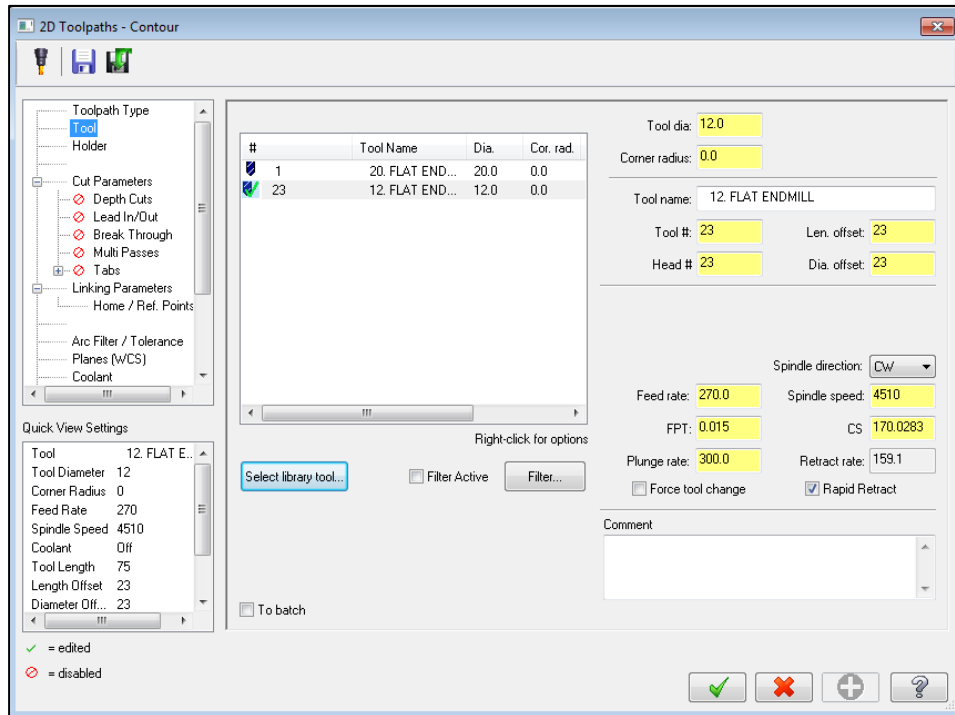


Figure 3.12: Tool parameters

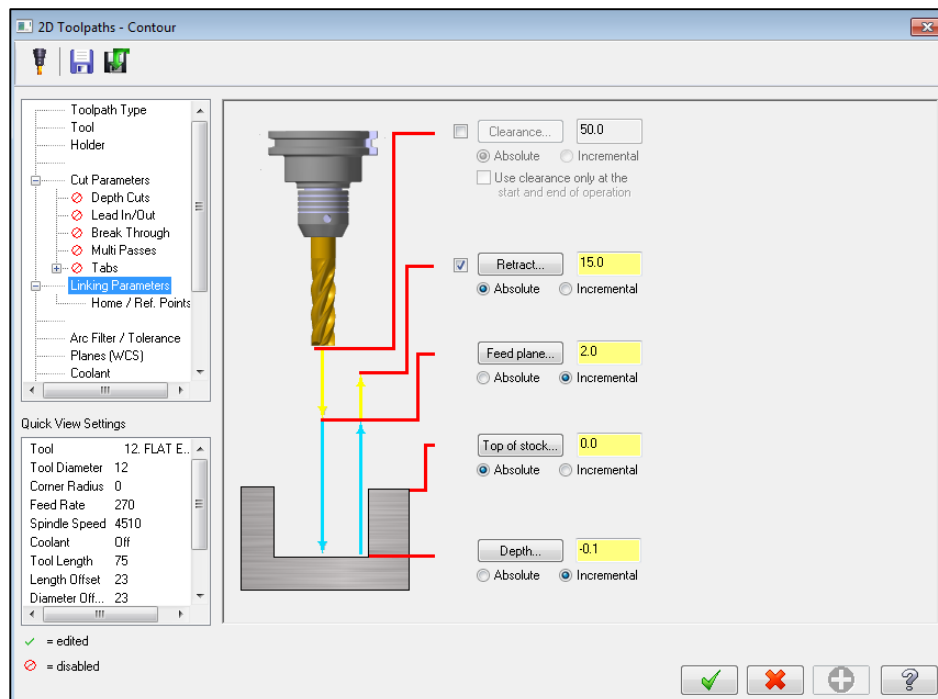
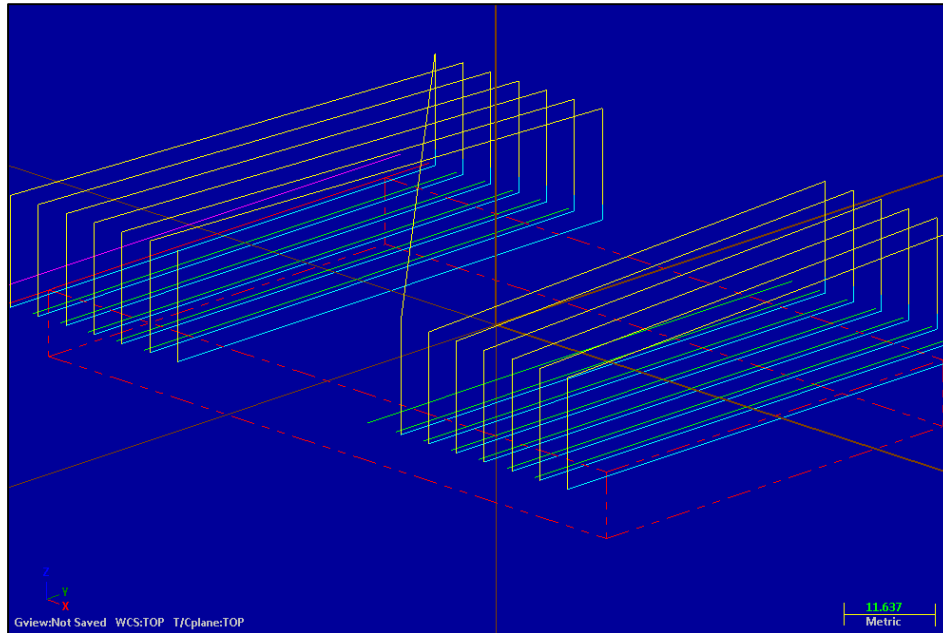
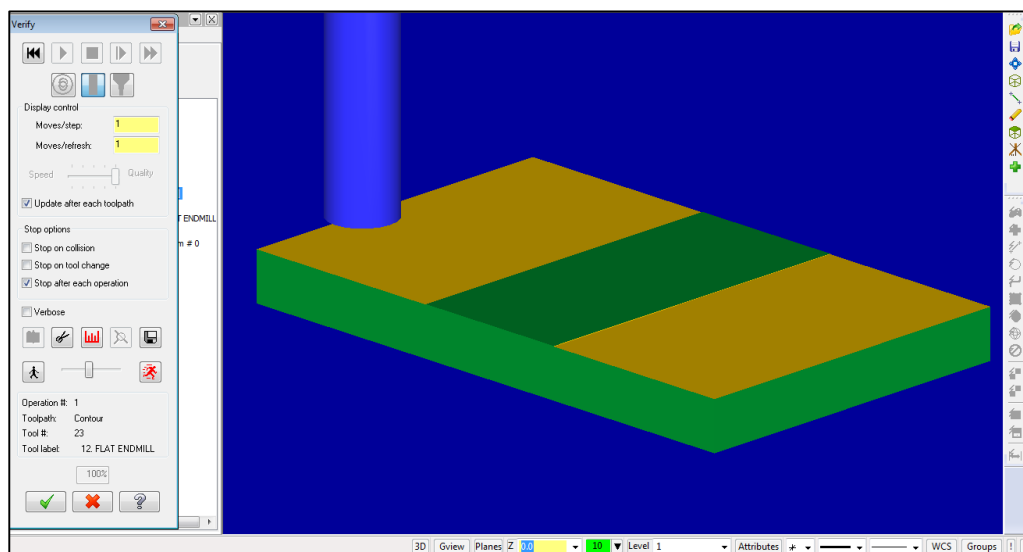


Figure 3.13: Linking parameters

Figure 3.14 shows the tool path design for the experiment while figure 3.15 shows the illustration of full cutting tool path using the software.



**Figure 3.14:** Tool path design



**Figure 3.15:** Tool path illustration



### 3.3.3 Tool Wear Measurement

The end mill insert was removed from the tool holder after every cut to measure its tool wear using an Olympus metallurgical microscope. The magnifying factor used was 10x and the tool wear was measured using the computer software on the photo captured using the camera on the microscope. Figure 3.16 shows the measurement process using the microscope.

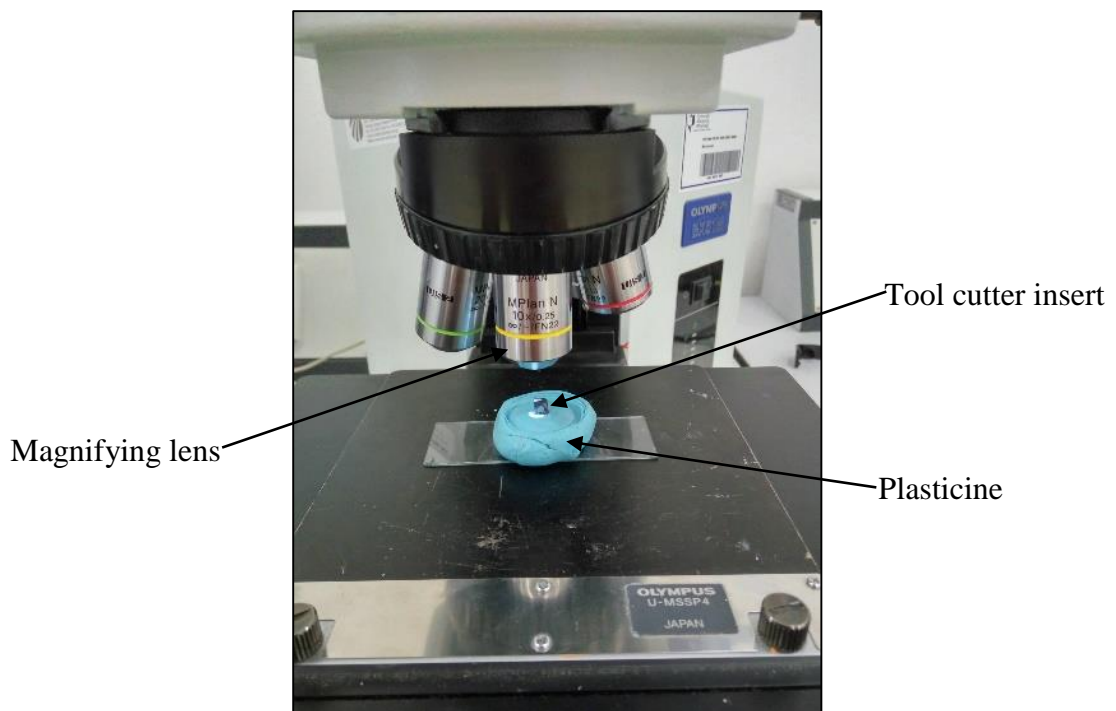


**Figure 3.16:** Tool wear measurement

Figure 3.17 shows the flow chart of procedure to measure the tool wear using the microscope.

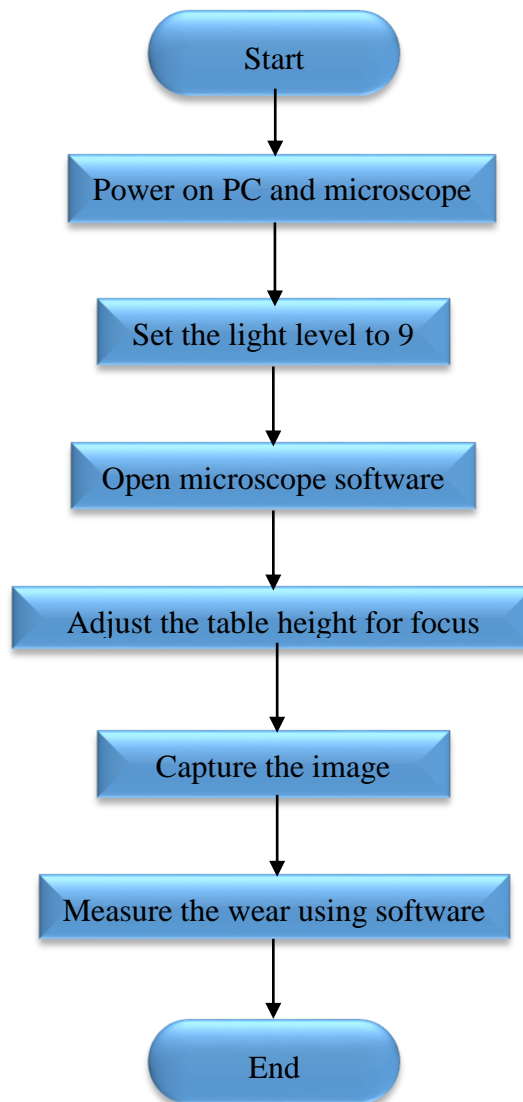


**Figure 3.17:** Tool wear measurement process

Figure 3.18 to 3.24 show the steps to measure the tool wear of the cutter insert. Both the computer and microscope was powered on first and the light level on the microscope was set to 9. The microscope software used to sync both of the equipment was opened and the height of the table was adjusted to show a focused image on the computer screen. The image was captured using the camera on the microscope and the tool wear was measured using the line feature in the software.



**Figure 3.18:** Computer and microscope system



**Figure 3.19:** Light level on microscope

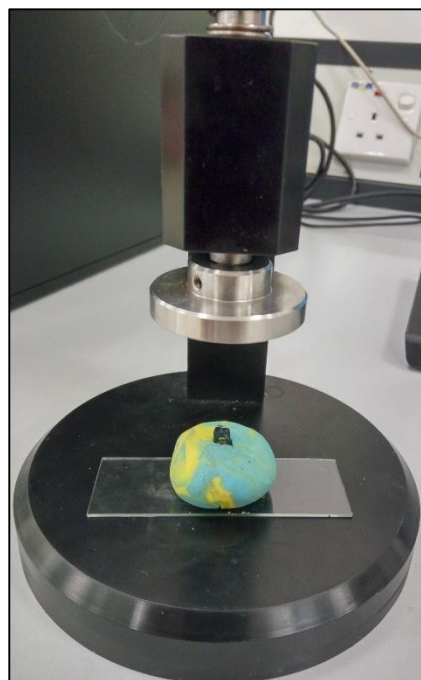


**Figure3.20:** Specimen preparation

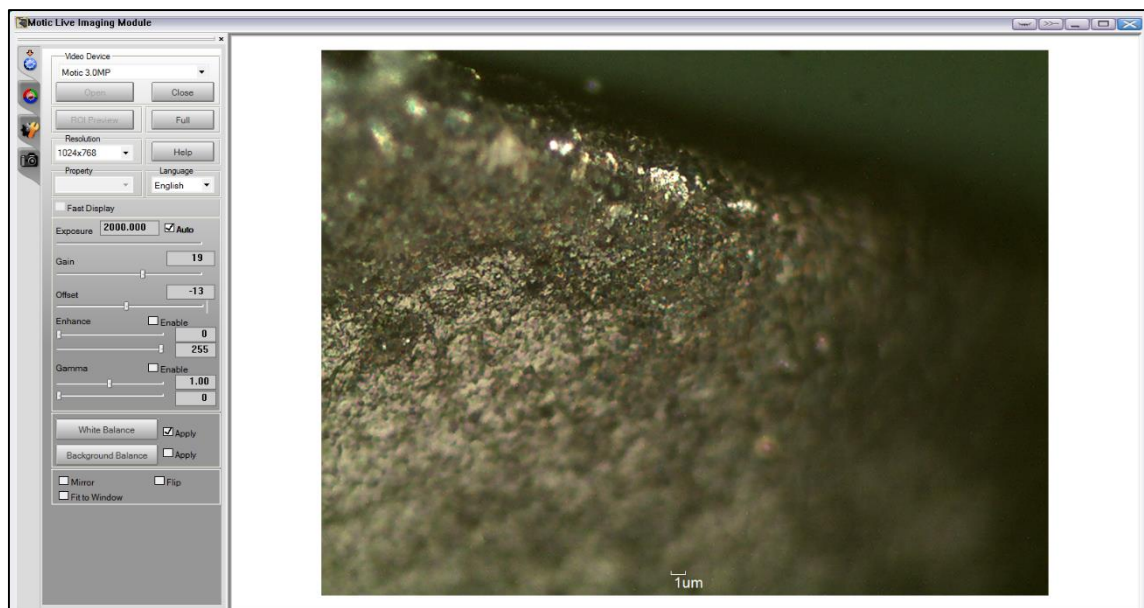


**Figure 3.21:** Microscope software

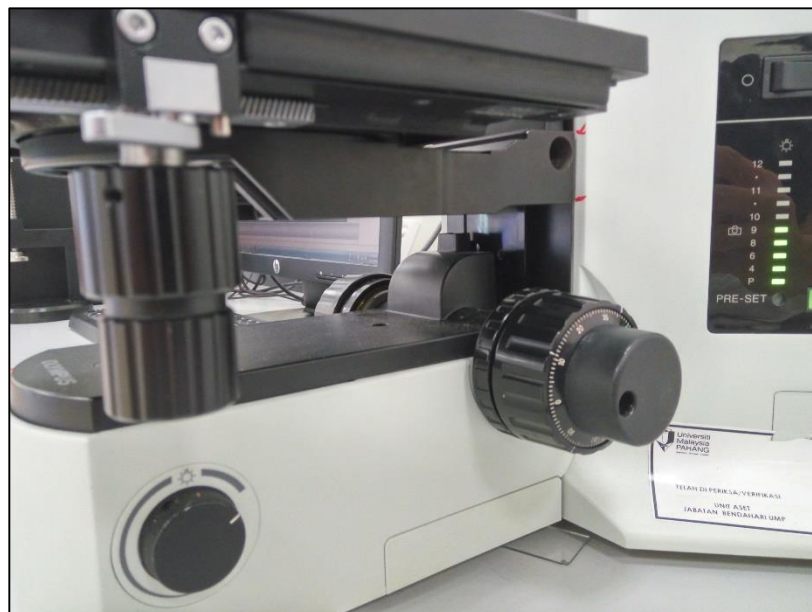


**Figure 3.22:** Table height adjustment

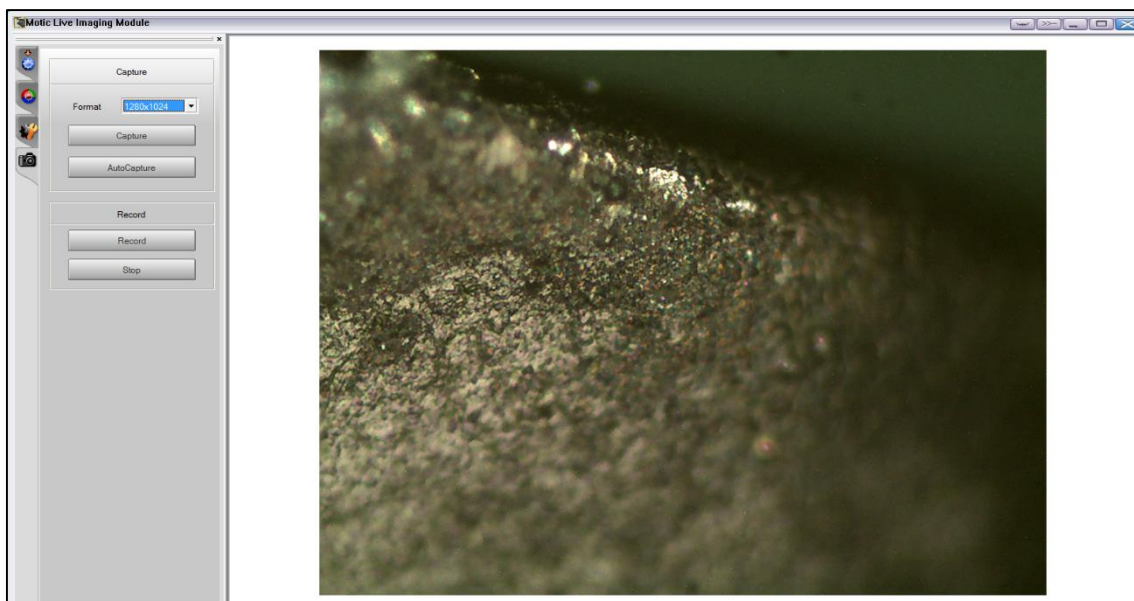


**Figure 3.23:** Image capture

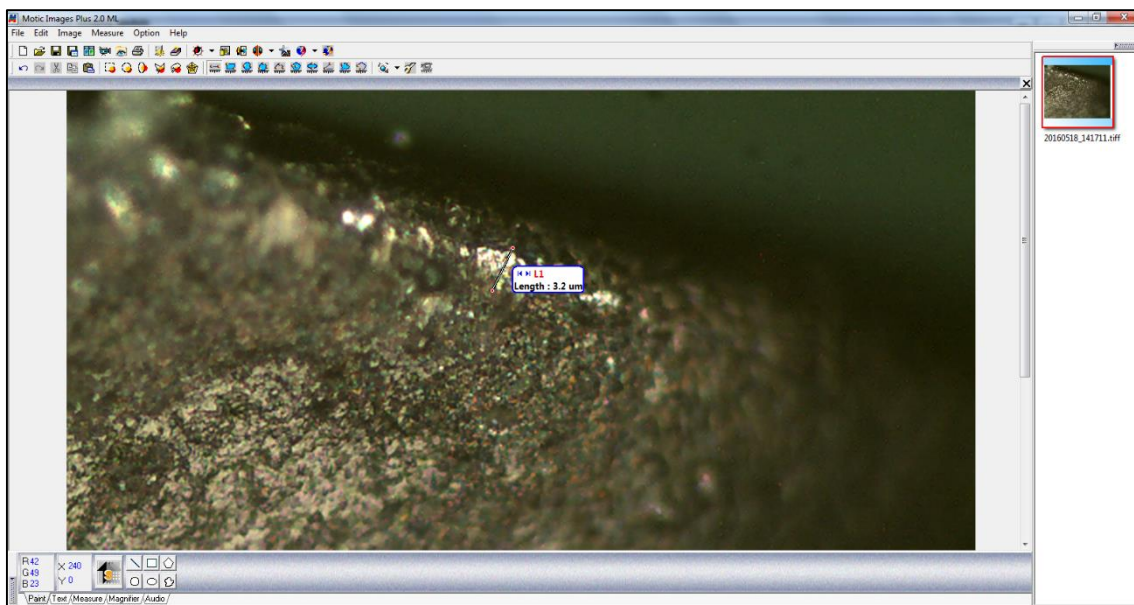


**Figure 3.24:** Wear measurement

### 3.3.4 Signal Acquisition and Processing

Normally the signal from the sensor will be amplified to make it meet the minimum requirement of the equipment. The signal from dynamometer was amplified to the range of  $\pm 5V$  for the maximum load. After that the signal was fed to the DAQ of computer and managed using the Dynoware software on the laptop. Figure 3.25 shows the flow chart to operate the dynamometer with the Dynoware software.

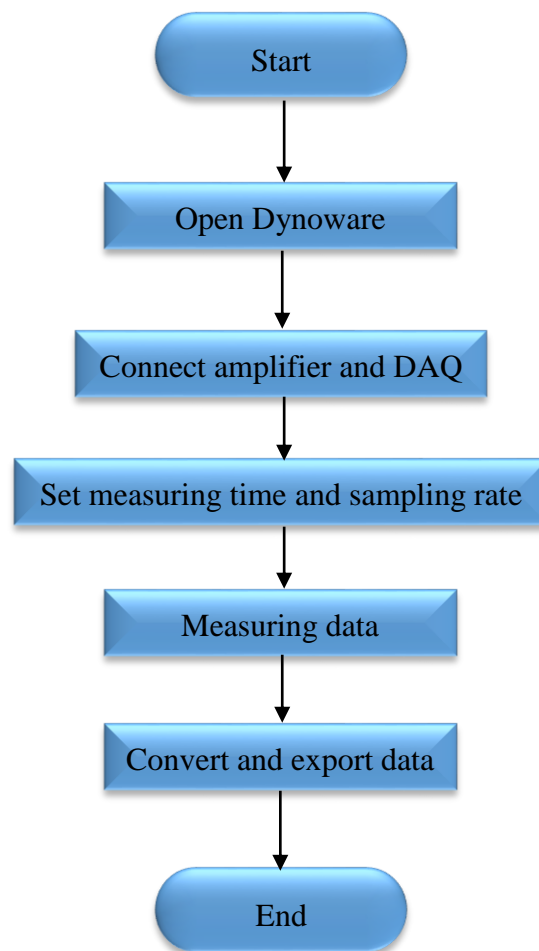


**Figure 3.25:** Data acquisition and export process

Figure 3.26 to 3.31 show the steps to acquire the data and export it from the dynamometer. The Dynoware software on the laptop was opened when the connection with the amplifier and dynamometer has been established. The total measuring time for every cut was set at 14 seconds and the sampling rate was 400 Hz. The start button on the Dynoware was pressed at the same time when the cutting cycle on the machine was started. Later the data was exported from the dynoware in the format of notepad file.

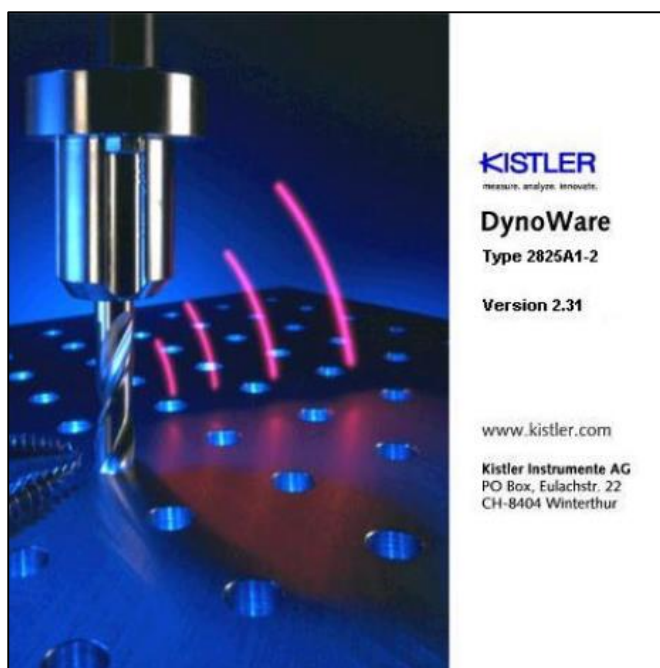


**Figure 3.26:** Dynoware





**Figure 3.27:** Amplifier Connection

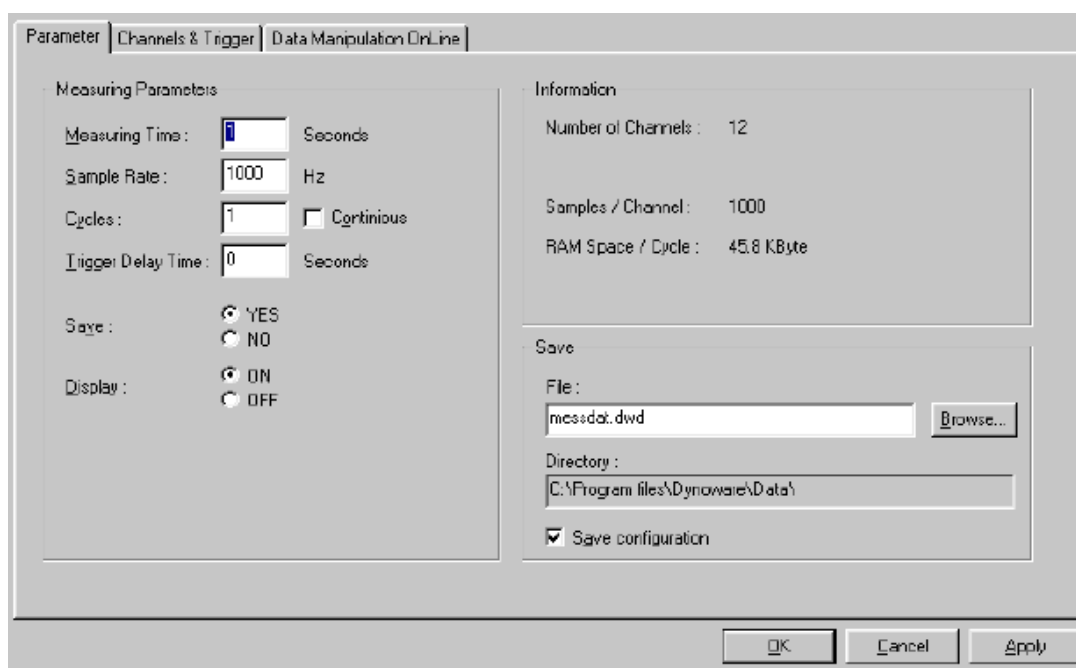


**Figure 3.28:** Measuring time and sampling rate

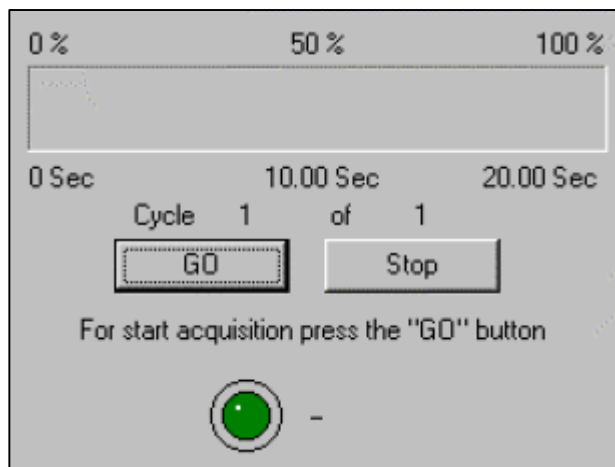


**Figure 3.29:** Sensor data measurement

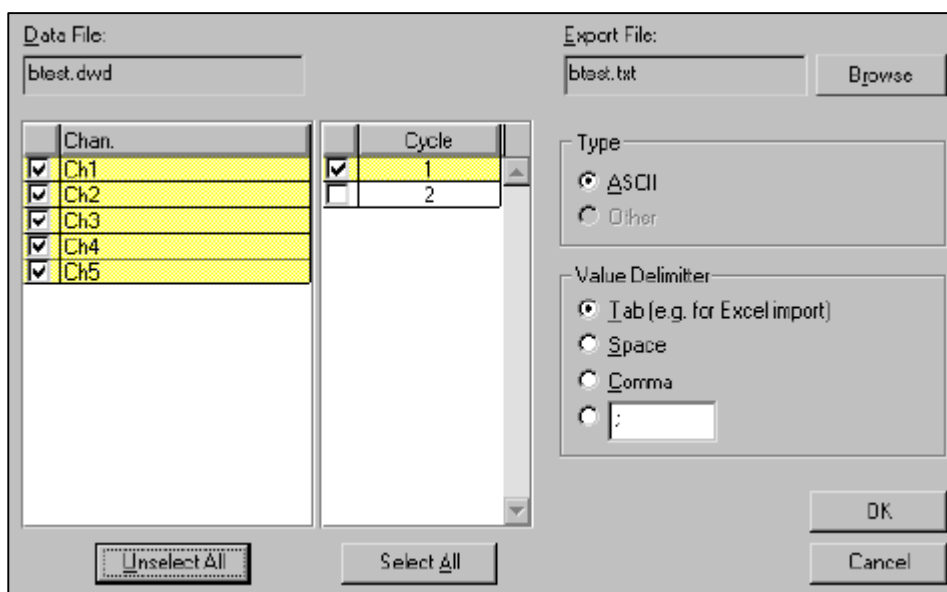
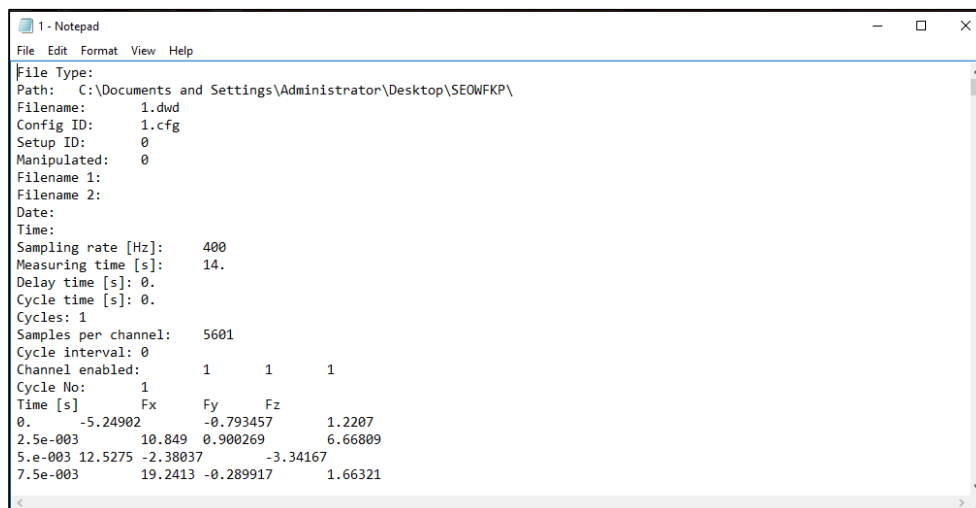


**Figure 3.30:** Data exportation



```

1 - Notepad
File Edit Format View Help
File Type:
Path: C:\Documents and Settings\Administrator\Desktop\SEOWFKP\
Filename: 1.dwd
Config ID: 1.cfg
Setup ID: 0
Manipulated: 0
Filename 1:
Filename 2:
Date:
Time:
Sampling rate [Hz]: 400
Measuring time [s]: 14.
Delay time [s]: 0.
Cycle time [s]: 0.
Cycles: 1
Samples per channel: 5601
Cycle interval: 0
Channel enabled: 1 1 1
Cycle No: 1
Time [s] Fx Fy Fz
0. -5.24902 -0.793457 1.2207
2.5e-003 10.849 0.900269 6.66809
5.e-003 12.5275 -2.38037 -3.34167
7.5e-003 19.2413 -0.289917 1.66321

```

**Figure 3.31:** Exported data

### 3.3.5 Features Extraction and Reduction

The statistical features were extracted from the raw signal data using the MATLAB software. Figure 3.32 shows MATLAB code used to extract the features from the signal.

```

%%Feature Extraction
Peak_TO_peak = (max(raw_data,[],1) - min(raw_data,[],1));

Standard_deviation = std(raw_data);

Kurtosis = kurtosis(raw_data);

Average = mean(raw_data);

Skewness = skewness(raw_data);

Variance = var(raw_data);

RMS = rms(raw_data);

Max = max(raw_data);

Factors = [Average,Kurtosis,Peak_TO_peak,Skewness,RMS,Standard_deviation,Variance];

```

**Figure 3.32:** Features extraction

After the features have been extracted, the features were reduced to the few most important features. The method used was the stepwise regression from the MATLAB software. Figure 3.33 shows the code used to reduce the features.

```
%% Features Reduction  
  
Factors = [Average,Kurtosis,Peak_TO_peak,Skewness,RMS,Standard_deviation,];  
  
stepwisefit(Factors,Tool_Wear,'penter',0.05,'premove',0.10);
```

**Figure 3.33:** Features reduction

### 3.3.6 Support Vector Machine Regression Model Training

The Support Vector Machine Regression model was trained using the MATLAB. The function used to train the model was *fitrsvm* [16] and the function used to predict the tool wear was *predict* [17]. The *fitrsvm* function will give a fully trained regression model using the predictor's value and the respond value. The *predict* function was used to predict the respond of the model for the input predictors value. Figure 3.34 shows the process to predict the tool wear using Support Vector Machine Regression model.

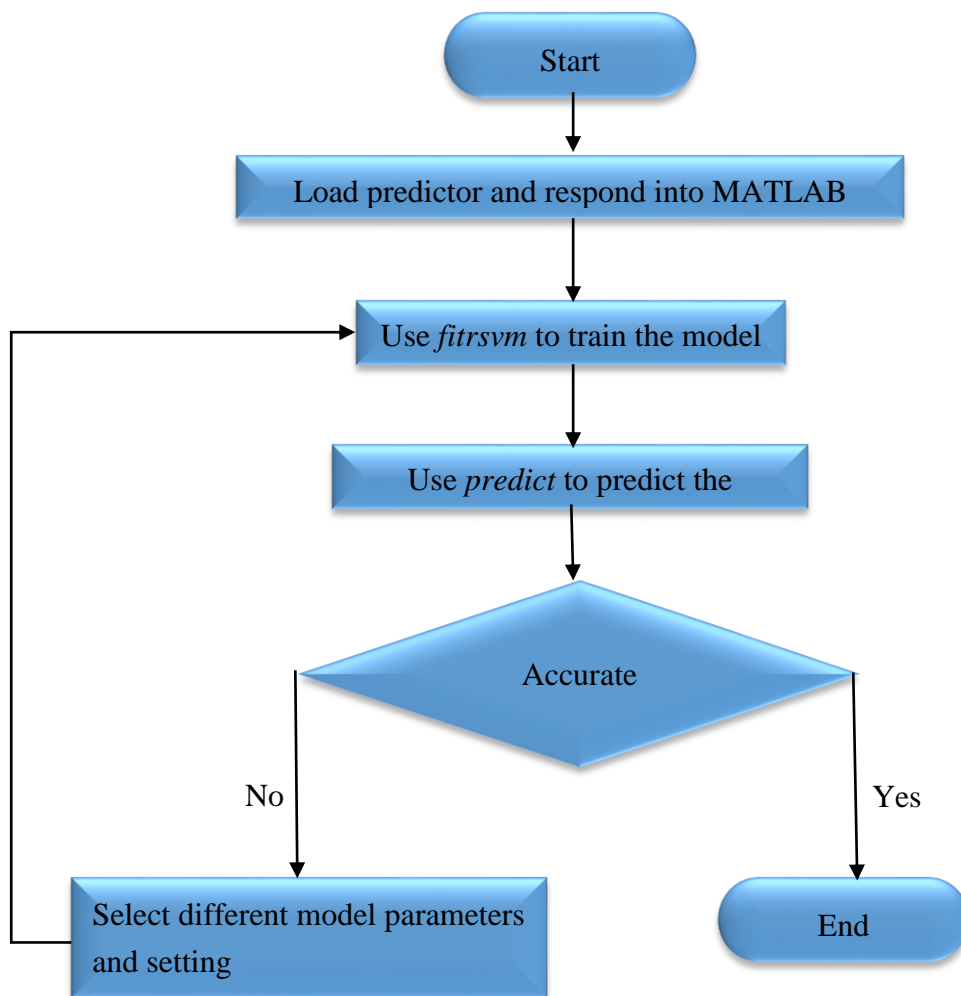


**Figure 3.34:** Support Vector Machine regression model training

Figure 3.35 shows the predictors and respond used to build the prediction. The data was loaded into a table format. Average and kurtosis were the predictors while tool wear was the predictor.

	1	2	3	4	5	6	7	8	9	10	11	12	13
	Average	Kurtosis	Tool_Wear										
1	-1.2461	6.9060	3.7000										
2	-1.2447	6.9132	3.8000										
3	-1.2496	6.8416	4.8000										
4	-1.2427	7.2262	5.5000										
5	-1.2359	7.3394	7.8000										
6	-1.2339	6.9406	7.9000										
7	-1.2440	7.0705	9.1000										
8	-1.2316	7.2125	9.3000										
9	-1.2407	7.5146	9.5000										
10	-1.2377	7.5633	9.5000										
11	-1.2165	7.5728	9.6000										
12	-1.2156	7.4288	9.7000										
13	-1.2298	7.4963	9.8000										
14	-1.2305	7.6755	9.9000										
15	-1.2140	7.7342	10										
16	-1.2068	8.0240	10.2000										
17	-1.2194	8.0635	10.5000										
18	-1.2005	7.8971	10.9000										
19	-1.1934	7.9018	11.2000										

**Figure 3.35:** Predictors and respond

After that, the prediction model was trained using the *fitrsvm* function and tested with the *predict* function. Figure 3.36 shows the code and respond of the *fitrsvm* function while figure 3.37 shows the code and respond of the *predict* function. The *fitrsvm* code showed the information of the model trained in the command window and the *predict* code showed the prediction result in the command window. If the result from the *predict* function was not accurate, the model will be retrain using *fitrsvm* function in different coding.

```

Command Window
>> mdl=fitrsvm(tbl,'Tool_Wear','KernelFunction','gaussian','KernelScale','auto','Standardize',true)

mdl =

RegressionSVM
    PredictorNames: {'Average' 'Kurtosis'}
    ResponseName: 'Tool_Wear'
    CategoricalPredictors: []
    ResponseTransform: 'none'
    Alpha: [19x1 double]
    Bias: 16.6850
    KernelParameters: [1x1 struct]
    Mu: [-1.1826 8.5267]
    Sigma: [0.0434 1.1285]
    NumObservations: 50
    BoxConstraints: [50x1 double]
    ConvergenceInfo: [1x1 struct]
    IsSupportVector: [50x1 logical]
    Solver: 'SMO'

Properties, Methods

```

**Figure 3.36:** *fitrsvm* function code

```

Command Window
>> yfit=predict(mdl,tbl)

yfit =

    4.7170
    4.8166
    4.7393
    6.5148
    8.1550
    6.8838
    5.3361
    8.1435
    9.2580
    9.7471
    10.5812
    10.7160
    9.7040
    10.5334
    10.6513
    11.2128
    11.4159
    11.3538
    12.0056
    12.6174
    11.0809
    13.3921
    13.6632
    14.0638

```

**Figure 3.37:** *predict* function code

### 3.3.7 Artificial Neural Network Model Training

The artificial neural network model was trained using the *nnstart* [18] GUI in the MATLAB. The feature used was the input-output curve fitting. This feature can train a

feed forward back propagation artificial neural network to predict the tool wear. Figure 3.38 shows the training workflow for the Artificial Neural Network model.

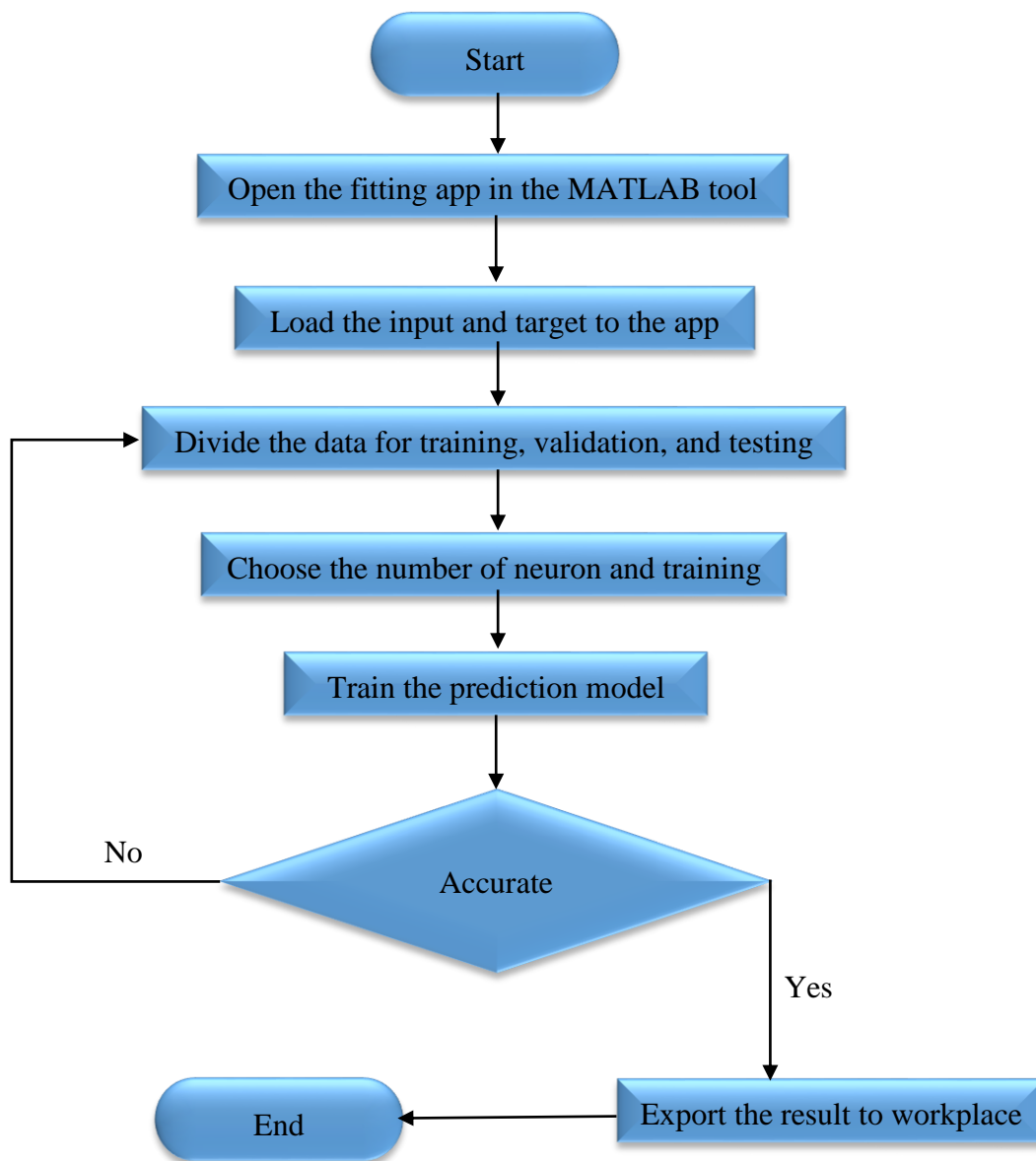


**Figure 3.38:** Artificial Neural Network model training

Figure 3.39 to 3.44 shows the step to train the Artificial Neural Network prediction model. In figure 3.39, the fitting app interface is shown and the loading of input and target data to the app is shown in the figure 3.40.



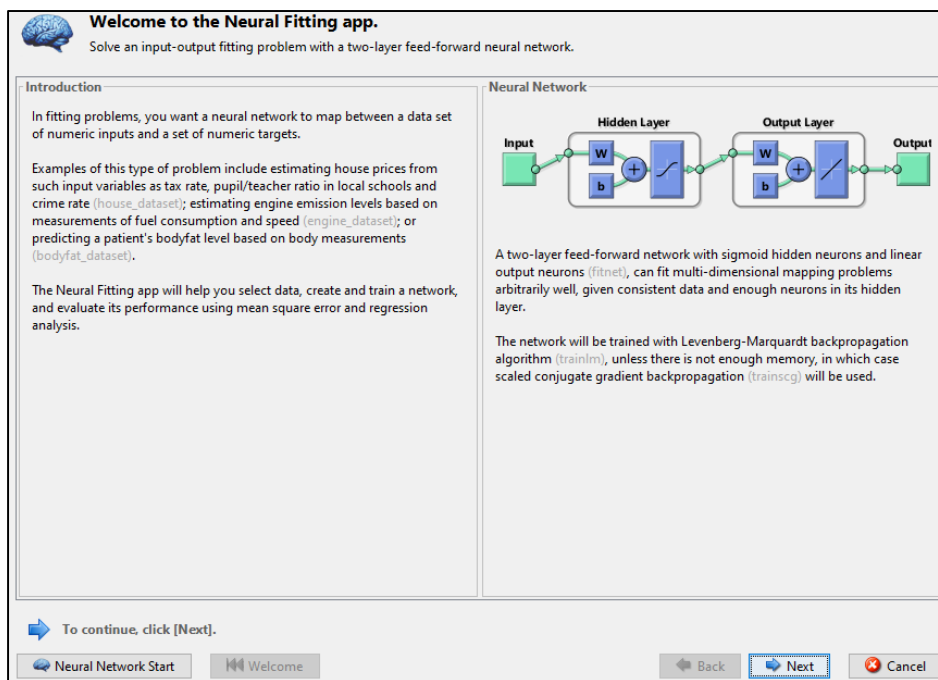


Figure 3.39: Neural fitting app

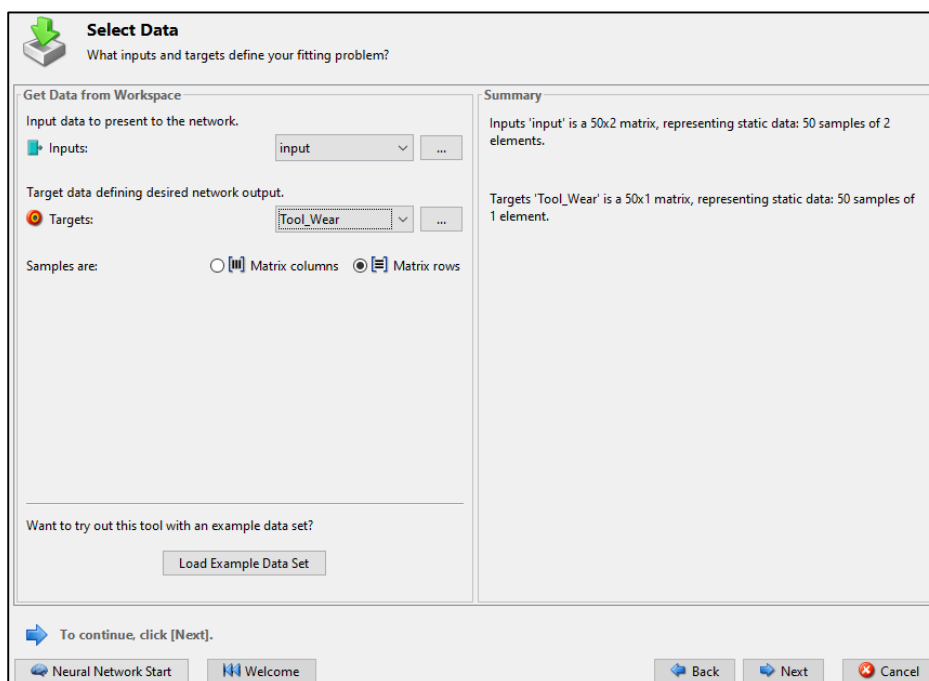


Figure 3.40: Data loading

Figure 3.41 shows the allocation of data for training, validation, and testing while figure 3.42 shows the selection for number of neurons in the hidden layer and the network architecture.

**Validation and Test Data**  
Set aside some samples for validation and testing.

Select Percentages

Randomly divide up the 50 samples:

Category	Percentage	Number of Samples
Training:	70%	34 samples
Validation:	15%	8 samples
Testing:	15%	8 samples

Restore Defaults

Explanation

Three Kinds of Samples:

- Training:** These are presented to the network during training, and the network is adjusted according to its error.
- Validation:** These are used to measure network generalization, and to halt training when generalization stops improving.
- Testing:** These have no effect on training and so provide an independent measure of network performance during and after training.

Change percentages if desired, then click [Next] to continue.

Neural Network Start Welcome Back Next Cancel

**Figure 3.41:** Validation and test data

**Network Architecture**  
Set the number of neurons in the fitting network's hidden layer.

Hidden Layer

Define a fitting neural network. (fitnet)

Number of Hidden Neurons:

Restore Defaults

Recommendation

Return to this panel and change the number of neurons if the network does not perform well after training.

Neural Network

Diagram illustrating the neural network architecture:

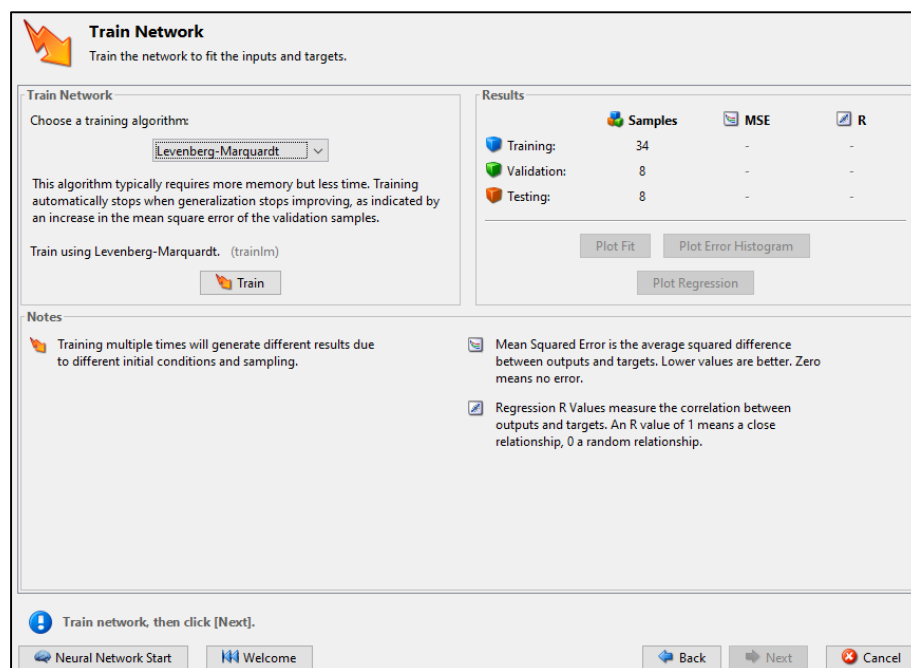
- Input: 2 neurons
- Hidden Layer: 10 neurons
- Output Layer: 1 neuron

Change settings if desired, then click [Next] to continue.

Neural Network Start Welcome Back Next Cancel

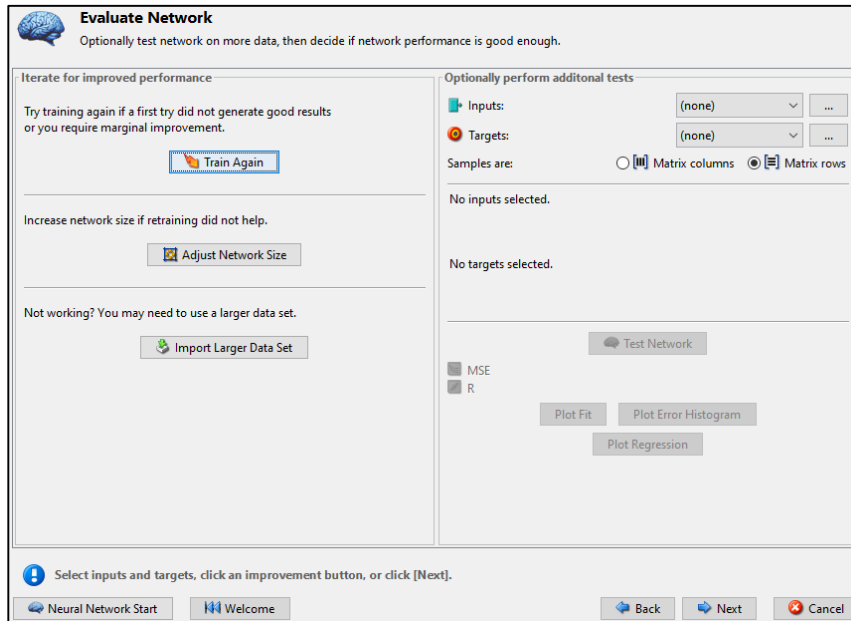
**Figure 3.42:** Neurons selection and network architecture

Figure 3.43 shows the training interface for the network. In the interface, the suitable training algorithm was selected to train the network and the performance of the network trained can be seen in that interface. The mean squared error and regression plot value were shown to indicate the model's performance.

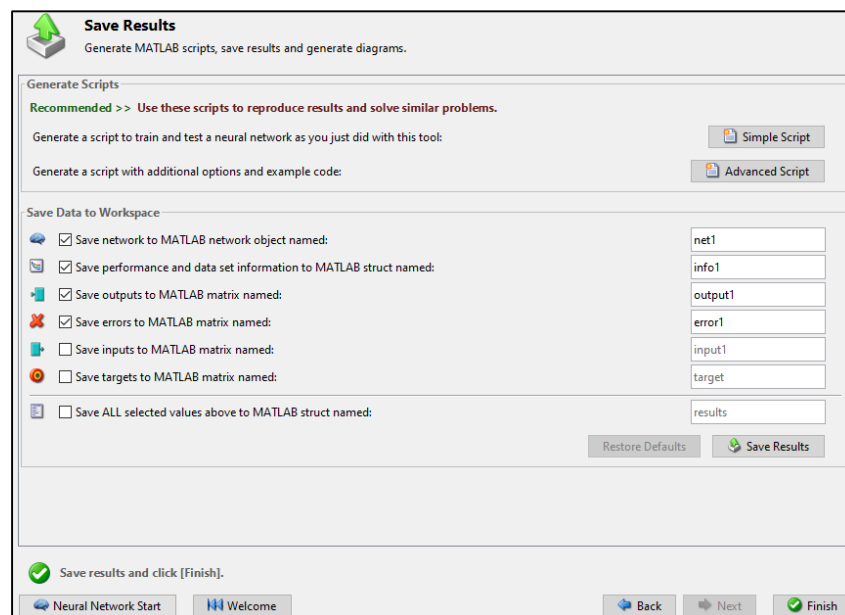


**Figure 3.43:** Training of network

If the performance of the network was not satisfying, it can be retrain using different numbers of neurons or different datasets. Figure 3.44 shows the retrain interface for the network.



**Figure 3.44:** Retraining interface



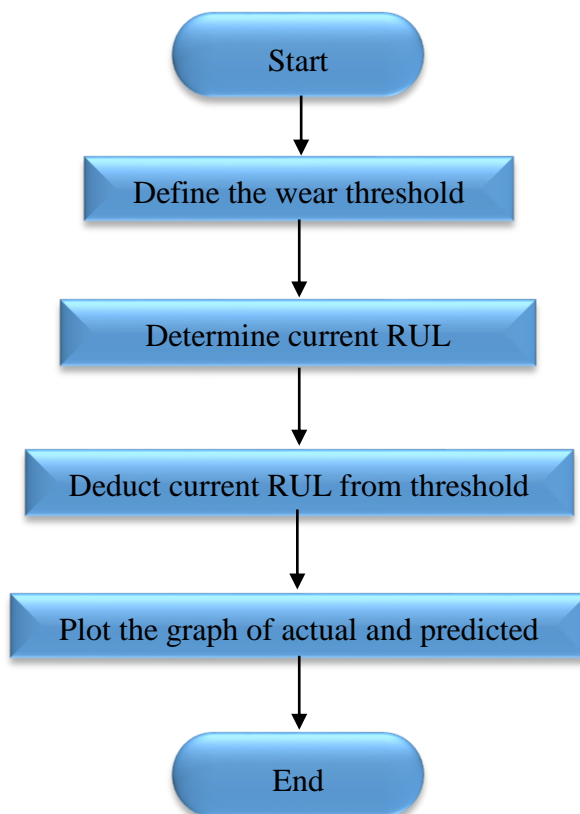
**Figure 3.45:** Network result saving

Figure 3.45 shows the saving of the outputs from the network prediction model. The results were exported to the workplace of the MATLAB software.

### 3.3.8 Predict for Remaining Useful Life

The remaining useful life for the tool insert was determined by setting a threshold value for it. In this project, the threshold was set as the tool can be used anymore at the end of the experiment. Therefore, the remaining useful life for a new insert was 50 and was 0 at the end of the experiment.

The remaining useful life was predicted using the predicted wear from the Support Vector Regression model and Artificial Neural Network model. Figure 3.46 shows the workflow to predict the remaining useful life.



**Figure 3.46:** Predicting remaining useful life

### 3.4 HARDWARE AND SOFTWARE APPLICATION

The hardware and software will be used in this project are the CNC milling machine, wire cut machine, metallurgical microscope, coated carbide insert, stainless steel, dynamometer, amplifier, Mastercam, and MATLAB. We will discuss all these hardware and software needed in the following section.

#### 3.4.1 MAKINO Milling Machine



**Figure 3.47:** Makino KE55 CNC milling machine

Milling machine is one of the most commonly available machine we can find in any machining workshop. The figure 3.47 shows a Makino KE55 CNC milling machine that we are going to use in this project for the facing process for the workpiece. This machine is very user friendly as it can reduce the tiresome set up process needed perform by the operator. It can perform many kinds of operation such as oblique cutting, circular

cutting, and tapping. It is desirable for a single part run for its speed, reliability, and accuracy. The figure 3.48 shows the specifications of this machine.

7.5 HP Vertical CNC Knee Mill			
Machine Type:	Milling Machine		
Num. of Axes:	3		
Work Support:	Knee		
Column Construction:	Single	Column Style:	Travelling
Operation Type:	CNC		
CNC Brand:	Fanuc ProEN		
TABLE/WORK SUPPORT			
Table Size L x W (in.)	31.500 x 14.750		
Max. Workpiece Weight (lbs)	550		
SPINDLE(S)			
Num. Main Spindles	1		
Orientation	Vertical		
Taper	# 40		
Top RPM	4,000 Opt: 6,000		
Horse Power (30 min rating)	8.00		
# Speed Ranges	2		
Type	Quill		
TOOLING			
Primary Tool Carrier(s)	MANUAL		
Number of Tools	1 Opt. 1		
AXES AND TRAVELS			
Number of Axes: 3			
	Travel	Max Feed	Rapid Rate
X1	Std. 21.625 in.	197 ipm	472 ipm
Y1	Std. 12.625 in.	197 ipm	472 ipm
Z1	Std. 13.750 in.	197 ipm	197 ipm
WEIGHTS AND MEASURES			
Machine Dimensions (l x w x h)(in.)	78 x 82		
Machine Weight (lbs)	6,600		
Spindle Nose To Table (Max)	17.750		
Spindle Nose To Table (Min)	3.937		

**Figure 3.48:** Specifications for Makino KE55 [19]

Source: Makino KE55 7.5 HP Vertical CNC Knee Mill Techspex.

### 3.4.2 HAAS Milling Machine



**Figure 3.49:** HAAS milling machine VF-6

Figure 3.49 shows the HAAS milling machine VF-6 used for the experiment. This machine is equipped with 20HP using dual vector drive and the maximum spindle speed is 7500 rpm. The coolant system is through spindle coolant system [20]. The machine is CNC controlled and incorporated with Mastercam for its machining operation. Figure 3.50 shows the controller of the machine where the status is displayed.



**Figure 3.50:** Control unit



### 3.4.3 Wire Cut Machine



**Figure 3.51:** Sodick VZ 300L wire cut machine

Figure 3.51 shows the Sodick VZ 300L wire cut machine used to prepare the workpiece for the experiment. This machine features Sodick's well-known Linear Motor Technology. The VZ Series is a low investment, basic model of WEDMs that can provide the quality we look for when using a wire cut machine. This machine has a higher levels of accuracy and cutting speeds when compared to the High End Sodick EDM models [21].

The machine has a large capacity worktank that comprises a vertical access door for ergonomic accessibility. The machine requires less working space by using the sliding door and its can prevent water drip totally to secure a safer workplace. It is also energy efficient as its energy consumption is 60% lower than other wire cut machine. Table 3.2 shows the specification of the machine [21].

**Table 3.2:** Wire cut machine specification [21]

Specification	Value
X - axis travel	350 mm
Y - axis travel	250 mm
Z - axis travel	220 mm
U, V axis travel	80 x 80 mm
Wire diameter range (min ~ max)	0.10 ~ 0.30 mm
Work tank dimensions (W x D)	810 x 650 mm
Maximum workpiece weight	500 kg
Distance from floor to table top	900 mm
Machine tool dimensions	1,895 x 2,180 x 1,960 mm
Machine weight	2,400 kg

Source: VZ300L Wire EDM

#### 3.4.4 Metallurgical Microscope



**Figure 3.52:** Olympus BX51M metallurgical microscope

Figure 3.52 shows the Olympus BX51M metallurgical microscope used in this project. This microscope give adaptability for a diverse category of materials science and industrial applications. It has an illuminator which can minimize the complex steps that are always needed when operating a microscope. Its magnifying power varies from 5x to 50x.

### 3.4.5 End Mill Insert



**Figure 3.53:** End mill insert

Figure 3.53 shows the type of insert used in this project. The insert was from Ceratizit with model CTPM240. The yellow colour triangle in the hexagon represent the stainless steel and the black colour square means the tool is specialized for the usage on stainless steel while the empty square means the extended use of the insert [22].

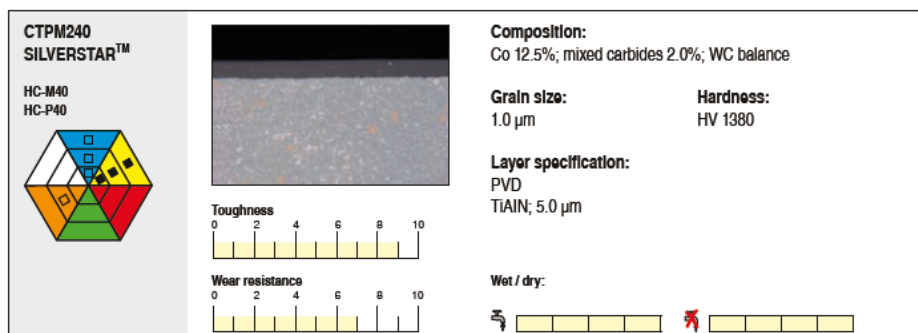


**Figure 3.54:** Insert specification [22]

Source: Innovation Product Highlight

Figure 3.54 shows the specification of the insert. The insert has its coated layer under the series of SILVERSTAR. This kind of coating is best for high performance machining in interrupted machining process or on material which is hard to machine. This cutter performs best for the stainless steel when it is use together with coolant [22]. The coating layer is made up of TiAlN using a PVD method. The wear resistance of this insert is 7 out of 10 while its toughness is 9 out of 10.

### 3.4.6 Workpiece Material

Uddeholm Stavax ESR was the material used in the experiment. It is a premium stainless mould steel for small and medium inserts and cores. Uddeholm Stavax ESR combines corrosion and wear resistance with excellent polishability, good machinability and stability in hardening. It is able to lower the mould maintenance cost and the production cost [23]. Figure 3.55 shows the physical data of the workpiece material.

Temperature	20°C (68°F)	200°C (390°F)	400°C (750°F)
Density, kg/m <sup>3</sup> lbs/in <sup>3</sup>	7 800 0.282	7 750 0.280	7 700 0.277
Modulus of elasticity N/mm <sup>2</sup> tsi psi	200 000 12 900 29.0 × 10 <sup>6</sup>	190 000 12 300 27.6 × 10 <sup>6</sup>	180 000 11 600 26.1 × 10 <sup>6</sup>
Coefficient of thermal expansion /°C from 20°C /°F from 68°F	– –	11.0 × 10 <sup>-6</sup> 6.1 × 10 <sup>-6</sup>	11.4 × 10 <sup>-6</sup> 6.3 × 10 <sup>-6</sup>
Thermal conductivity* W/m °C Btu in/(ft <sup>2</sup> h °F)	16 110	20 138	24 166
Specific heat J/kg °C Btu/lb, °F	460 0.110	– –	– –

**Figure 3.55:** Workpiece physical data [23]

Source: UDDEHOLM STAVAX® ESR

### 3.4.7 Dynamometer

A stationary dynamometer is often the connecting element between the machine table of the machine tool and the workpiece. The workpiece is fastened on the dynamometer with which the reaction forces in manufacturing processes such as milling or drilling are measured. The tool is placed on the dynamometer with a suitable tool holder. Depending on the structure, the forces that arise are recorded by one or more multi-component force sensors and are available at the connector of the dynamometer in the form of charge signals.



**Figure 3.56:** Dynamometer 9257B

Figure 3.56 shows the dynamometer with workpiece on it. The dynamometer used in this project was the Kistler 9257B stationary multi-component dynamometer with top plate 100x170 mm up to 10 kN. The dynamometer is for universal use. The handy size and the ideal measurement range for many applications have made Type 9257B the most frequently built multi-component dynamometer. The connection with the machine table is accomplished with lateral flanges with oblong holes [24]. Figure 3.57 shows the technical data of the dynamometer.

Technical Data	Type	9257B
Measuring range		
$F_x, F_y$	kN	-5 ... 5
$F_z$	kN	-5 ... 10
Calibrated measuring range		
$F_x, F_y$	kN	0 ... 5
	kN	0 ... 0,5
$F_z$	kN	0 ... 10
	kN	0 ... 1
Sensitivity		
$F_x, F_y$	pC/N	$\approx -7,5$
$F_z$	pC/N	$\approx -3,7$
Natural frequency		
$f_n(x), f_n(y)$	kHz	$\approx 2,3$
$f_n(z)$	kHz	$\approx 3,5$
Pretensioning direction		vertical
Operating temperature range	°C	0 ... 70
LxWxH	mm	170x100x60
Weight	kg	7,3
Degree of protection IEC/EN 60529 (w. conn. cable)		IP67
Connection		Fischer flange 9 pol. neg.

**Figure 3.57:** Dynamometer technical data [24]

Source: Kistler product catalog

### 3.4.8 Amplifier

The charge amplifier carry out a charge conversion function by changing the charge at the input to the amplifier, to voltage at the output. The gain of a charge amplifier is stated in units of mV/pC. The gain of the amplifier will not be affected by the

capacitance and can be adjusted from the component inside. This allows the amplifier can be calibrated very accurately.

Figure 3.58 shows the type 5070A multi-channel charge amplifier for multi-component force measurement and figure 3.59 shows the specifications. This charge amplifier was developed especially for multi-component force measurement. Due to its large and continuously adjustable measuring ranges and the wide frequency range, this device is suitable in measuring chains with stationary Dynamometers for cutting force measurement [24].



**Figure 3.58:** Amplifier type 5070A



Technical Data	Type	5070A...
Number of channels		
Type 5070Ax0xxx		4
Type 5070Ax1xxx		8
Type 5070Ax2xxx		8 with 6-component summing calculator
Measuring range FS, optional	pC	±200 ... 200 000
	pC	±600 ... 600 000
Measuring ranges adjustment		continuous
Frequency range (-3 dB)	kHz	≈0 ... 45
Output signal	V	±10
Supply voltage	VAC	100 ... 240
Input signal	Type/ connector	Piezoelectric, optional with: – BNC neg. – Fischer 9 pol. neg.
Output signal	Type/ connector	D-Sub 15 pol. neg.
Degree of protection IEC/EN 60529		IP40
Interface, optional		RS-232C RS-232C + IEEE-488
Case, optional		– 19" cassette for rack mounting – Desktop unit with support bracket – 19" cassette with panel mounting set
Other features		– Display of peak values – Display of mechanical measurands

**Figure 3.59:** Amplifier specifications

Source: Kistler product catalog

### 3.4.9 Mastercam

Mastercam is the most widely used CAM software worldwide and remains the program of choice among CNC programmers. Mastercam Mill is the next generation of

the popular program, delivering the most comprehensive milling package with powerful new toolpaths and techniques. Mastercam Mill delivers fast, easy, industry-proven NC programming that lets you make the most of your machines [25].

The Mill suite of CAD/CAM tools is focused on delivering speed and efficiency to your shop. Since milling covers a huge range of disciplines—basic and complex 2D cutting to single-surface and advanced 3D milling—Mastercam offers an equally wide range of tools to make sure you can get your job done right. Mastercam also offers streamlined multiaxis cutting. Figure 3.60 shows the Mastercam logo.



**Figure 3.60:** Mastercam logo [25]

Source: Mastercam

#### **3.4.10 MATLAB**

MATLAB is a software using a high level language and has an interactive environment that is commonly used worldwide by the engineers and scientists. We are able to visualize our ideas using this software and the collaboration across different disciplines is possible. As an example, MATLAB can be used to run simulations for us to determine the optimal parameter for a process [26]. This software is used in this project for the extraction and reduction of the data and predict the remaining useful life of the

end mill using the support vector machine toolbox available in the MATLAB. The figure 3.61 shows the logo for the MATLAB.



**Figure 3.61:** MATLAB Logo [26]

Source: MATLAB - The Language of Technical Computing.

## **CHAPTER 4**

### **RESULTS AND DISCUSSIONS**

#### **4.1 INTRODUCTION**

This chapter provides all the relevant results from the experiment and the raw data analysis available from Prognostics Health and Management Society. The data from Prognostics Health and Management Society Competition 2010 was used to train the prediction models to acquire the theoretical background knowledge for the remaining useful life prediction. The preliminary data from the models will be shown and analyze in this chapter before the analysis of the experimental data.

The results of the actual tool wear measurement, raw data features extraction process, features reduction and selection process, Artificial Neural Network model training, Support Vector Regression model training, and the remaining useful life prediction will be displayed here. The performance of the models from this project will be compared with each other. Other than that, all the results will be interpreted to explain the difference between the models trained using different methods..

## 4.2 PHM SOCIETY DATA ANALYSIS

The procedures to assess the tool wear and predict the remaining useful tool life described in the methodology are applied on the experimental raw data taken from the prognostics and health management society data challenge competition. The dataset contains raw data of 315 cutting process of the end mill. The cutter used in the experiment was a three flute ball nose end mill while the sensors used in the experiment were force sensors, vibrations sensors, and acoustic emission sensor. The models trained using this PHM data was served as the theoretical model to build the prediction model for my own experiment. Table 4.1 shows the conditions of the experiments.

**Table 4.1:** Cutting Condition

<b>Spindle Speed</b>	<b>Feed Rate</b>	<b>Depth of Cut Y (radial)</b>	<b>Depth of Cut Z (radial)</b>	<b>Sampling Frequency</b>
<b>10400 RPM</b>	1555 mm/min	0.125mm	0.2mm	20kHz

The graph of the raw data from the different sensors during first cut and last cut are shown in the figure 4.1 to figure 4.3 below. The raw data used in this project was the data from the force sensor.

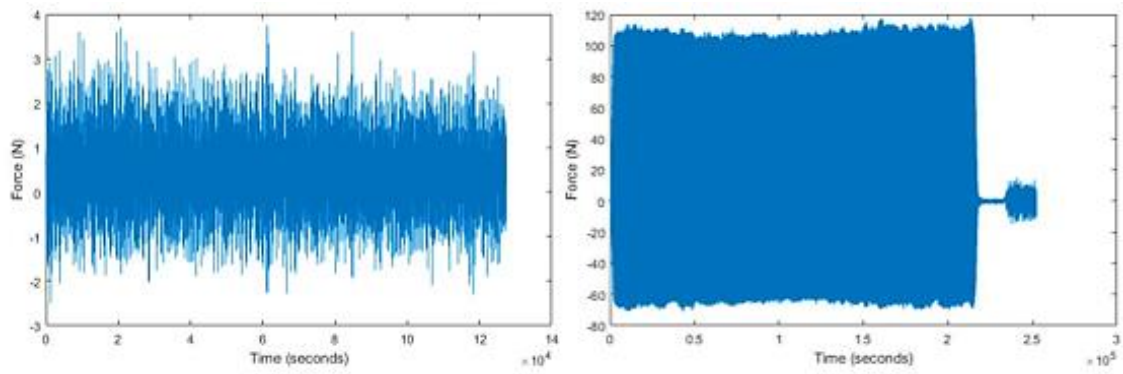


**Figure 4.1:** Raw data from force sensor during first cutting process (left) and final cutting process (right)

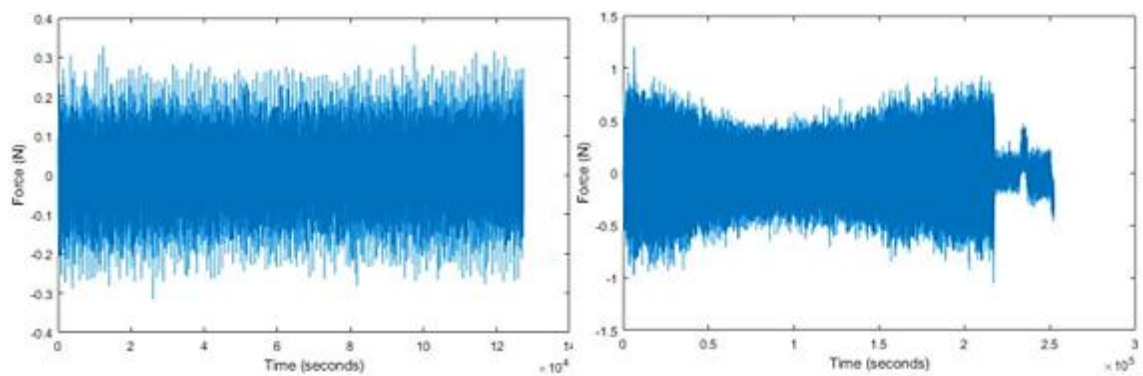


**Figure 4.2:** Raw data from vibration sensor during first cutting process (left) and final cutting process (right)

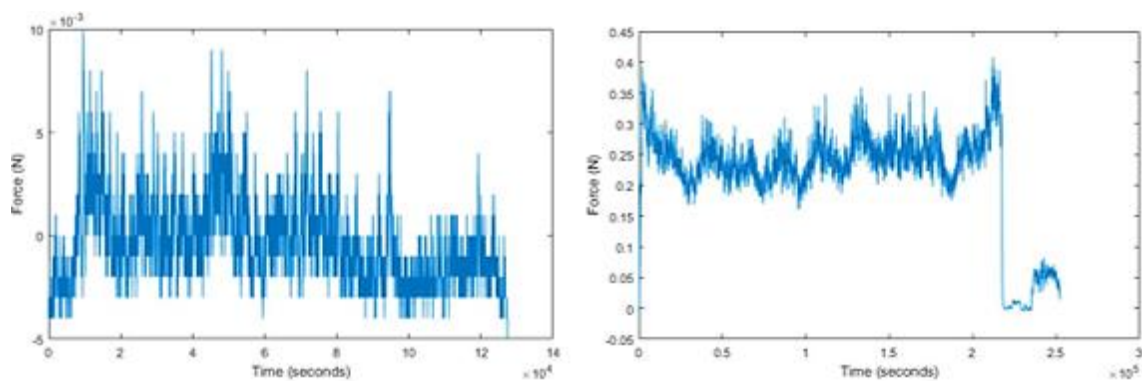


**Figure 4.3:** Raw data from acoustic sensor during first cutting process (left) and final cutting process (right)

#### 4.2.1 Raw Data Features Extraction

The force sensor raw data went through the extraction process to acquire the statistical features from the data. These statistical features are mean, kurtosis, total amplitude, skewness, root mean square, standard deviation, and maximum level. Table 4.2 shows the statistical features.

**Table 4.2:** Significant statistical features

No.	Important Statistical Features
1	Mean
2	Kurtosis
3	Total amplitude
4	Skewness
5	Root mean square
6	Standard deviation
7	Maximum level

#### 4.2.2 Features Reduction and Selection

All of the features listed in the table 4.2 are important, but when there are too many features involved in the building of model, the established correlated model will possess undesirable calculation performance [4]. Stepwise regression was used in this project to select the most appropriate features to train the model. Table 4.3 shows the setting of the stepwise regression.

**Table 4.3:** Stepwise regression parameters

<b>Input Parameters</b>	<b>Value</b>
<b>Initial model</b>	None included
<b>Entrance tolerance</b>	0.05
<b>Exit tolerance</b>	0.10
<b>Information display</b>	On
<b>Number of steps</b>	Infinity
<b>Scale</b>	Off

**Table 4.4:** Features selection result from stepwise regression

<b>Features</b>	<b>Coefficients</b>	<b>P-value</b>	<b>Status</b>
<b>Mean</b>	-0.0203	0.2211	Out
<b>Kurtosis</b>	-13.8775	6.7262e-17	In
<b>Total amplitude</b>	0.5626	4.6475e-10	In
<b>Skewness</b>	-27.2321	3.9430e-11	In
<b>Root mean square</b>	-0.0242	0.2603	Out
<b>Standard deviation</b>	-0.6854	0.0434	In
<b>Maximum level</b>	-0.0213	0.2013	Out



According to the table 4.4, four features were selected by the stepwise regression as their p-value were smaller than the selection requirement of 0.05. They were the kurtosis, total amplitude, skewness, and standard deviation. These four features have the most significant influence on the estimation of tool wear and prediction of the remaining useful too life. These four features were used as the input to train the prediction models.

### 4.2.3 Support Vector Regression (SVR) Model

The features selected were used to train a support vector regression prediction model. The four features were the predictor and the tool wear were used as the response for the regression model. The table 4.5 shows the properties and parameters of the model trained for this project.

**Table 4.5:** Support vector machine regression model

<b>Property</b>	<b>Value</b>
<b>Predictor names</b>	'kurtosis', 'total amplitude', 'skewness', 'standard deviation'
<b>Respond name</b>	'Tool wear'
<b>Standardize data</b>	Yes
<b>Kernel</b>	Gaussian
<b>Kernel scale</b>	Auto
<b>Solver</b>	Sequential Minimal Optimization
<b>Box constraints</b>	27.8526
<b>Epsilon</b>	2.7853
<b>Mu</b>	2.1395, 79.5112, 0.0393, 17.9830
<b>Sigma</b>	0.2501, 60.2180, 0.1455, 15.2199

Referring to the table 4.5, the four predictor names were kurtosis, total amplitude, skewness, and standard deviation while the respond name was tool wear. The box constraint which is also called the C parameter used to train the model was 27.8526 and the epsilon,  $\epsilon$  has the value of 2.7853. The Mu in table 4.5 is the mean value of the predictors data arranged in the sequence of kurtosis, total amplitude, skewness, and standard deviation. Other settings can be seen clearly from the table above.

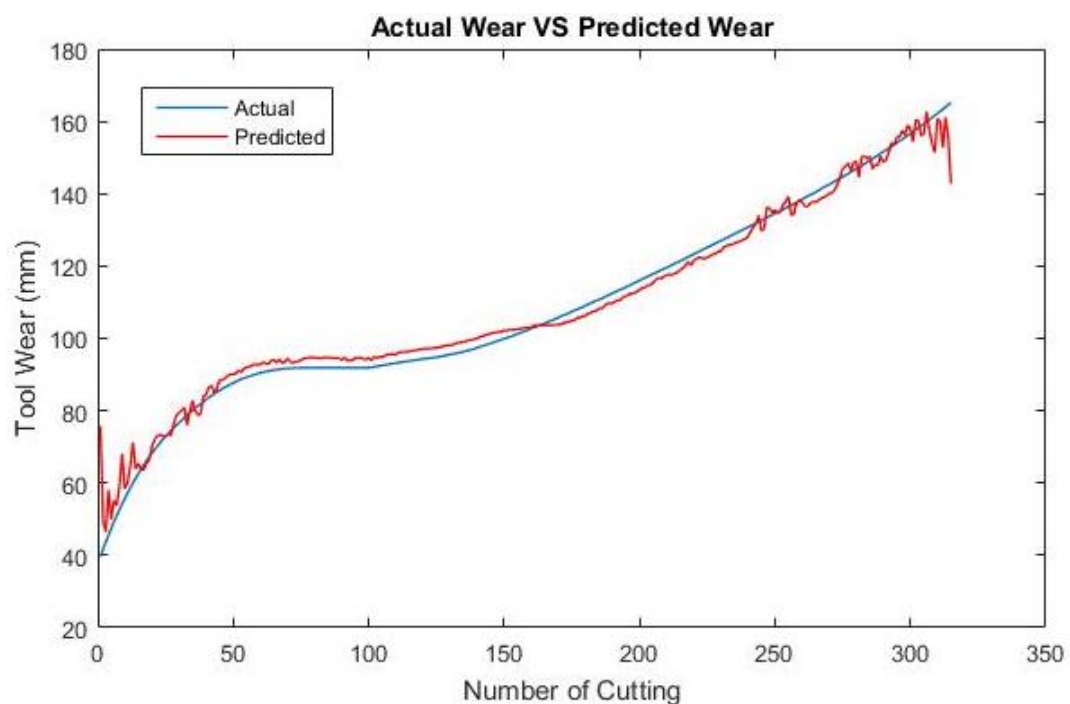


**Figure 4.4:** Comparison between actual wear and predicted wear of SVR

The result of actual wear and the predicted wear from the support vector machine regression model is shown in the figure 4.4. There was a total of 315 cuts performed using the end mill and the respective actual tool wear after each cut was recorded. The blue colour line graph was the progression of actual tool wear while the red colour line graph was the progression of the predicted tool wear.

#### 4.2.4 Artificial Neural Network Model

The Artificial Neural Network model was trained using the same data for the training of support vector machine regression model, which are the same 4 features and the actual tool wear. Figure 4.5 shows the feedforward network architecture of the neural model.

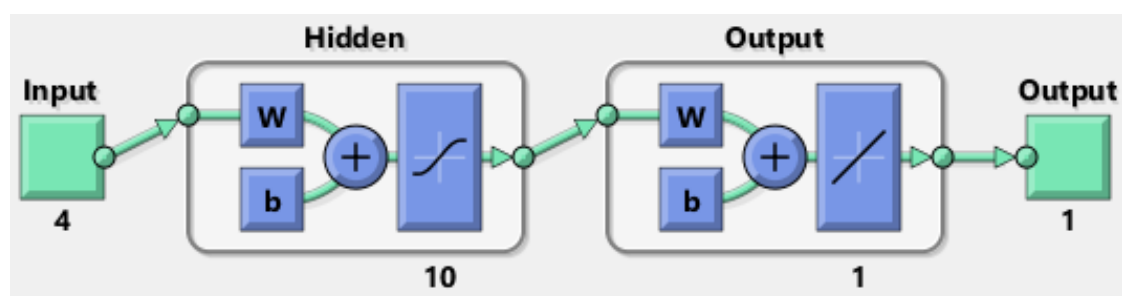


Figure 4.5: Neural Network Architecture

Table 4.6: Artificial Neural network setting

Parameters	Description
Data division	Dividerand
Training function	Trainlm
Hidden layer transfer function	Tansig
Output layer transfer function	Purelin
Maximum number of epochs to train	1000
Maximum training time	Infinity
Performance	MSE
Performance goal	0
Minimum performance gradient	1e-7
Maximum validations failure	6

Table 4.6 shows the settings of the neural network during the training process. The settings are the standard default for the training of the Artificial Neural Network. More explanation will be provided with the experimental data analysis.

**Table 4.7:** Mean Square Error and regression of the model

<b>Subset</b>	<b>Samples</b>	<b>MSE</b>	<b>Regression</b>
<b>Training</b>	221	0.608592	0.999608
<b>Validation</b>	47	0.613508	0.999549
<b>Testing</b>	47	2.70535	0.998181

Table 4.7 shows the result for Mean Square Error value and the regression fit of the three subsets. Both training, validation, and training data have a small MSE value. This means that the network has a good performance and the performance will be best when the MSE is zero. Figure 4.6 shows the line graph plotted using the MSE of both training, validation, and testing data. The graph shows that the validation error reached a minimum value at the 141 epochs with a value of 0.61351. The training process was continued for 6 more epochs before it was stopped.

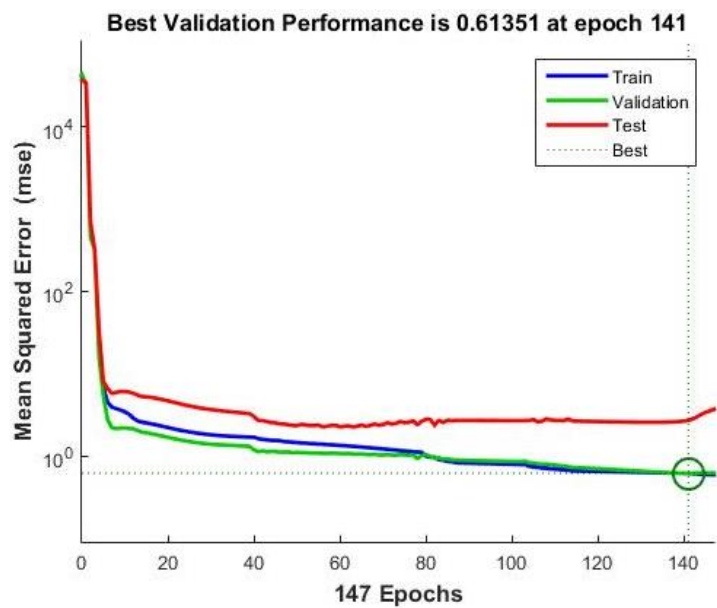


Figure 4.6: Mean Square Error

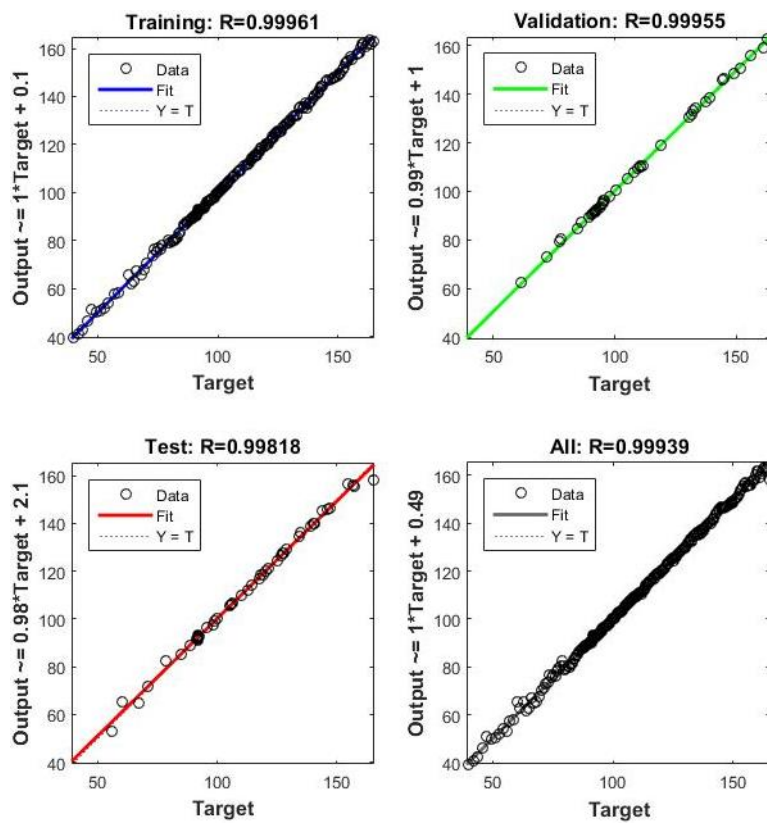
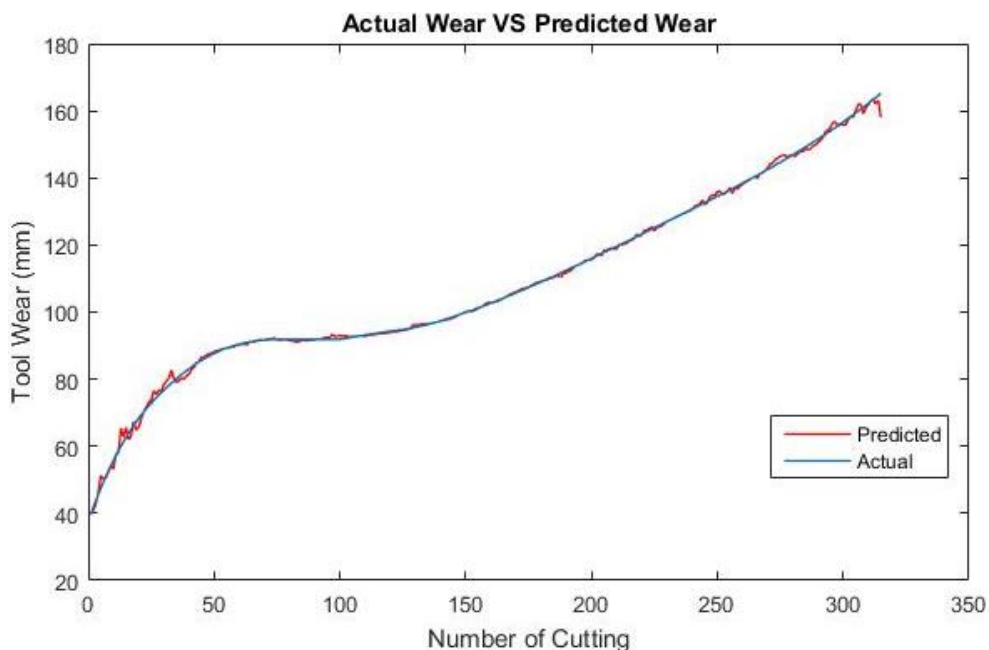


Figure 4.7: Regression plot

Figure 4.7 shows the regression plot for the training, validation, testing, and overall data. The R value is same as the regression value in the table 4.7. The value from both training, testing and testing fit very well to the regression model. This means the accuracy of the model is high as a perfect fit was almost achieved.



**Figure 4.8:** Comparison between actual wear and predicted wear of neural network

The result of actual wear and the predicted wear from the support vector machine regression model is shown in the figure 4.8. There was a total of 315 cuts performed using the end mill and the respective actual tool wear after each cut was recorded. The blue colour line graph was the progression of actual tool wear while the red colour line graph was the progression of the predicted tool wear.

The predicted wear using the Artificial Neural Network is more accurate than the Support Vector Regression model. This can be seen from the figure 4.5 and figure 4.9

where the predicted wear is more alike as the actual wear. The values for the actual wear and predicted wear were later used for the prediction of remaining useful life.

#### 4.2.5 Remaining Useful Life (RUL) Prediction

The predicted tool wear was used to predict the remaining useful life. The remaining useful life were calculated using the same formula stated in the chapter 4.6.

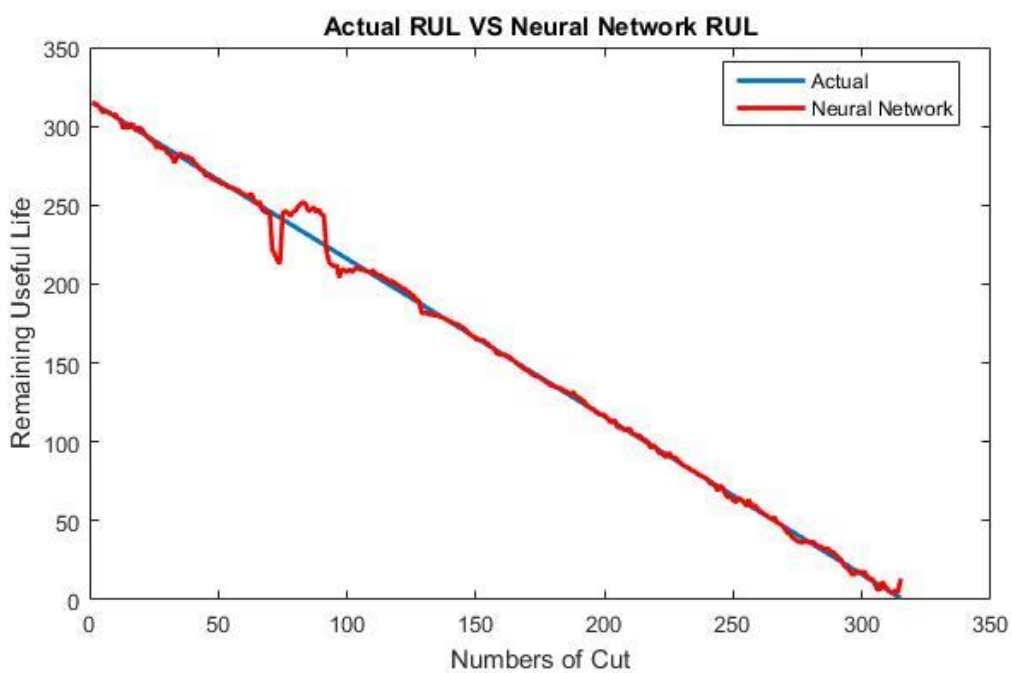


**Figure 4.9:** Comparison between actual RUL and neural network RUL

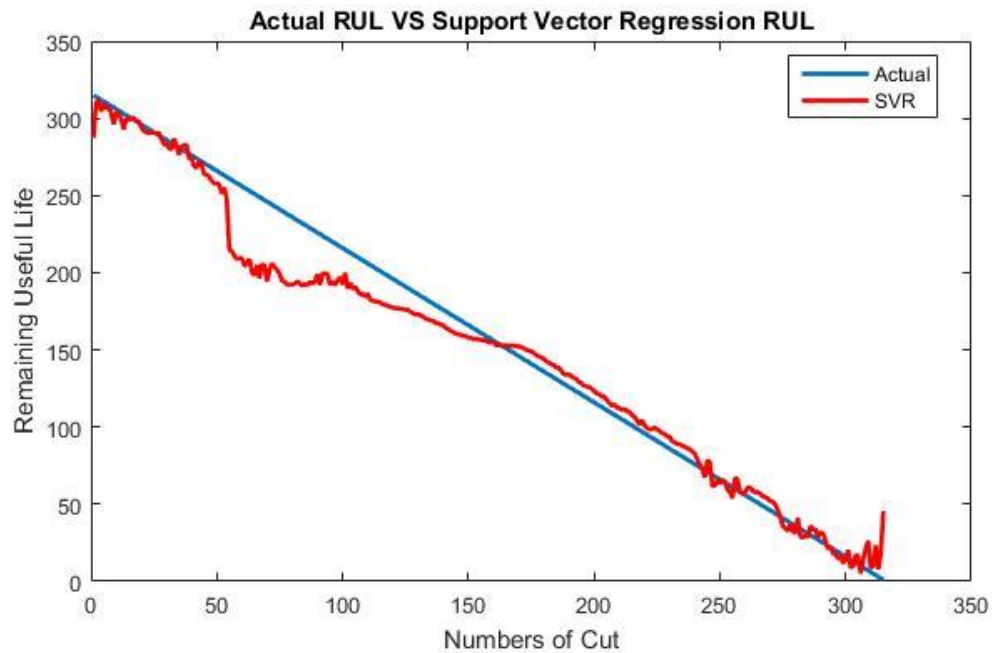


**Figure 4.10:** Comparison between actual RUL and Support Vector Regression RUL

Figure 4.9 and figure 4.10 show the graph of actual tool life versus the predicted wear acquired from the Artificial Neural Network model and the Support Vector Regression model. The predicted RUL from the Artificial Neural Network model is better as it can give a result nearer to the actual RUL. This meant the neural model trained in this project has the higher performance compared to the Support Vector Machine Regression model trained.

#### 4.2.6 Performance Assessment

The performance assessment process is same as for the model trained using the experimental data. However, two more performance measures were used to assess the performance of neural network trained using the PHM data, which were the R squared value ( $R^2$ ) and the Mean Square Error (MSE). The performance of the models trained



using the PHM data in this project were compared with the existing model trained using same data.

R squared value is a coefficient to determine the proportionate size of discrepancy in the tool wear and the four features selected as the input for the model training. More variability will be explained by the regression model if the R squared value is large. Mean Square Error is a measure of how close a fitted line is to data points. For every data point, you take the distance vertically from the point to the corresponding y value on the curve fit (the error), and square the value. The smaller the Mean Squared Error, the closer the fit is to the data.

**Table 4.8:** Performance assessment for SVM Regression model

	<b>Trained Model</b>	<b>Existing Model</b>
<b>Accuracy</b>	0.90	0.87
<b>Precision</b>	17.85	5.74
<b>MAPE</b>	29.13	6.41

Table 4.8 shows the performance of the trained SVR model and it was compared with the performance of existing model. The accuracy is better if the value is nearer to 1 while the precision and MAPE symbolise a better performance with a smaller value. According to the table, the model trained in this project has a slightly better accuracy than the existing model, with 3% improvement in accuracy. The existing model has the much better precision and MAPE than the trained model with values of 12.11 and 22.72 respectively. The existing model possess a better performance due to the different features extraction and reduction method.

The existing model used the Wavelet Packet Decomposition (WPD) method to extract the features. The detailed energy coefficient for the signal in the first six level of decomposition is calculated. The higher discrimination of the signal can be retain as the WPD can analyze higher frequency domain of a signal. After this, the features extracted will be reduced. The method used here were two nonlinear reduction method which are EM-PCA and ISOMAP. A trend will be obtained from these reduction methods and the trend is also called as a health indicator. The health indicator will be mapped to the regression model using the technique of support vector regression to predict the RUL of the cutter [5].

**Table 4.9:** Performance assessment for neural network model

	Trained Model	Existing Model
<b>Accuracy</b>	0.97	0.87
<b>Precision</b>	5.20	14.49
<b>MAPE</b>	7.21	24.76
<b>R<sup>2</sup></b>	0.97	0.98
<b>MSE</b>	0.61	335.66

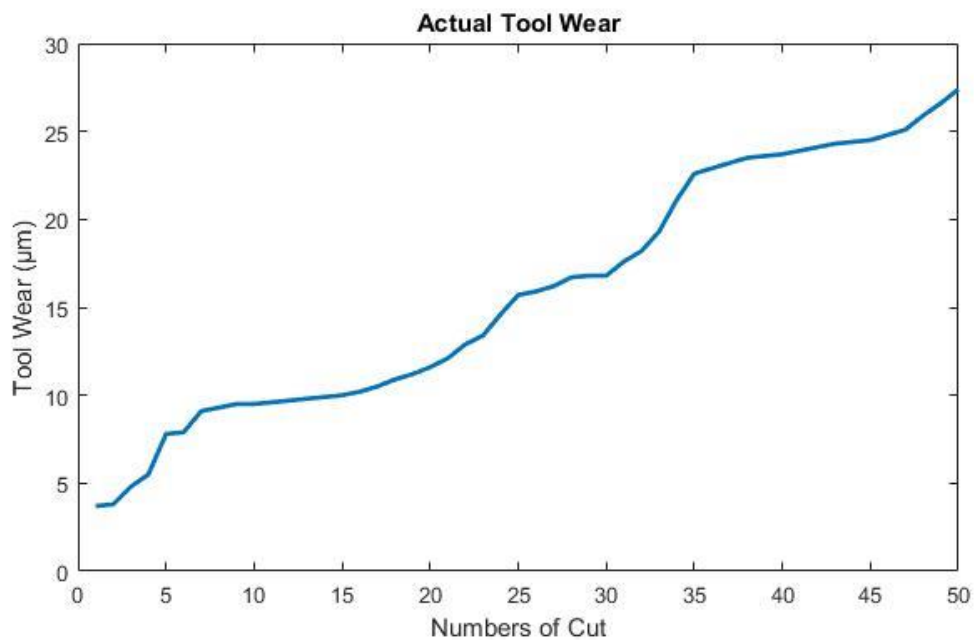
Table 4.9 shows the performance of the trained neural model and it was compared with the performance of existing model. The model trained in this project is generally better than the existing model in all aspect except the R<sup>2</sup> value. The value is just slightly better than the model from this project.

The Mean Squared Error (MSE) is a measure of how close a fitted line is to data points [27]. The performance of the neural network model is based on the Mean Squared Error (MSE) value. The MSE value indicates the validation performance at its minimum

point. The smaller the value means the data is fitted better, hence better performance. The existing model has a very big MSE value, thus its performance is not at the best. The difference in the MSE value was due to the different neural network model training method.

### 4.3 ACTUAL TOOL WEAR MEASUREMENT

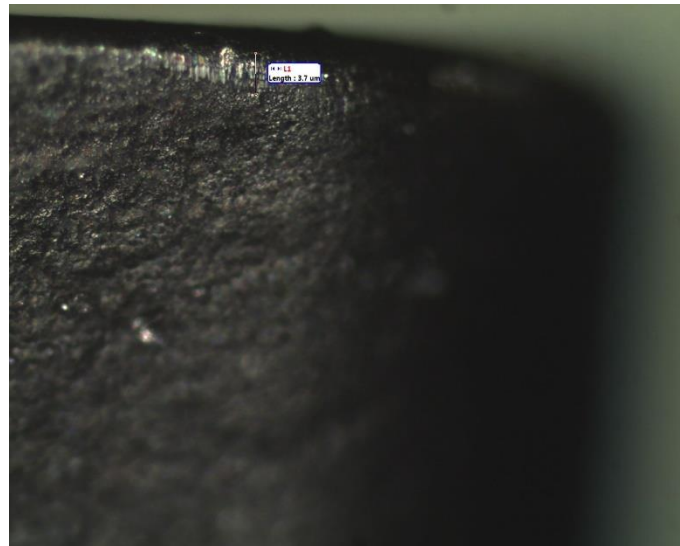
The experiment conducted were 50 cuts on the STAVAX ESR stainless steel with axial depth of cut 0.1mm. After every cut, the end mill insert was brought to the Olympus metallurgical microscope to measure the flank wear.



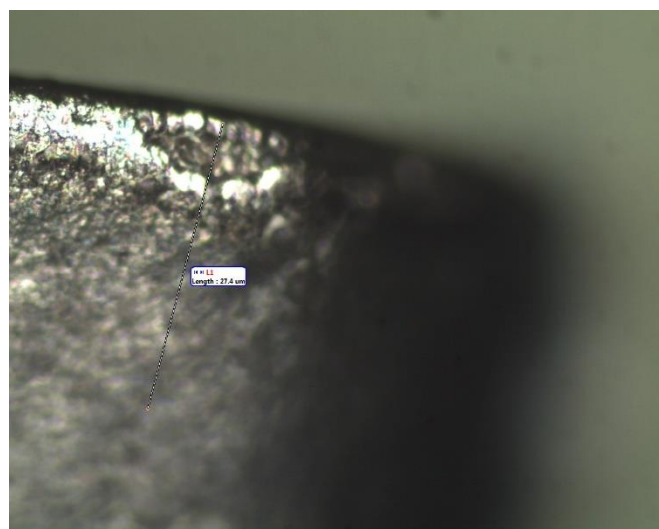
**Figure 4.11:** Actual tool wear of end mill

Figure 4.11 shows the actual tool wear measured. The tool wear increases when the numbers of cutting increases. This actual tool wear were used as the target to train the

prediction model using Support Vector Regression method and neural network method. Figure 4.12 shows the tool wear image after the first cutting process while figure 4.13 shows the tool wear image after the last cutting process.



**Figure 4.12:** Tool wear after first cutting process



**Figure 4.13:** Tool wear after last cutting process

#### 4.4 RAW DATA FEATURES EXTRACTION

The force sensor raw data went through the extraction process to acquire the statistical features from the data. These statistical features include the informative signature of the system. There are 10 different types of features presented in the available journal [28]. The table 4.10 shows the 7 most important statistical features for a force sensor identified from the literatures available.

**Table 4.10:** Important statistical features

No.	Important Statistical Features
1	Mean
2	Kurtosis
3	Total amplitude
4	Skewness
5	Root mean square
6	Standard deviation
7	Maximum level

#### 4.5 FEATURES REDUCTION AND SELECTION

All of the features listed in the table 4.10 are important, but when there are too many features involved in the building of model, the established correlated model will possess undesirable calculation performance [4]. Normally the selection of the features is random, so this can cause that some of the features selected were actually provided the identical information or may provide useless information for computation. This situation will increase the learning cost and the time taken for training [28].

Stepwise regression was used in this project to select the most appropriate features to train the model. It is a standard procedure to include or remove the elements from a multilinear model according to their importance in the regression model. It starts with an initial model and the analytical capability of bigger and smaller model will be compared later. The p-value of the statistic is measured to investigate the model with the presence of absence of a potential element [29].

If an element is not in the current model, the null hypothesis for it will be that the element will have a coefficient of zero if it is added to the model. The element will be included to the model if there is enough evident to ignore the null hypothesis. On the other hand, if the element is included in the current model, the null hypothesis for that element will be it has a zero coefficient. The element will be remove from the model if there is enough evident to reject the null hypothesis [29]. Table 4.11 shows the setting of the stepwise regression.

**Table 4.11:** Stepwise regression setting

<b>Input Parameters</b>	<b>Value</b>
<b>Initial model</b>	None included
<b>Entrance tolerance</b>	0.05
<b>Exit tolerance</b>	0.10
<b>Information display</b>	On
<b>Number of steps</b>	Infinity
<b>Scale</b>	Off

There was no initial element included in the initial model of the stepwise regression. The p-value for an element to enter the selection is smaller than 0.05 and it will be removed from the selection if its p-value is larger than 0.10. The maximum steps

in the regression is set to infinity and the elements were not scaled before the fitting process. All the relevant information and results from the regression model were displayed on the command window of MATLAB.

**Table 4.12:** Features selection result from stepwise regression

Features	Coefficients	P-value	Status
Mean	68.4452	7.2032e-05	In
Kurtosis	3.5226	4.8643e-07	In
Total amplitude	0.0897	0.5664	Out
Skewness	5.5010	0.4620	Out
Root mean square	0.5706	0.0877	Out
Standard deviation	0.2343	0.7501	Out
Maximum level	-0.1404	0.2873	Out

According to the table 4.12, two features were selected by the stepwise regression as their p-value were smaller than the selection requirement of 0.05. They were the mean and kurtosis. These two features have the most significant influence on the estimation of tool wear and prediction of the remaining useful too life. These four features were used as the input to train the prediction models.

#### 4.6 SUPPORT VECTOR REGRESSION (SVR) MODEL

The features selected were used to train a Support Vector Regression prediction model. The two features were the predictor and the tool wear were used as the response for the regression model. The regression model was trained using the MATLAB support vector machine regression function included in the statistics and machine learning toolbox

version R2015b. The table 4.13 shows the properties and parameters of the model trained for this project.

**Table 4.13:** Support vector machine regression model

<b>Property</b>	<b>Value</b>
<b>Predictor names</b>	'mean', 'kurtosis',
<b>Respond name</b>	'Tool wear'
<b>Standardize data</b>	Yes
<b>Kernel</b>	Gaussian
<b>Kernel scale</b>	Auto
<b>Solver</b>	Sequential Minimal Optimization
<b>Box constraints</b>	10.1557
<b>Epsilon</b>	1.0156
<b>Mu</b>	-1.1826, 8.5267
<b>Sigma</b>	0.0434, 1.1285

Referring to the table 4.13, the two predictor names were mean and kurtosis while the respond name was tool wear. The predictors' data were centered and divided each column by the standard deviations to standardize it. There were several different kernels such as linear, polynomial, Gaussian, and radial basis function can be applied to the support vector regression model. However, according to the established work, it has shown that Gaussian kernel can give the best performance for the model [5].

The Gaussian kernel measured with a support vector is an exponentially decaying function in the input feature space. It will has the maximum value at the support vector and decreasing steadily in every directions throughout the support vector. This let the kernel to have a hyper spherical contour. The kernel scale used in this project was set to auto where the MATLAB will select a suitable scale factor by a heuristic measure. This



heuristic method applies subsampling technique, so estimates acquired by this method can be different for different purpose of Support Vector Machine Regression model [30].

Other than that, the table shows that the solver for the support vector machine regression model was the Sequential Minimal Optimization (SMO). This algorithm is able to train the Support Vector Machine faster. The training process needs to solve a very huge quadratic programming (QP) optimization problem. SMO will create a group of smallest probable QP problems by dividing the big QP problem. Analytic method will be used to solve these tiny QP problem, which prevents the implementation of a time-consuming numerical QP optimization as an inner loop [31].

Furthermore, the box constraint which is also called the C parameter used to train the model was 10.1557 and the epsilon,  $\epsilon$  has the value of 1.0156. The Mu in table 4.5 is the mean value of the predictors data arranged in the sequence of mean then kurtosis.

The C parameter and the epsilon value determines the performance and complexity of the model. The epsilon value will influence the numbers of support vector included for the prediction process. If a larger value of epsilon was selected, the numbers of support vector included for prediction will be lesser thus makes the model less complex. On the other hand, the C parameter represent the compromise between the model complexity and the amount of difference permit during the optimization process. The using of a large C parameter will result in a less complex model. The selection of epsilon value and C parameter is still an active field of research [32].

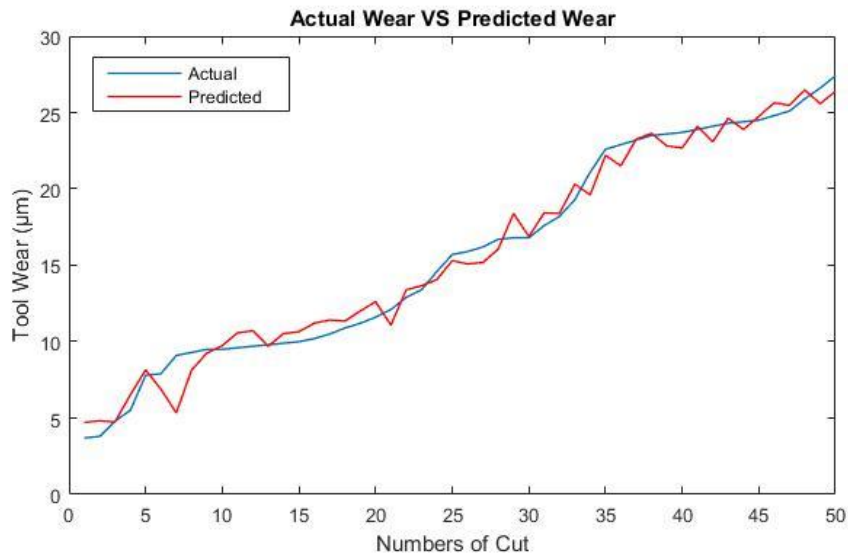


**Figure 4.14:** Comparison between actual wear and predicted wear of SVR

The result of actual wear and the predicted wear from the Support Vector Machine Regression model is shown in the figure 4.14. There was a total of 50 cuts performed using the end mill and the respective actual tool wear after each cut was recorded. The blue colour line graph was the progression of actual tool wear while the red colour line graph was the progression of the predicted tool wear. The actual wear showed a smoother curve while the predicted wear contained a zig-zag shape with some deviation from the actual wear and has more fluctuation at the beginning of the cutting process. This was due to some fitting error in the regression model. The values for the actual wear and predicted wear were later used for the prediction of remaining useful life.

#### 4.7 ARTIFICIAL NEURAL NETWORK MODEL

The Artificial Neural Network model was trained using the same data for the training of support vector machine regression model, which are the same 2 features and

the actual tool wear. Figure 4.15 shows the feedforward network architecture of the neural model.

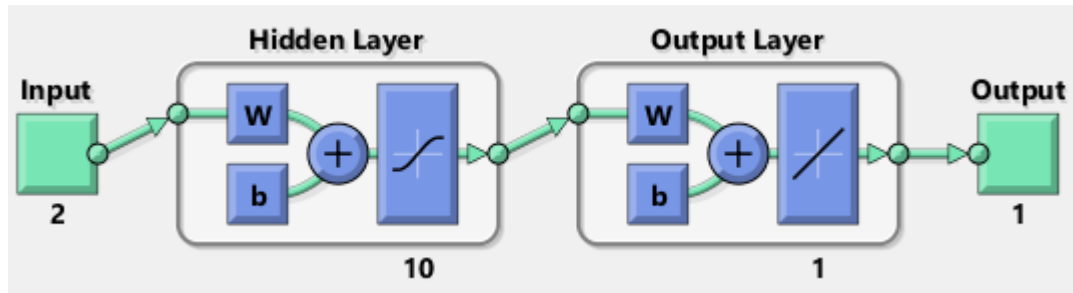


**Figure 4.15:** Neural network architecture

This architecture contained two layers which are the hidden layer and the output layer. There was 10 neurons in the hidden layer and 1 neuron in the output layer. Great result can be achieved by using single hidden layer, but more layers can be used if the result is not satisfying. The number of neurons determines the power of the neural network, so by increasing the number of neurons, the power of the network will be improved. However, increase the number of neurons will also causes more fitting to be done and potentially lead to overfitting [33].

**Table 4.14:** Neural network setting

<b>Parameters</b>	<b>Description</b>
<b>Data division</b>	Dividerand
<b>Training function</b>	Trainlm
<b>Hidden layer transfer function</b>	Tansig
<b>Output layer transfer function</b>	Purelin
<b>Maximum number of epochs to train</b>	1000
<b>Maximum training time</b>	Infinity
<b>Performance</b>	MSE
<b>Performance goal</b>	0
<b>Minimum performance gradient</b>	1e-7
<b>Maximum validations failure</b>	6

Table 4.14 shows the settings of the neural network during the training process. The data was divided randomly using the dividerand function before it was used as the input to train the network. The training function used was trainlm which was based on the Levenberg-Marquardt algorithm. Tan-sigmoid transfer function was used in the hidden layer and the purelin linear transfer function was used at the output layer for the fitting purpose. The model was set to train for a maximum of 1000 epochs and no restriction was given on the training time so it can be trained for an infinity time.

The performance criteria was based on the mean squared error (MSE) where it was set to zero as the best performance goal. Moreover, the performance gradient will become smaller during the training process as the model reaches the minimum performance and the training process will stop when the gradient is less than 1e-7. The maximum validation failure was the successive iterations where the performance in the validation failed to reduce. The maximum continuous failure was set to 6 and the training will stop if this limit was exceeded [34].

**Table 4.15:** Mean Square Error and regression of the model

Subset	Samples	MSE	Regression
Training	34	2.76062	0.983495
Validation	8	1.98153	0.971191
Testing	8	3.14558	0.981849

Table 4.15 shows the result for Mean Square Error value and the regression fit of the three subsets. The subsets are the training set, validation set, and training set. It is a general practise to separate the data into these three subsets. In the training set, the data are used to calculate the gradient and revise the weights and biases continuously. In the validation subset, the error was being observed in the training phase. Normally, the error for both the training and validation will reduce at the beginning of the training process. The validation error will start to increase when the data has been over fitted in the network. During the minimum validation error, the weights and biases were recorded and saved [35].

According to table 4.15, both training, validation, and training data have a small MSE value. This means that the network has a good performance and the performance will be best when the MSE is zero. Figure 4.16 below shows the line graph plotted using the MSE of both training, validation, and testing data. The graph shows that the validation error reached a minimum value at the 3 epochs with a value of 1.9815. The training process was continued for 6 more epochs before it was stopped. The graph for the testing and validation data have the similar shape and this shows that there were no big problems occurred during the training process. If the test curve had increased significantly before the validation curve increased, then it is possible that some overfitting might have occurred [36].

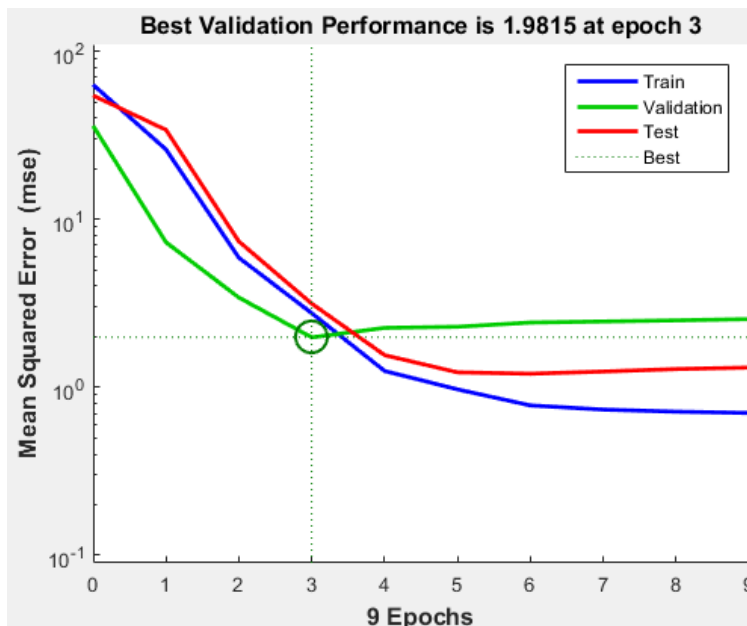


Figure 4.16: Mean Square Error

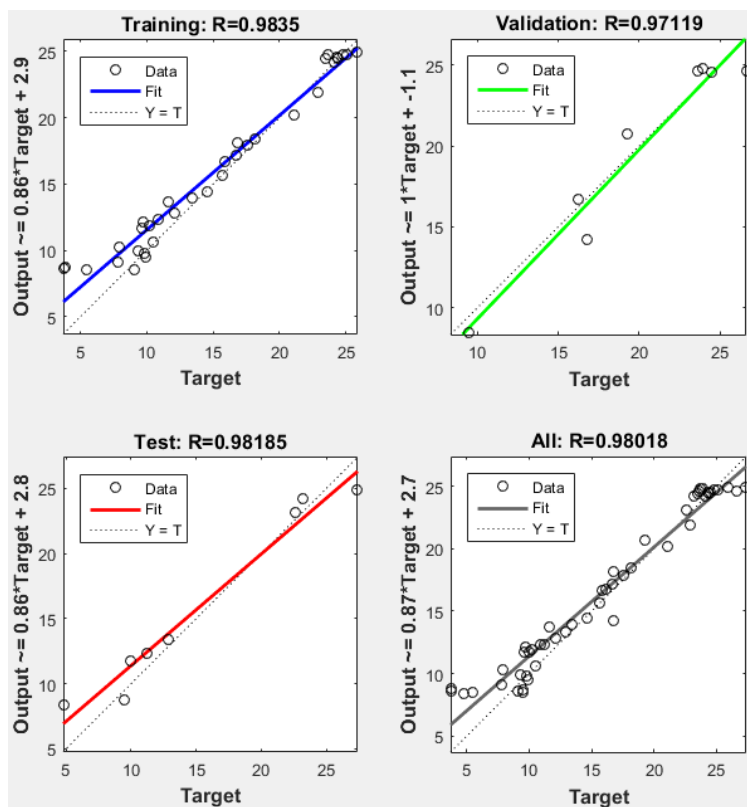
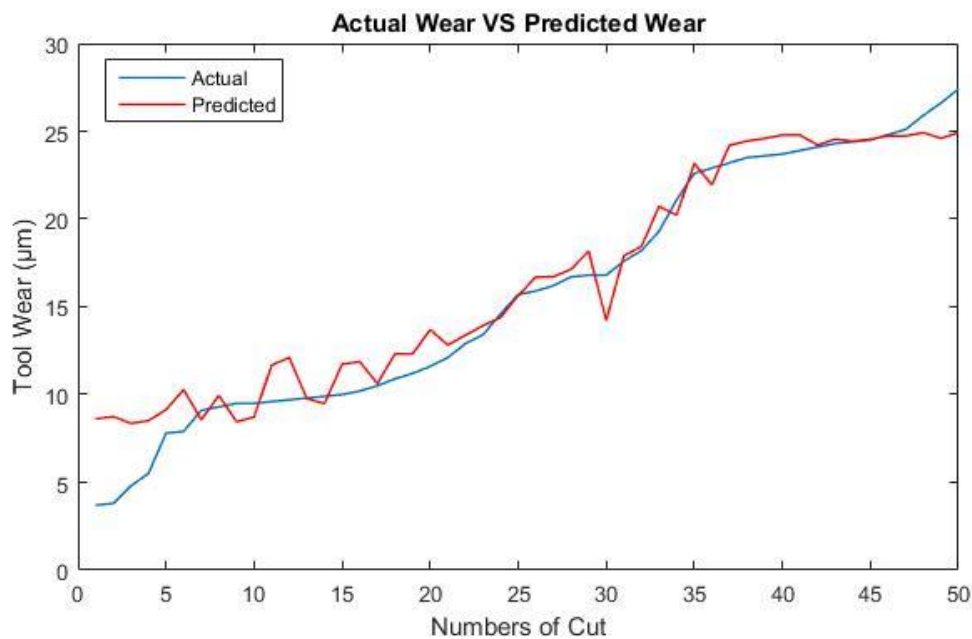


Figure 4.17: Regression plot

Figure 4.17 shows the regression plot for the training, validation, testing, and overall data. The R value is same as the regression value in the table 4.15. The dashed line in each plot represents the perfect result – outputs = targets. The solid line represents the best fit linear regression line between outputs and targets. The R value is an indication of the relationship between the outputs and targets. If  $R = 1$ , this indicates that there is an exact linear relationship between outputs and targets. If R is close to zero, then there is no linear relationship between outputs and targets [36].



**Figure 4.18:** Comparison between actual wear and predicted wear of neural network

The result of actual wear and the predicted wear from the Support Vector Machine Regression model is shown in the figure 4.18. There was a total of 50 cuts performed using the end mill and the respective actual tool wear after each cut was recorded. The blue colour line graph was the progression of actual tool wear while the red colour line graph was the progression of the predicted tool wear.

The actual wear showed a smoother curve while the predicted wear contained some deviation from the actual wear and has more fluctuation at the beginning and the final of the cutting process. This was due to some prediction error in the neural network. The predicted wear using the Artificial Neural Network is less accurate than the Support Vector Regression model. This can be seen from the figure 4.15 and figure 4.19 where the predicted wear is more alike as the actual wear from the support vector regression model. The values for the actual wear and predicted wear were later used for the prediction of remaining useful life.

#### **4.8 REMAINING USEFUL LIFE (RUL) PREDICTION**

The predicted tool wear was used to predict the remaining useful life. The remaining useful life can be calculated using the following formula:

$$RUL(t) = t_f - t \quad (4.1)$$

The  $t_f$  is the final time where the end mill cannot be used anymore. In this project, we assumed the end mill will reach the threshold value or its end of service life at the end of 50 cuts. On the other hand,  $t$  is the actual time where the remaining useful life was computed. A graphical illustration for the calculation of remaining useful life is shown at the figure 4.19 [3].



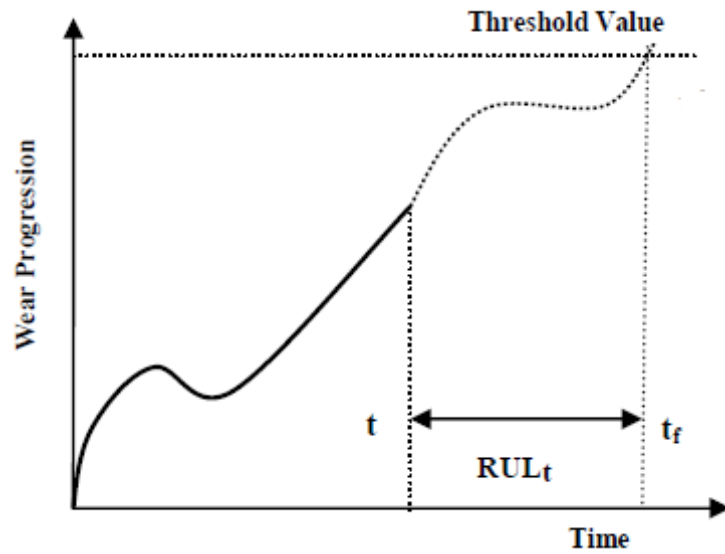


**Figure 4.19:** Illustration for remaining useful life calculation [3]

Source: Predicting remaining useful life of high speed milling cutters based on Artificial Neural Network

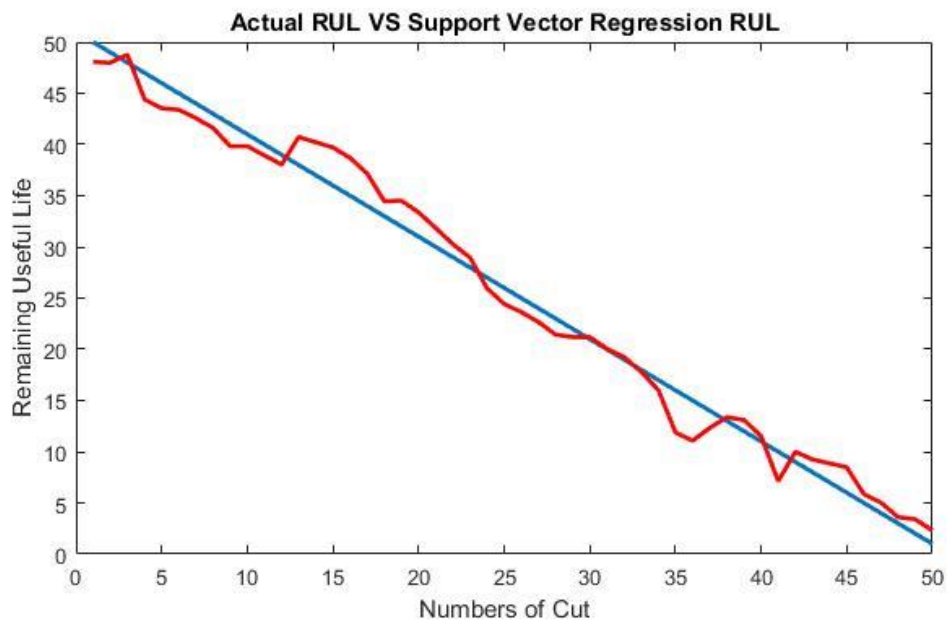


**Figure 4.20:** Comparison between actual RUL and Support Vector Regression RUL

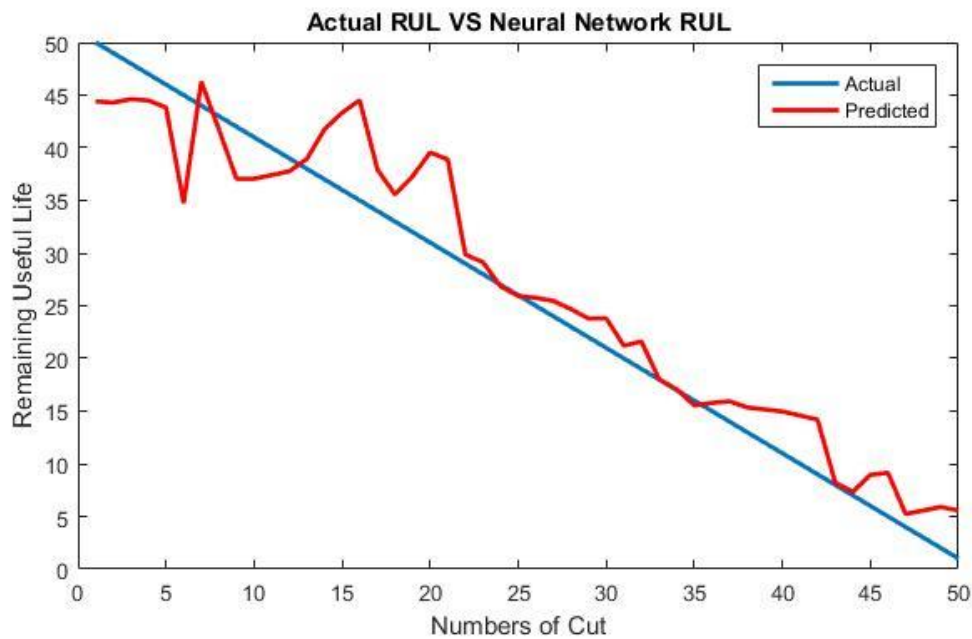


**Figure 4.21:** Comparison between actual RUL and Artificial Neural Network RUL

Figure 4.20 and figure 4.21 show the graph of actual tool life versus the predicted wear acquired from the Support Vector Regression model and the neural network model. The predicted RUL from the Support Vector Regression model is better as it can give a result nearer to the actual RUL. This means the Support Vector Regression model trained in this project has the better performance compared to the neural network model trained.

#### 4.9 PERFORMANCE ASSESSMENT

The performance assessment process is important to determine whether the train RUL prediction model is suitable for the real life application or not. The prognostic measures used to determine the performance for models were the accuracy, precision, and Mean Absolute Percentage Error (MAPE).

Accuracy is the measure of worthiness for the prediction result. The result of the accuracy will be near to 1 if the prediction is accurate and vice versa. The formula for the accuracy is shown as following:

$$Accuracy = \frac{1}{N} \sum_{n=1}^N e^{-\frac{|RUL_{actual}(n) - RUL_{predicted}(n)|}{RUL_{actual}(n)}} \quad (4.2)$$

Where the  $RUL_{actual}(n)$  is the real RUL of the cutter,  $RUL_{predicted}(n)$  is the predicted RUL acquired from the prediction model at cutting process  $n$ , and the  $N$  is the total number of prediction.

Precision is the measure of the distribution for the prediction error around the mean. The formula to calculate the precision is shown as following:

$$Precision = \sqrt{\frac{\sum_{n=1}^N (\varepsilon(n) - \epsilon)^2}{N}} \quad (4.3)$$

Where the  $\varepsilon(t)$  is the  $RUL_{actual}(n) - RUL_{predicted}(n)$  and  $\epsilon$  is equal to  $\frac{1}{N} \sum_{n=1}^N \varepsilon$

Mean Percentage Absolute Error (MAPE) calculate the average error in percentage. It is calculated using the following formula:

$$MAPE = \frac{1}{N} \sum_{n=1}^N \left| \frac{100 \cdot \varepsilon(n)}{RUL_{actual}(n)} \right| \quad (4.4)$$

**Table 4.16:** Performance assessment for models trained

	<b>Support Vector Regression</b>	<b>Neural Network</b>
<b>Accuracy</b>	0.90	0.83
<b>Precision</b>	1.90	3.73
<b>MAPE</b>	12.59	28.68

Table 4.16 shows the performance of the trained SVR model and neural network model. They were compared against each other. The accuracy is better if the value is nearer to 1 while the precision and MAPE symbolise a better performance with a smaller value. According to the table, the Support Vector Regression model has a slightly better accuracy than the neural network model as it was 9% more accurate. The precision and the MAPE of the Support Vector Regression model are also better than the neural network model. The precision was 1.83 better and MAPE was 16.09 better. It possess a better overall performance than the neural network model.

The performance of the support vector regression model and the neural network model are affected by its data. Some data set will perform better with the neural network but some will perform better with the support Vector Regression model. This means the performance of the model will be affected by the suitability of datasets. However, the average performance for both the Support Vector Regression model and neural network model are the same [37].

The neural network has two main disadvantages when compared with Support Vector Regression. The first one is that the neural network will normally converge at the local minima instead of the global minima. Sometimes, this will cause the model to have the problem that it cannot get the full picture of the situation. The other disadvantage that

causes the Support Vector Regression to perform better than the neural network in the real practise is that neural network is more susceptible to overfitting, where this is the biggest problem in neural network [38].

According to the work done by Yang Shao and Ross S. Lunetta in “Comparison of support vector machine, neural network, and CART algorithms for the land-cover classification using limited training data points”, it has shown that the performance of the Support Vector Machine with limited training data is better than the Neural Network. It can achieve a higher accuracy. The performance gap between these two methods will be narrowed when the number of training data has been increased. This also shows the performance of the Support Vector Machine is less prone to the influence of the training data available [39].

## **CHAPTER 5**

### **CONCLUSION AND RECOMMENDATIONS**

#### **5.1 INTRODUCTION**

This chapter will conclude the finding acquired from this project. The limitation of the project will be discussed and recommendations will be proposed for future work to improvement this project.

#### **5.2 CONCLUSION**

In conclusion, the remaining useful life of the end mill cutter has been predicted in this project. Different prediction methods were also been implemented and compared using the MATLAB software.

The Support Vector Regression model has a slightly better accuracy than the neural network model as it was 9% more accurate. The precision and the MAPE of the Support Vector Regression model are also better than the neural network model. The precision was 1.83 better and MAPE was 16.09 better. It possess a better overall performance than the neural network model.

According to the project, both of the prediction methods are suitable for the prediction of remaining useful life as both of them are having an accuracy of over 80%. However, Support Vector Machine Regression method is the best method for prediction of remaining useful life.

### **5.3 RECOMMENDATIONS**

The scope of the project was limited to determine the remaining useful life on and end mill cutter. However, there are times in the industries where the tool cutter will still be continued to use even when it has exceeded the wear threshold limit. The tool will be used until the products produced are below the minimum requirement for quality assurance.

Therefore, a surface roughness test can be included as the future work for this project. By doing this, the surface finish of the workpiece can be determined and whether a tool can be used exceeded its remaining useful life can be discovered. Sometimes the surface finish roughness of the workpiece after the end of RUL for the cutter will still be within the limits of quality and specifications limits. This can prevent the wastage of the tool cutter since industries are more concern about the most cost effective solution available.

## REFERENCE

This thesis is prepared based on the following references;

1. Engin, S., & Altintas, Y. (2001). Mechanics and dynamics of general milling cutters. PartII: Inserted cutters. *International Journal of Machine Tools and Manufacture*, 41(15), 2213–2231.
2. Dolinšek, S., Šuštaršič, B., & Kopač, J. (2001). Wear mechanisms of cutting tools in high speed cutting processes. *Wear*, 250-251, 349–356.
3. Jain, A. K., & Lad, B. K. (2015). Predicting Remaining Useful Life of High Speed Milling Cutters based on Artificial Neural Network, (February).
4. Li, X., Lim, B. S., Zhou, J. H., Huang, S., Phua, S. J., Shaw, K. C., & Er, M. J. (2009). Fuzzy Neural Network Modelling for Tool Wear Estimation in Dry Milling Operation, 1–11.
5. Benkedjough, T., Medjaher, K., Zerhouni, N., & Rechak, S. (2015). Health assessment and life prediction of cutting tools based on support vector regression. *Journal of Intelligent Manufacturing*, 26, 213–223.
6. Ahmed, W. (2013). Advantages and Disadvantages of Using MATLAB/ode45 for Solving Differential Equations in Engineering Applications. *International Journal of Engineering*, (7), 25–31.
7. Introduction to MATLAB for Engineering Students. *Northwestern University, Version*, (August).
8. Metal Cutting and Cutting Tool: Factors Affecting Tool Life. (n.d.). Retrieved from <http://metalcuttingandcuttingtool.blogspot.my/2008/03/factors-affecting-tool-life.html>



9. CLIMB & CONVENTIONAL MILLING ENHANCING TOOL LIFE & MACHINE PERFORMANCE. (n.d.), 48(888).
10. Dang, J. W., Zhang, W. H., Yang, Y., & Wan, M. (2010). Cutting force modeling for flat end milling including bottom edge cutting effect. *International Journal of Machine Tools and Manufacture*, 50(11), 986–997.
11. Kumar, K. S., & Sreenivasulu, B. (2015). Optimization and Process Parameters of CNC End Milling For Aluminum Alloy 6082, 2(1), 1–6.
12. Hamdan, A., Sarhan, A. A. D., & Hamdi, M. (2012). An optimization method of the machining parameters in high-speed machining of stainless steel using coated carbide tool for best surface finish. *The International Journal of Advanced Manufacturing Technology*, 58(1-4), 81–91.
13. Vijay, S., & Krishnaraj, V. (2013). Machining Parameters Optimization in End Milling of Ti-6Al-4V. *Procedia Engineering*, 64, 1079–1088.
14. Liew, W. Y. H., & Ding, X. (2008). Wear progression of carbide tool in low-speed end milling of stainless steel. *Wear*, 265(1-2), 155–166.
15. Repo, J. (2010). *Condition Monitoring of Machine Tools and Machining Processes using Internal Sensor Signals. Thesis.*
16. Mathworks. 2016. *fitrsvm*. [ONLINE] Available at: <http://www.mathworks.com/help/stats/fitrsvm.html>. [Accessed 10 May 2016].
17. Mathworks. 2016. *predict*. [ONLINE] Available at: <http://www.mathworks.com/help/stats/compactregressionsvm.predict.html>. [Accessed 10 May 2016].

18. Mathworks. 2016. *Fit Data with a Neural Network*. [ONLINE] Available at: <http://www.mathworks.com/help/nnet/gs/fit-data-with-a-neural-network.html>. [Accessed 10 May 2016].
19. Techspex. 2002. *Makino KE55 7.5 HP Vertical CNC Knee Mill*. [ONLINE] Available at: [http://www.techspex.com/machining-centers/makino\(2612\)/1625](http://www.techspex.com/machining-centers/makino(2612)/1625). [Accessed 10 May 2016].
20. Haas Automation Inc. 2016. *CNC Verticals: 50 - 64 Inch X-Axis*. [ONLINE] Available at: [http://www.haascnc.com/we\\_spec1.asp?id=VF6/40&sizeID=50\\_64INCH\\_VMC#gsc.tab=0](http://www.haascnc.com/we_spec1.asp?id=VF6/40&sizeID=50_64INCH_VMC#gsc.tab=0). [Accessed 10 May 2016].
21. Sodick. 2016. *VZ300L Wire EDM*. [ONLINE] Available at: <http://www.sodick.com/products/wireedm/vz300l.htm>. [Accessed 9 May 2016].
22. Ceratizit. 2014. *Innovation Product Highlight*. [ONLINE] Available at: [http://www.ceratizit.com/uploads/tx\\_extproduct/files/GD\\_KT\\_PRO-04370814\\_SEN\\_ABS\\_V1.pdf](http://www.ceratizit.com/uploads/tx_extproduct/files/GD_KT_PRO-04370814_SEN_ABS_V1.pdf) [Accessed 10 May 2016].
23. Bohler Uddeholm US. (2013). *UDDEHOLM STAVAX® ESR (420, Modified)*. [ONLINE] Available at: [http://www.bucorp.com/stavax\\_esrp.html](http://www.bucorp.com/stavax_esrp.html) [Accessed 10 May 2016].
24. Kistler. 2014. *Product Catalog*. [ONLINE] Available at: <https://www.kistler.com/fileadmin/files/divisions/sensor-technology/cuttingforce/960-002e-05.14.pdf> [Accessed 10 May 2016].
25. Mastercam. 2016. *Milling Solutions*. [ONLINE] Available at: <http://www.mastercam.com/en-us/Solutions/Milling-Solutions>. [Accessed 10 May 2016].
26. Mathworks. 2016. *The Language of Technical Computing*. [ONLINE] Available at: <http://www.mathworks.com/products/matlab/>. [Accessed 10 May 2016].

27. Vernier. 2011. *What are Mean Squared Error and Root Mean Squared Error?*. [ONLINE] Available at: <http://www.vernier.com/til/1014/>. [Accessed 16 May 2016].
28. Weihua Li Tielin Shi Guanglan Liao Shuzi Yang, (2003), "Feature extraction and classification of gear faults using principal component analysis", *Journal of Quality in Maintenance Engineering*, Vol. 9 Iss 2 pp. 132 – 143.
29. Mathworks. 2016. *stepwisefit*. [ONLINE] Available at: <http://www.mathworks.com/help/stats/stepwisefit.html>. [Accessed 16 May 2016].
30. Gaussian, T., 1855. 3. The Gaussian kernel.
31. Platt, J.C., 1998. Sequential Minimal Optimization : A Fast Algorithm for Training Support Vector Machines. , pp.1–21.
32. Omitaomu, O.A., Jeong, M.K. & Hines, J.W., 2016. On-Line Prediction of Motor Shaft Misalignment Using Fast Fourier Transform Generated Spectra Data and Support Vector Regression. , 128(November 2006), pp.1019–1024.
33. Mathworks. 2016. Create, Configure, and Initialize Multilayer Neural Networks. [ONLINE] Available at: <http://www.mathworks.com/help/nnet/ug/create-configure-and-initialize-multilayer-neural-networks.html>. [Accessed 16 May 2016].
34. Mathworks. 2016. *Train and Apply Multilayer Neural Networks*. [ONLINE] Available at: <http://www.mathworks.com/help/nnet/ug/train-and-apply-multilayer-neural-networks.html>. [Accessed 16 May 2016].
35. Mathworks. 2016. Improve Neural Network Generalization and Avoid Overfitting. [ONLINE] Available at: <http://www.mathworks.com/help/nnet/ug/improve-neural-network-generalization-and-avoid-overfitting.html>. [Accessed 16 May 2016].

36. Mathworks. 2016. Analyze Neural Network Performance After Training. [ONLINE] Available at: <http://www.mathworks.com/help/nnet/ug/analyze-neural-network-performance-after-training.html>. [Accessed 16 May 2016].
37. Cross Validated. 2012. Neural networks vs support vector machines: are the second definitely superior?. [ONLINE] Available at: <http://stats.stackexchange.com/questions/30042/neural-networks-vs-support-vector-machines-are-the-second-definitely-superior>. [Accessed 16 May 2016].
38. Stackoverflow. 2013. What are advantages of Artificial Neural Networks over Support Vector Machines?. [ONLINE] Available at: <http://stackoverflow.com/questions/11632516/what-are-advantages-of-artificial-neural-networks-over-support-vector-machines>. [Accessed 16 May 2016].
39. Shao, Y. & Lunetta, R.S., 2012. ISPRS Journal of Photogrammetry and Remote Sensing Comparison of support vector machine , neural network , and CART algorithms for the land-cover classification using limited training data points. , 70, pp.78–87.

## APPENDICES

### A BUDGET PLAN

No	Equipment/Material	Supplier	Price per Unit (RM)	Unit	Sub Total (RM)
1	Cast iron	YG	60	1	60
2	Stainless Steel	Yuh Field OEM	114	1	114
3	Vibration Sensor	Sparkfun	13.2	2	26.4
4	Acoustic emission sensor	Soundwell	1318	2	2636
5	Current Sensor	Sparkfun	44	1	44
6	High Pass Filter	Eagle	13.2	2	26.4
7	Low Pass Filter	Drake	27	1	27
8	Amplifier	Omega	368	1	368
9	Data Acquisition Board	MC	439	1	439
10	Milling Electricity Cost	TNB	50	1	50
11	Two Flute End Mill	Ouke	2.2	16	35.2
				Total (RM)	3826





**C CAD PROGRAM**

%

O0000(SEOW FKP)

(DATE=DD-MM-YY - 12-01-80 TIME=HH:MM - 23:37)

(MCX FILE - C:\USERS\CNC\DESKTOP\SEOW FKP.MCX-5)

(NC FILE - C:\USERS\CNC\DESKTOP\SEOW FKP.NC)

(MATERIAL - ALUMINUM MM - 2024)

( T23 | 12. FLAT ENDMILL | H23 )

N100 G21

N102 G0 G17 G40 G49 G80 G90

N104 T23 M6

N106 G0 G90 G54 X51. Y38.5 A0. S4510 M3

N108 G43 H23 Z15.

N110 Z2.

N112 G1 Z-.1 F300.

N114 Y-38.5 F270.

N116 G0 Z15.

N118 X46. Y38.5

N120 Z2.

N122 G1 Z-.1 F300.

N124 Y-38.5 F270.

N126 G0 Z15.

N128 X41. Y38.5

N130 Z2.

N132 G1 Z-.1 F300.

N134 Y-38.5 F270.

N136 G0 Z15.

N138 X36. Y38.5

N140 Z2.

N142 G1 Z-.1 F300.

N144 Y-38.5 F270.

N146 G0 Z15.

N148 X31. Y38.5

N150 Z2.

N152 G1 Z-.1 F300.

N154 Y-38.5 F270.



N156 G0 Z15.  
N158 X26. Y38.5  
N160 Z2.  
N162 G1 Z-.1 F300.  
N164 Y-38.5 F270.  
N166 G0 Z15.  
N168 X21. Y38.5  
N170 Z2.  
N172 G1 Z-.1 F300.  
N174 Y-38.5 F270.  
N176 G0 Z15.  
N178 X-49. Y38.5  
N180 Z2.  
N182 G1 Z-.1 F300.  
N184 Y-38.5 F270.  
N186 G0 Z15.  
N188 X-44. Y38.5  
N190 Z2.  
N192 G1 Z-.1 F300.  
N194 Y-38.5 F270.  
N196 G0 Z15.  
N198 X-39. Y38.5  
N200 Z2.  
N202 G1 Z-.1 F300.  
N204 Y-38.5 F270.  
N206 G0 Z15.  
N208 X-34. Y38.5  
N210 Z2.  
N212 G1 Z-.1 F300.  
N214 Y-38.5 F270.  
N216 G0 Z15.  
N218 X-29. Y38.5  
N220 Z2.  
N222 G1 Z-.1 F300.  
N224 Y-38.5 F270.  
N226 G0 Z15.  
N228 X-24. Y38.5  
N230 Z2.

N232 G1 Z-.1 F300.

N234 Y-38.5 F270.

N236 G0 Z15.

N238 X-19. Y38.5

N240 Z2.

N242 G1 Z-.1 F300.

N244 Y-38.5 F270.

N246 G0 Z15.

N248 M5

N250 G91 G28 Z0.

N252 G28 Y0. A0.

N254 M30

%